The dynamics of angioplasty: Effects of vascular bed and lesion morphology

by

Vishal Saxena

Submitted to the
Department of mechanical engineering
in partial fulfillment of the requirements for the degree of

MASTER OF SCIENCE IN MECHANICAL ENGINEERING
at the
MASSACHUSETTS INSTITUTE OF TECHNOLOGY

February 2001

Author .....
.....
Department of Mechanical Engineering
January 19, 2001

Certified by .....
.....
Elazer R. Edelman
Thomas D. and Virginia W. Cabot Professor, Harvard-MIT Department of Health Sciences and Technology

Accepted by .....
.....
Ain A. Sonin
Chairman, Departmental Committee on Graduate Students

The dynamics of angioplasty:
Effects of vascular bed and lesion morphology

By
Vishal S. Saxena

Submitted to the department of Mechanical Engineering
on January 19, 2001, in partial fulfillment of the
Requirements for the degree of Master of Science in
Mechanical Engineering

ABSTRACT

This thesis sought to examine the influence of the vascular bed on the tissue response to endovascular stent implantation. Closed form analytic solutions were obtained for the different beds studied. Ideal arteries were considered of normal, tapered, curved, or eccentric morphology. The application of the stent boundary conditions in the appropriate defining equations produced the desired strains and stresses. It was found that even severe curvature could not produce stresses that came close to those obtained with tapered and eccentric vessels. The highest absolute stresses (circumferential) in the curved, tapered, and eccentric vessels were 38.158 kPa, 59.117 kPa, and 97.721 kPa respectively. For comparison, the stresses in 'normal' vessels are 38 kPa. Eccentric vessels produced the highest variation in stresses (66%) followed by variations in the tapered vessel (27%). In contrast blood pressure loading created far lower stresses, and shear forces from blood flow were negligible (~ 0.63 Pa and 0.9 Pa for the aorta and renals).

In the tapered bed, the maximal stress principally arose was at the smallest diameter location of the arterial wall. This corresponded to a maximum level of strain at the smallest diameter section of the tapered vessel wall (in a vessel with a monotonically decreasing diameter or in other words in a vessel with a constant taper, this corresponds to either the top or the bottom portion of the vessel).

Thus, one design that alleviates this problem inputs a uniform strain, not a uniform displacement, in the arterial wall. This minimizes both the absolute stresses and the variation in axial stresses (ideally, the variation should approach zero in the 'constant-strain stent'.

In conclusion, the eccentric vessel imposes far higher stresses than other vessel geometries, with the tapered geometry following close behind. The curved vessel stresses are negligible.

Thesis Supervisor: Elazer R. Edelman
Title: Thomas D. and Virginia W. Cabot Professor, Harvard-MIT Department of Health Sciences and Technology

Acknowledgements

It was my turn to jump. "should I jump or should I not jump?" that if it weren't the question, would certainly be something else (it would be a sentence that could, for instance, end with a diminutive period. It could also end with a pastrami, but we won't get into that). I looked out past the door of the plane now cruising at a gruesome 20,000 ft over some rectangular blobs of something my mind quite couldn't convince itself of being nice meadows where I would have a soft landing. What it (my mind) could easily convince itself was that a jump from a height of say 20,000 ft could easily turn into a pretty hard landing on some unforgiving piece of meadowy land if—and this 'if' didn't look too big of an 'if'—my parachute decided to be slightly stubborn that warm nice day.

"Looks pretty far, doesn't it?" I said, hoping to gain some time; because the people behind me, for some insane reason wanted to give their parachutes a chance to be slightly stubborn in a quick hurry. "What do you think?" I asked my friend. His reply? "Well, I believe the parachute won't let you down." Hmm, when people use the word "believe", they are usually not quite sure of the outcome. Otherwise, they wouldn't need to believe, they would be sure. My mind began computing outcomes. What chance is there that this oversized umbrella does a flip on me (like those carbon atoms undergoing SN2 reaction)? What if the parachute sprung a leak? What is the chance that that would happen? .02 percent? How about the overall chance of my landing not so softly? 0.7%? What my friend should have said was: "I believe you have a 10% chance of failure in the parachute."

I didn't jump.

Where are the acknowledgements? Surely, you aren't asking yourself that question? Well, first of all, I had to throw this nonsense somewhere, and assuming that you 'believe' as I firmly do, that the rest of this catachresis—I mean, thesis, honestly—is not so, then...I lost track of the sentence.

And second, here they are.

My thanks to Elazer for providing me with the opportunity for working on this project. His guidance and insights were invaluable in helping me formulate a coherent problem statement and in helping me obtain the closed form solutions to the different models that were studied.

Jim Squire's advice and help are truly appreciated.

My Parents have provided me with the motivation and the courage to pursue my dreams and goals. It perhaps can be said with not a little justification that one is truly defined by one's goals (if one doesn't demur to being 'defined'), and my gratitude to them is immeasurable.

TABLE OF CONTENTS

CONTENTS		Page
Abstract		**2**
Acknowledgements		**3**
List of Figures		**6**
List of Tables		**7**
Terminology		**8**
Chapter	**Title**	
1	**Historical background / Literature review**	**9**
	1.1 Cardiovascular diseases	*9*
	1.2 The structure of the arterial wall	*12*
	1.3 Thesis outline	*15*
2	**Theory / Assumptions**	**16**
	2.1 Arterial Mechanics	*16*
	2.2 Stent types	*18*
	2.3 Remodeling	*21*
	2.4 Compensatory enlargement	*23*
	2.5 Material composition of the plaque	*24*
	2.6 The zero stress state of the artery	*24*
	2.7 The incompressibility assumption	*26*
	2.7.1 The relationship of Poisson's ratio to incompressibility: Isotropic case, small strain	*26*
	2.7.2 The relationship of Poisson's ratio to incompressibility: Isotropic case, large strain	*30*
	2.7.3 Orthotropic Incompressible Poisson's ratio value constraints	*32*
	2.7.4 ADINA—using orthotropic material properties	*34*
	2.7.5 Incompressibility—orthotropic material	*36*
	2.8 Axial stretch ratio of 1.5—explanation and discussion	*49*
3	**Materials / Methods**	**40**
	3.1 Force-displacement (F/D) characteristic for a self-expanding stent	*40*
	3.2 Recoil	*42*
	3.3 Arterial Bed	*43*
	3.3.1 Derivation of longitudinal and circumferential stresses in different types of arterial geometries	*44*
	3.3.2 Non tapered, concentric, straight (non-curved) vessels	*48*
	3.3.3 Curved vessel	*50*
	3.3.4 Eccentric vessel	*52*
	3.3.5 Tapered vessel	*54*
	3.3.5.1 Tapered stent in a tapered vessel	*55*
	3.3.5.2 Non-tapered stent in a tapered vessel	*58*
	3.4 The inapplicability of using thermal shell elements in modeling stent expansion within arteries	*60*
	3.5 Verification of the eccentric vessel data using ABAQUS	*62*
	3.6 Failure	*63*

3.6.1 Chronic-dynamic case: 'Time to fatigue' determination with cyclic loading 64
3.6.1.1 Mechanics of stent deformation 64
3.6.2 Fatigue determination 66
4 Results **74**
4.1 Self-expanding force displacement relationship 74
4.2 Acute force determination 74
4.3 Effect of arterial bed 75
4.4 Inapplicability of using thermal shell elements 78
4.5 Fatigue life determination 79
5 Discussion **81**
5.1 Effect of arterial bed 83
5.2 Inappropriateness of using thermal elements 86
6 Future work **89**
Appendices
App. A Matlab file to calculate the stiffness matrix entries 91
App. B Data used to obtain the force-displacement characteristics of a self-expanding stent 93
App. C Determination of force to be used in fatigue testing 95
App. D Calculation of fatigue life 98
App. E Matlab file to find the pressure that will cause ave($strain_{local}$) = a specified global strain in a curved vessel 99
App. F Matlab file to find the stress vs strain curve for an eccentric vessel 102
App. G Matlab file to find the stress vs strain curve for a tapered and non-tapered stent in a tapered vessel 104
App. H Matlab code to find variation of Poisson's ratio with strain 105
References **106**

List of Figures

No.	Title	Page
1	The arterial wall	12
2	Connective tissue conceptualized	13
3	The arterial stress-strain characteristics	17
4	A conceptual representation of balloon vs. self expanding stents	19
5	A self-expanding stent being deployed	20
6	The zero stress state of the artery	25
7	Coordinate system term representation	27
8	Poisson's ratio variation with strain	32
9	Force-displacement analysis setup	41
10	Detail of the transparency set up	42
11	Direction of principal stresses in a cylinder	45
12	Derivation of longitudinal stresses	46
13	Circumferential stresses in normal vessels	49
14	Circumferential stresses in curved vessel	50
15	Derivation of stresses in a curved vessel	51
16	Derivation of eccentric stresses	53
17	Tapered vessel, tapered stent	56
18	Tapered stent in tapered vessel (cut-away)	57
19	Non-tapered stent in a tapered vessel	58
20	Definition of C, E, and T (curvature, eccentricity, and taper	60
21	Finite element model of the curved vessel	61
22	Crowning	64
23	Crimping	65
24	Deployment	65
25	Components of the cyclic load shown with hypothetical profiles	67
26	Composite hypothetical profile of the dynamic forces seen by the stent	68
27	Palmgren Miner rule	69
28	Determination of 'a'	71
29	Stress-strain characteristics for a self-expanding stent	75
30	Variation of circumferential stress with curvature	76
31	Effect of stenting a tapered vessel with tapered and non-tapered stents	77
32	Eccentric vessel. Comparison of FEA results with the closed form analytic solution	78
33	Variation of maximum stress with eccentricity through use of thermal shell elements	79
34	Model of the eccentric vessel in ABAQUS	85
35	Application of the same strain at two different points leads to stresses opposite to what is expected	87
36	Each thermal shell element shows strain regardless of global constraints	88
37	Forces on a stent modeled as a cylindrical tube	95
38	Force balance on a tube	96

List of Tables

No.	Title	Page
1	Assumptions / Problems	44
2	Variation in Parameters	60
3	Loading vs. time frame of loading	63
4	The different components of cyclic load occur at different frequencies	67
5	Data used to obtain the self-expanding force-displacement characteristic	93

Terminology

Adventitia	The outer layer of the arterial wall
Angiogram	An x-ray photograph of a vessel (or any cavity) by use of a radio-opaque dye
CSA	Cross-sectional area
EEL	External elastic lamina
IEL	Internal elastic lamina
Intima	The thin layer of (endothelial) cells lining the inside of the arterial wall
Late loss	Angiographic lumen reduction (45)
Lesion	A region in the artery where there is 'deposition' of material leading to a decrease in the size of the lumen.
Lumen	The inside (hollow part) of a tube—in the artery, this is where blood flows.
Media	The middle portion of the arterial wall
Neointimal hyperplasia	A proliferation of smooth muscle cells from the media next to the intima usually leading to a decrease in lumen size.
Ostium	The region where the aorta joins the renal artery(in general any region where two tubes intersect)
Ostial lesion	A lesion seen at the ostium (usually characterized by its appearance beginning in the region a little bit down into the renals from the aorta (distal to the aorta) extending upto and into the aorta.
Plaque rigidity	The higher the level of lipid content in the plaque the less rigid it is and the less able it is to withstand a stress.
Stenosis	Any blockage (of a vessel or tube) in the body. For instance, it can refer to the arteries, veins (although stenoses in veins are rare), urinary tract etc. Further, a Stenosis is also defined mathematically as a % narrowing: Stenosis = Plaque area / IEL CSA * 100%

Chapter 1 Historical background/Literature review

1.1 Cardiovascular diseases

Cardiovascular diseases are the major cause of illness and death in the US. These include diseases and deaths from pathological alteration of the coronary, carotid, and renal arteries that supply blood to the heart, brain, and kidneys respectively. Because of the severity, frequency, and early onset, diseases stemming from blockage of the coronary arteries have been most extensively studied, followed by those stemming from the carotids. Renovascular disease can produce hypertension and end stage renal failure, and is associated with a high mortality rate [1]. However, the renal arteries themselves have been the object of less study. Renal artery stenting has recently been gaining ground as a modality for treatment of renal artery stenosis or blockage. Apart from hypertension, reduction in kidney function and a concomitant reduction in the size of the kidneys can result from stenoses that are of a severity greater than 60% [2].

The late seventies saw a new treatment design in the battle against cardiovascular disease. Until then, arterial blockage was usually treated with bypass surgery, wherein a vein—typically from the patient's own leg—was extracted and then used to channel the flow of blood around the blocked area through a bypass vein graft. For complete blockages and for multiple vessel blockages, this procedure is still the procedure of choice. However, for blockages that are restricted to one vessel and which still are able to maintain partial blood flow, balloon angioplasty, in which a balloon is snaked through the arterial bed with the aid of a guide wire, was successfully used for the first time in the late seventies. With good post-operative results, this procedure started to gain widespread usage.

Another procedure that had been tried since the sixties is stenting, where a tube is used to 'hold' the blocked artery open. Early results with the stent were not very encouraging, partially because the tube was solid—this prevented the supply of blood to the wall propped open—and partially because the stents caused a significant thrombus, or clot,

formation. With the advent of better designs and more hemocompatible materials, the eighties saw a renewed interest in these devices that has persisted till today. Stents are now combined with balloon angioplasty to provide a reliable and effective treatment for arterial blockage. However, restenosis, or *re*-development of a blockage over time, continues to be a problem. The process of restenosis is not completely understood. Biologic factors that respond to the mechanical insult caused during stenting are almost certainly involved. Stents are, however, more effective than the use of PTA or percutaneous transluminal angioplasty, or treatment of blockage with an inflated balloon, alone. Although, PTA and endovascular stenting both effectively relieve vascular stenoses [3], making their use in the coronary arterial tree routine, recoil and other phenomena, especially in ostial atherosclerotic lesions, limit the utility of angioplasty [4], and have increased interest in stenting [5]. For example, it is known that the ostial lesion often responds suboptimally to balloon angioplasty [6]. It has thus been proposed that all ostial stenoses may be successfully treated with stenting [7].

Extension of stent technology to ramifying branches, complex arterial lesions and other vascular beds may not be straightforward. For example, the effectiveness of these approaches in treating ostial atherosclerotic renal artery stenoses is limited. The carotid arteries pose dilemmas of their own by virtue of their morphology and their support of critical flow to the brain. The renal and carotid arterial systems provide a wonderful contrast to the coronary vascular bed for examination of critical elements in stent biology and design.

Arteries of different vascular beds are structurally diverse, reside in a range of milieus, are exposed to an assorted set of biochemical signals and are subject to variable loads. When considering the impact on the structural integrity of endovascular implants, all of these issues become important. The dimensional and structural heterogeneity of different arterial beds were studied to understand whether different design criteria might be required for stents in different vascular beds. Some researchers have shown that stenting as applied to different vascular beds produces different disease states and responses. For instance, Lankeren [8] has cited other authors as showing that stenting of the iliac arteries

is a satisfactory alternative to surgery, but of debatable benefit in the femoropopliteal arterial tree. If biologic effects can be assumed to remain constant across different beds, then it can be hypothesized that the difference in geometry and material parameters is a causative factor in the different types of responses seen. It is hoped that the disparate approach that has been taken so far in analyzing stenting in different types of arteries can be replaced by a unifying set of ideas delineating the different beds.

The goal of this thesis is to look at differences between the response of different arterial beds to stenting, as well as to look at design issues that optimize the use of stents in specific beds. Finite element techniques were used throughout the thesis to provide quantitative data on the issues involved. Closed form solutions, independent of the finite element technique, were also developed. It was found that considering the stent as a mesh of thermal shell elements defined on the inner surface of arteries modeled as tubes is not a useful technique for modeling stent expansion in arteries.

Although arterial walls are mechanical structures with corresponding material properties, and they have been modeled as such, they are as much if not more biologic structures that respond dynamically to any applied boundary conditions. Remodeling is one aspect of this response that has been postulated to have a biologic basis to mechanical insult [9]. Thus, it is clear that the biologic and mechanic properties are coupled, and their effects on each other cannot be neglected.

As mentioned above, not all stenoses may be suitable candidates for stenting or even balloon angioplasty. Severe or complete blockage of an artery or severe blockage that is not restricted to one artery generally disqualifies a lesion bed for either procedure. As shown by Ohki et al [10] in an ex vivo model, more embolic particles are produced in stenoses that are of a severity greater than 90% compared with lesser stenoses. For these reasons, stenoses chosen in this thesis were given an upper limit of approximately 90%.

1.2 The structure of the arterial wall

The artery can be divided into three main sections or tunics: the tunica intima comprised primarily of endothelial cells and a smattering of smooth muscle cells, the tunica media, an orderly arrangement of packets of vascular smooth muscle cells separated by elastic sheets or lamina and the outermost compartment of loosely packed fibrous material and interdigitating vessels and nerves, the tunica adventitia [11]. The most dense elastic laminae separate the media from the other compartments and they are labeled the *internal* and *external elastic laminae* respectively. (Fig. 1).

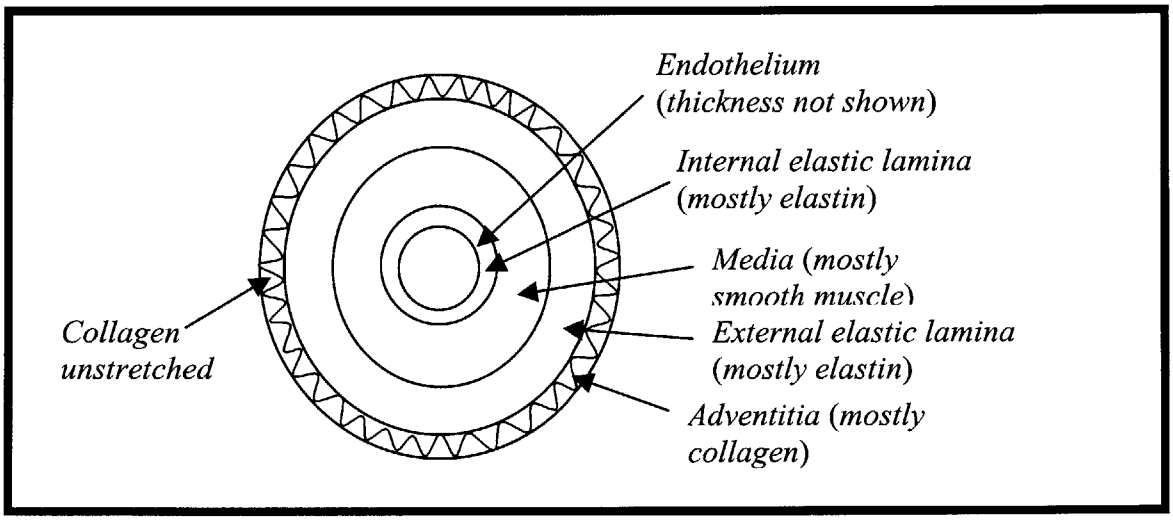

Figure 1 ***The arterial wall (not to scale).*** **Shown is a conceptual representation of the arterial wall. There is a wide variation in the relative thicknesses of the layers shown depending on the location in the vascular tree (with even the endothelium which in the normal vessel is one-cell thick becoming thicker (neointimal hyperplasia). Also, the elastin within the media occurs in bands. Adapted from Tickner [11].**

The arterial wall is therefore essentially arrays of smooth muscle cells supported by a network of connective tissue, and as the bulk of these cells are in the media it is this compartment that is most important for normal arterial tone.

The intima does not contribute significantly to the mechanical stiffness of the artery directly [12], until significant smooth muscle cell migration and proliferation can create a hyperplastic intimal lesion as a proliferative response to arterial trauma. The cells of the connective tissue synthesize, and break down, the macromolecular components. The components of the tissue outside the cell are termed the extracellular matrix. This is made up of fibrous and non-fibrous material (page 2, Silver, [13]). The fibrous part can be either collagen or elastin. Collagen essentially prevents the tissue from overextending and provides stiffness at high strains, while elastin is the component that is the energy storing component in the tissue. Finally, in addition to cells and connective support, which give shape and mechanical support to the blood vessel, the tissue also contain a significant amount of water and ions in hydrostatic equilibrium with the interstitial space (Page 7, Silver, [13]).

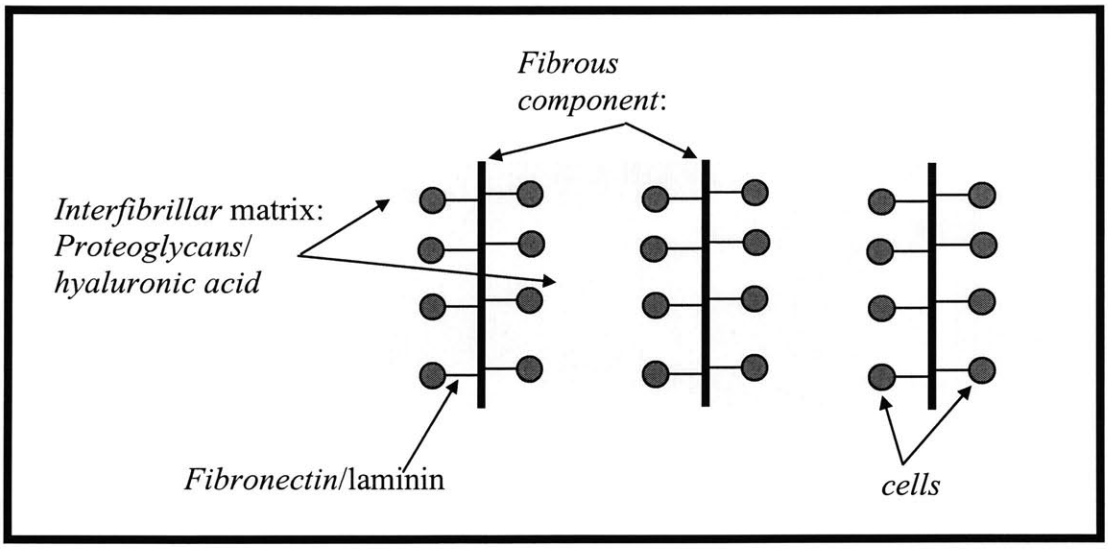

Figure 2 ***connective tissue conceptualized.*** **Depending on the 'resistance' in the interfibrillar matrix, the connective tissue can be of varying extensibility. For example, the interfibrillar matrix that makes up paper has a high level of friction to the fibrous components making paper very stiff (in its plane) [13]. The fibrous component provides the strength to the tissue (perhaps similar to steel in reinforced concrete)**

The high stiffness of collagen itself comes from the high content of the amino acid proline in collagen and the three-dimensional alignment of collagen fibers. The nonfibrous component of connective tissue is the interfibrillar matrix. As its name implies, it is found between the fibrous components of the tissue. It is made of hyaluronic acid and proteoglycans. The interfibrillar component binds the fibrous parts together and prevents friction between the fibers (page 3, Silver, [13]). The cells in the matrix are either attached to the fibers or are in close proximity to the fibers. The figure above gives a conceptual representation of the different tissue components.

When stenting is performed, the arterial wall mounts an orderly and coordinated response that includes reaction to both the balloon apposition force during stent inflation and the pressure applied by the stent during and subsequent to stent placement.

The arterial wall as depicted above is quite conceptual. Other than histology, no one way of looking at the arterial wall presents a complete picture. To look at the arterial wall in vivo, one either uses angiography or IVUS (intravascular ultrasound). Each emphasizes a specific element of the blood vessel wall. Angiography, for example, involves the radiological imaging of an artery after injection with a radio-opaque dye. While there is precise discrimination of the lumen and its contours angiography shows nothing of the vessel itself, and atherosclerotic lesions are *inferred* from the negative image they leave within the lumen.

In contrast, intravascular ultrasound (IVUS) provides excellent morphological data. The media appears hypoechoic while the adventitia is echoreflective [14]. This form of vessel layer property measurement has been shown to give an accurate representation of the vessel wall [14]. IVUS, however, is not a reliable technique for measuring the media thickness [14] as it is difficult to tell where the media ends and the plaque/intima begins. Changes in EEM cross sectional area, or the whole area—including the media, plaque and lumen—subtended by the plaque, are used as markers of enlargement of the vessel. Stents are highly echoreflective and show up clearly on IVUS [15]. The ultimate determinant of vessel morphology is histologic section. The internal elastic lamina or

IEL, for example shows up clearly. Fibrin, which is not differentially echoreflective in IVUS, and therefore does not show up in IVUS, stains differently
in the IEL from the surrounding wall material.

1.3 Thesis Outline

Above the treatment of the context and background for this work has been given, as has been given the general structure of the arterial wall. Chapter 2 looks at arterial mechanics as well as other assumptions on the boundary conditions that are relevant to arterial loading. These will help explain the conditions that were chosen as part of this study. Chapter 3 gives a description of the methods used, the experiments/simulations that were performed. Chapter 4 gives the results that were obtained. Chapter 5 deals with the discussion of results, and finally chapter 6 is a discussion of future work that is relevant in continuing this work.

Chapter 2 Theory / Assumptions

The following chapter presents some of the theoretical underpinnings of the analyses that were carried out. The general issue that this thesis deals with is interventions that lead to alleviation of the blockage in arteries. Thus, to start with, section 1 presents a correlation of the structure with the mechanical properties of the arterial wall to any loading. To gain an understanding of the arterial response to stenting, it must be realized that stenting can be of different types and the arterial response can vary depending on the stent type used. Section 2 therefore talks about the two general classes of stenting that are performed. The next two sections, remodeling, and compensatory enlargement deal with the arterial response to injury and/or restenosis. This response is mostly biologic. The next four sections deal with issues that are more mechanic and less biologic in modeling the arterial wall (although the two biologic response issues mentioned previously can and do change the mechanic factors). The section on structural loads gives the theory behind stent fatigue analysis, and the final section develops the equations relevant to the closed form analysis of the different arterial beds.

2.1 Arterial Mechanics

Analysis of arterial mechanics has a rich and long standing history. As far back as 1808, Thomas Young, after whom we have termed the modulus that describes the stiffness of a material [16], wrote of the various fluidic issues involved in the flow of blood through the circulatory system [16]. Since that time many have described critical elements in the arterial response to stress and strain. The mechanical properties of the artery are captured through the response of the two components that provide the majority of the mechanical resistance to deformation: elastin and collagen. Elastin is a flexible material that is responsible for the resistance at low strains. Collagen is much tougher. However, it is packed in a coiled structure such that at low strains it provides no resistance. As the coils expand out, collagen starts to resist deformation.

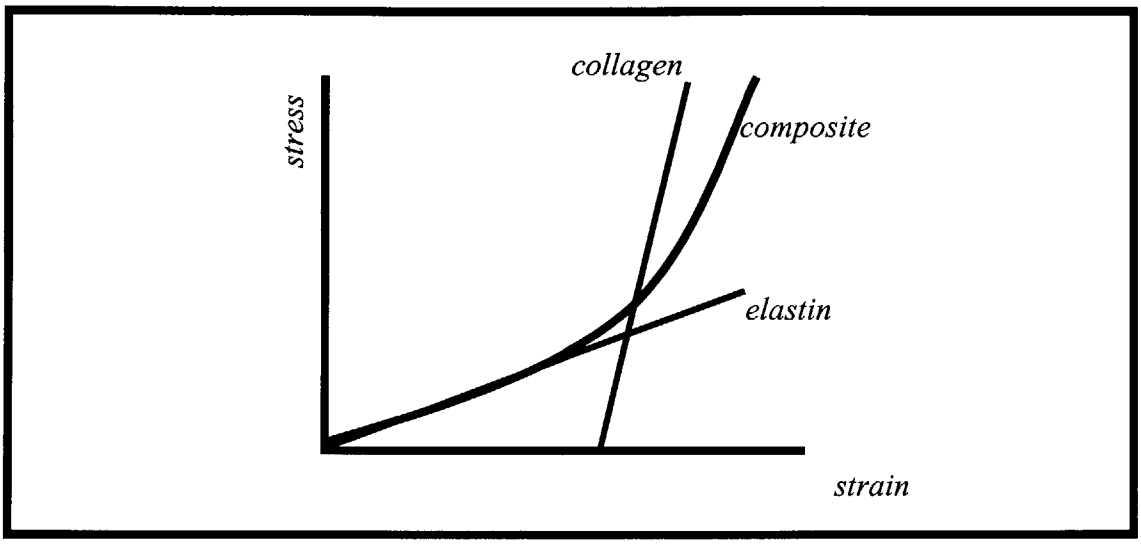

Figure 3 ***The arterial stress-strain characteristics.*** **The non-linear composite response of the arterial wall can be modeled as the superposition of two linear responses from for example, elastin and collagen. Elastin is the restorative element, and collagen is the element that prevents overextension.**

This can be appreciated from the coiled collagen in the adventitia (Fig. 1). It is because of the different responses at two different strain ranges that the arterial response to stretch is non-linear [17], [18] (Fig. 2). As can be seen, if small strain differences that are either at the low or the high end are imposed, linear properties can be assumed. This is the rationale behind a linear assumption by most investigators. Arterial mechanical properties can also vary depending upon whether the artery is muscular or elastic.

With the above background, the question arises: what is the best way to model the arterial response to loading or stretch? Should a fully non-linear, transversely-orthotropic, and hyperplastic assumption be used, or can simpler characteristics be assumed? Because the properties of the arterial wall change with large strains, investigators often forego the more complex analyses for simpler , and perhaps more intuitive analyses, assuming that as long as they are within a narrow range of strains, the simpler assumptions are valid. The idea of using an "incremental" quantity was perhaps first proposed by Krafka, who also showed that the response curve for an artery is a superposition of two responses [19].

Often, for lack of data on the more complex models, investigators are forced to stay with simpler models.

2.2 Stent types

In general there are two types of stents: self-expanding and balloon-expanded. Within these two broad categories are endless variations. Self-expanding stents are placed using a system similar to the one shown below (Fig. 4) in which a spring-like stent is inserted at the site of occlusion. Both stents are placed by the use of a catheter that is snaked through the arterial tree through an appropriate incision—usually at the groin. Self-expanding stents are typically made of nitinol which is a temperature dependent memory allow. It can be made to 'remember' what shape it had at the time of its formation under a given temperature. Once the nitinol self-expanding stent is placed at the site of occlusion, and as the sheath that covers it is removed, it starts to regain its memory at the body temperature and expands. Or the stent can simply be made of a spring-like material that expands as the stent sheath is removed.

In older designs, once the stent was partially expanded inside the arterial lumen, it was impossible to reposition the stent. However the Magic Stent allows the partially deployed stent to be recovered and repositioned (Kutryk, [20]). There are other issues such as non-uniform appositional contact between the stent and the arterial wall as the stent is expanded that give this stent a disadvantage vis-à-vis the balloon expanded stent. A balloon expanded stent is simply plastically deformed with the help of a compliant or non-compliant balloon so that it molds to the arterial configuration.

Such plethora of designs has prompted the obvious question: does stent type influence the outcome? In the United States, treatment has been limited to the use of balloon-expandable stents [21].

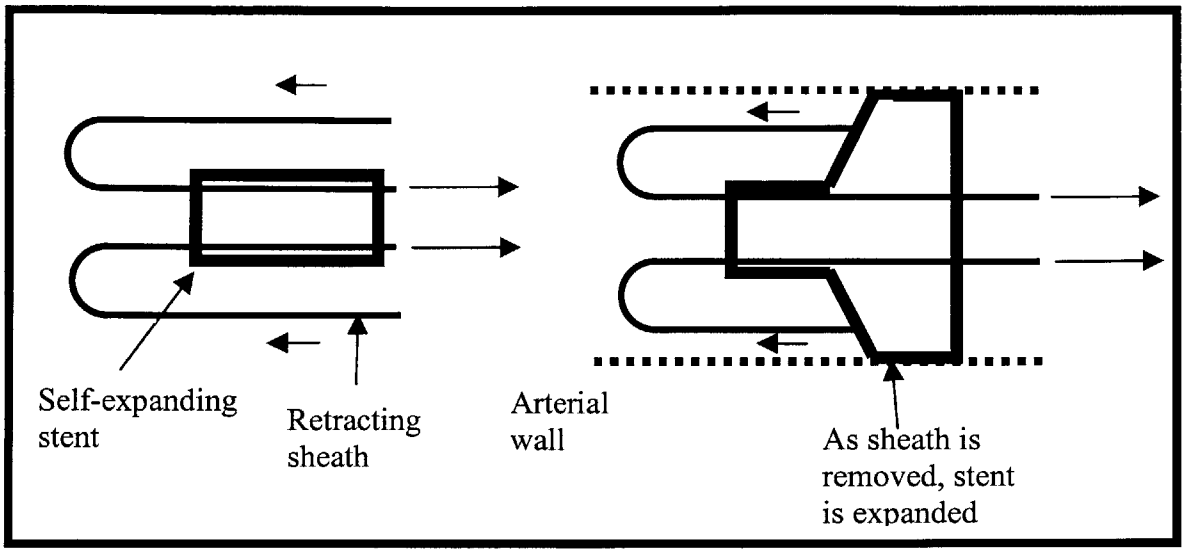

Figure 4 *A self-expanding stent being deployed.* The left figure shows the sheath that covers the stent being retracted. On the right is shown a partially deployed stent. The thick rectangle on the left is the undeployed stent. As the sheath encasing the stent is retracted by being pulled to the right (the right arrows in the left figure), the upper part of the sheath that covers the stent moves left and exposes the stent. The uncovered stent then because of its springiness or its temperature memory opens out. The figure on the right shows the stent in the process of being deployed, and therefore the left half of the stent is still in the original position being held in place by the sheath covering it.

Let's look at why balloon-expandable stents are the design of choice in the US. Balloon-expandable stents that are expanded using a non-compliant balloon obtain in the artery a constant displacement boundary condition, while the self-expanding stent simply comes to rest at an equilibrium dictated by the balance between the force that the stent imposes on the artery and the stress with which the artery resists this force. Thus, it is harder to control the displacement that the self-expanding stent obtains in the arterial wall. Further, if the plaque is fairly incompliant, the self-expanding stent may not be of much use at all if its force of expansion on the artery is lower than the plaque resistance. Thus, a self-expandable stent may provide for more uncertainty in the outcome of the stenting procedure.

However, having said this, one study with animals [21] has reported a "greater late gain" (which means that over a period of time which is not acute, there is a greater increase with lumen size in the self-expanding stent) with the self-expanding stent. This could be because the self-expanding stent obtains a higher level of 'compensatory enlargement' in the arterial wall. The next section (section 2.3) talks about the possible mechanism. The uncertainty in the use of the self-expanding stent in acute outcome vis-à-vis its putative long term benefit may however limit its utility.

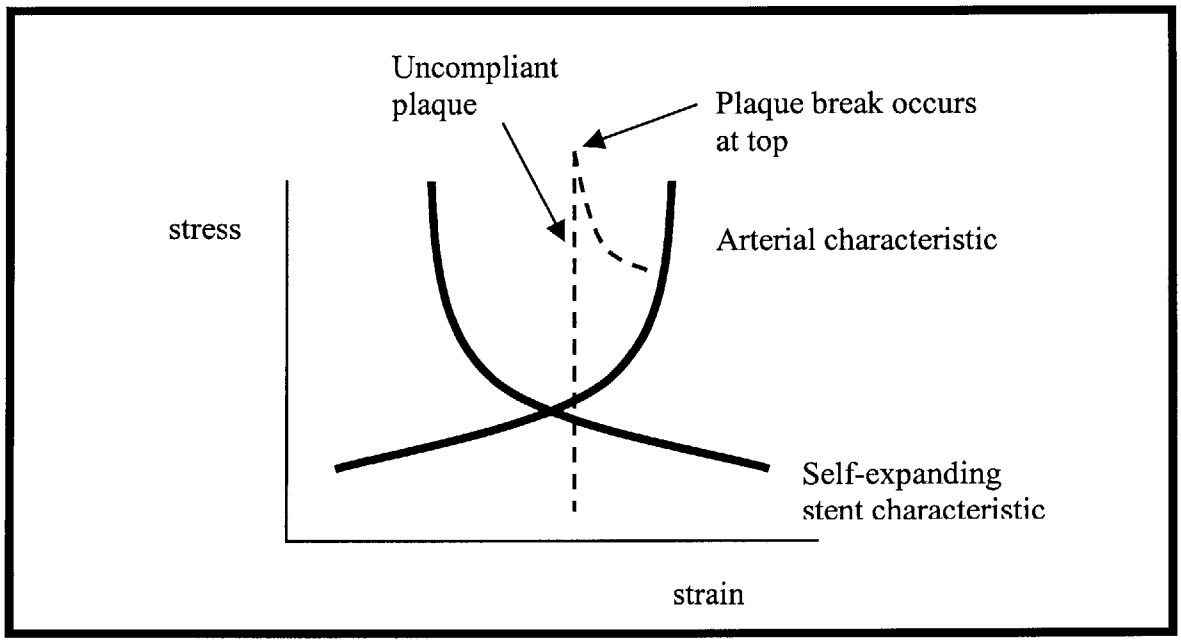

Figure 5 ***A conceptual representation of balloon vs self expanding stents.*** **The left curve shows the self-expanding and the right the arterial characteristic. The dotted line is a tough plaque representation.**

This can be made clearer by looking at Figure 4. As shown in Figure 29 in Chapter 4, the self-expanding stent characteristic shows an approximate exponential decline, while the arterial wall from Figure 3 shows an approximate exponential increase. Stenting an arterial wall that follows this profile with a self-expanding stent will produce a point of equilibrium shown by the intersection of the two solid curves in Figure 4. However, if the resistance in the arterial wall comes from a tough plaque, the arterial characteristic will look more like the dashed line. A self-expanding stent if it does not input a force greater

than the peak of the plaque characteristic will fail to obtain any expansion in the arterial wall.

2.3 Remodeling

It has been observed that lack of compensatory mechanisms and/or constriction of the vessel wall [8], [22] may play a bigger role in restenosis (post angioplasty without stenting) than neointimal hyperplasia. Remodeling is the term used to describe any and all changes that are attendant within the arterial wall with changes in boundary conditions: hypertension, changes in wall shear, angioplasty, stenting, etc. Remodeling itself can be constrictive or dilutive (compensatory enlargement). One of the ways that stenting may provide better outcomes is through its ability to restrict recoil [14] in the artery—or rather stop it altogether. As discussed next, stenting creates one form of 'compensatory' enlargement where the compensation is forced upon the arterial wall. Not much is understood about the mechanism of recoil or constriction or compensatory enlargement.

Is compensatory enlargement possible with stenting? The answer may depend on the type of stent that is being studied. As the artery remodels in response to the stresses imposed by the stents, a self-expanding stent will continue to impose a radial force, while a balloon-expanded stent simply holds the artery in place. The balloon-expandable stent will 'stop' pushing on the artery once the artery relieves the stresses imposed at the new equilibrium radius through either material addition or through a change in its compliance.

There are two different paradigms involved: a balloon-expanded stent is expanded to the "correct" diameter desired, while a self-expanding stent is hopefully sized and selected such that it helps the artery obtain its final "correct" diameter with gradual radial push. The difference is one of acute and gradual recovery of the patent lumen.

Perhaps the ability of a self-expanding stent to effect increases in diameter with time is a result of compensatory enlargement. The artery in response to the self-expanding stent

somehow 'gives' such that the diameter increases, and it 'gives' slowly over time—the definition of compensatory enlargement. This in one sense gives credence to the mechanical theory of compensatory enlargement—because it is a mechanical event that the enlargement that is seen is a result of. One may then ask why the response is not instantaneous—in other words, why does the artery not instantly expand with the force applied by the self-expanding stent? First, it may be instructive to look at the mechanical theory behind compensatory enlargement.

Oniki [23] has proposed a purely mechanical basis for compensatory enlargement. The rationale behind this proposal is that a mechanical basis is simpler. It is also supported by other events that are seen in compensatory enlargement—for instance, compensatory enlargement is seen early in the stenosis process when the adventitia has room to grow. It is usually not seen later in the process of stenosis formation. The mechanical growth is seen simply as an increase in diameter with the material addition that occurs circumferentially. This increase in circumference (and therefore diameter) can only be seen if there is circumferential addition of material. It will not be seen with radial addition.

Viscoelasticity effects may answer the question raised in the paragraph previous to the one above. Also material addition itself takes time as the biologic response manifests as a material addition. The artery may simply take its time in 'responding' to the applied stresses. Material addition in the circumferential direction effects a change in diameter because it applies additional stresses that the artery needs to resolve to maintain equilibrium with own 'ability' to resist deformation. Radial addition does not have this effect. Rather if anything, it would lower the stresses.

The animal model results that seem to show that self-expanding stents are superior to balloon expanded stents [21] may then validate some of the other findings that have been reported [24], [25], [26]. A balloon expanded stent, because of its inherent inability to compensatorily enlarge (because it doesn't push on the arterial wall) may then have a larger propensity towards higher restenosis compared to a self-expanding stent. As the

artery responds to a mechanical insult or injury with neointimal hyperplasia, the self-expanding stent is able to counter this with an outward expansion.

Perhaps in a balloon-expanded stent, the material addition occurs primarily in the radial direction. Because no 'push' is applied with a relieving of stresses in the arterial wall, no circumferential addition of material can result as an instance of neointimal hyperplasia. The only material that can be added is radial. This analysis then perhaps refines the concept that bigger is better [27]. Perhaps the gain in vessel diameter that is obtained can be more effectively achieved with a consistent and slow push on the arterial wall (as seen in a self-expanding stent) versus that obtained quickly with a balloon expanded stent.

Another study in pigs has shown that self-expanding stents follow the arterial contour as it expands and constricts with the blood pulsatile pressure while balloon expanded stents detach during the expansion [28]. This may also play a role in the greater neointimal hyperplasia seen with balloon-expanded stents.

As mentioned in section 2.3 however, the uncertainty in the acute response to self-expanding stents may limit their usefulness.

2.4 Compensatory enlargement

Glagov was perhaps the first to discuss the importance of a compensatory enlargement of the stenotic vessel [29]. As the lumen narrows with the buildup of plaque within it, a compensatory mechanism within the artery through a pathway not understood [23] tends to bring the lumen size back to its original level by expanding the artery outward. Furthermore, this compensatory mechanism is only able to bring the vessel back to its patent lumen size for stenoses that are no larger than 40%. In this case stenosis is defined as the ratio of plaque area to the original lumen area. The lumen area is the area subtended by the internal elastic lamina. Compensatory enlargement of the vessel has been extensively studied in the coronaries, but is also present in the carotids [30] and may be present in the renals [31] and other arteries.

It has also been observed that after balloon angioplasty, the ability of the vessel to undergo compensatory vessel enlargement, rather than solely its neointimal response may be responsible for restenosis in a hypercholesterolemic rabbit model [24]. In another study [25], it was shown that in diabetics there is a reduced propensity for compensatory enlargement, and that this is the cause of coronary artery stenosis in such patients. It is known that diabetic patients have a higher propensity of developing atherosclerotic disease [32]. Understanding the process of compensatory enlargement may lead to a better understanding of restenosis and also may lead to more effective treatments for atherosclerosis.

2.5 Material composition of the plaque

It has been hypothesized that plaque composition is a better determinant of a plaque's rupture potential than its size [33]. Those plaques that are at risk of rupture contain "a soft, lipid-rich core that is covered by a thin and inflamed cap of fibrous tissue. Compared with intact caps, the ruptured ones usually are thinner and contain less collagen (responsible for tensile strength), fewer smooth muscle cells (the smooth muscle cells synthesize collagen synthesizing), and many more macrophages (collagen degrading cells)" [33]. Lendon et al also showed that macrophage density correlates with a decrease in the strength of the atherosclerotic plaque cap [34]. Lipid lowering therapy has been shown to reduce the occurrence of cardiac events significantly [35]. Thus, lesion material properties are important in the study of atherosclerosis. But predisposition to rupture does not lead to rupture in all plaques. Extrinsic factors such as the circumferential stress at the plaque are also important in determining whether a certain lesion will rupture [36].

2.6 The zero stress state of the artery

Any elastic material that when stretched returns to its unstretched configuration if the stretching force or boundary condition is removed. Take for example an artery. An artery is made of elastic material which is mostly elastin. See section 1.2, the structure of the

arterial wall. If the artery is pressurized as it is when blood pressure is applied to the inside of the artery, the artery stretches. As the blood pressure pulsates about a mean, the artery expands and contracts.

In trying to determine the stresses and strains in a modeled system, it is important to start with the unstressed configuration as the baseline. Otherwise, the results will be off. For instance, if a stretchable material is already stretched, and then an additional stretch is applied, it would be incorrect to assume that the starting position had zero stress and strain. Similarly, in finding the stresses in an artery that is modeled as being expanded by a balloon or a stent, it is important to know what configuration of the artery corresponds to a zero stretch in the artery. Surprisingly, the unstressed state of the artery is not a circular tube with the blood pressure removed. This was shown by Fung [37] in the following way. If the closed tube configuration of the artery is unstressed, then if it is cut longitudinally, it should remain as it is, or at least the circumference should not decrease. The artery, however, when slit longitudinally assumes a slightly opened out state. This state is the zero stress state of the artery. Figure 6 makes this clearer.

To find the stress configuration of an artery, it is important to know its zero-stress state. However, in the simulations presented in this thesis, the in-vivo closed configuration was assumed to have a stress state of zero.

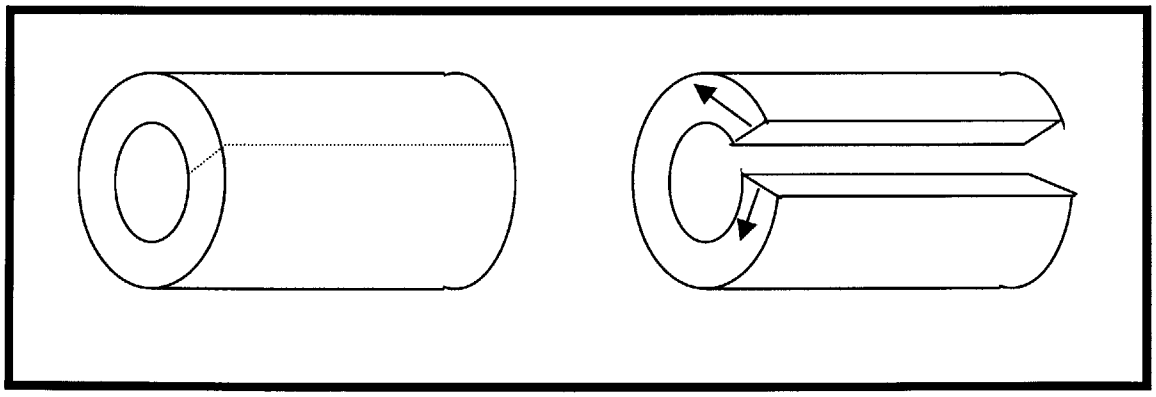

Figure 6 ***The zero stress state of the artery.*** **The artery when it is cut longitudinally opens out because of the pre-stress in the closed configuration. If there were no pre-stress in the vessel, it would not have opened out with the axial incision.**

2.7 The incompressibility assumption

The artery can be considered to be incompressible [38]. This is because the arterial wall is essentially made up of water. The assumption of incompressibility means that with any deformation imposed on the arterial wall (such as with stents), the volume of the artery remains constant. The constancy of the volume of the arterial wall is best expressed in terms of the Poisson's ratio. This is explained next. The discussion starts with the isotropic small strain case and extends to the isotropic large strain case. Finally, the incompressibility relationship is expressed for the orthotropic small strain case.

2.7.1 The relationship of Poisson's ratio to incompressibility: Isotropic case, small strain

An isotropic material is one whose properties are constant in all directions. Although an artery is not isotropic—it is transversely isotropic (a discussion of this is delayed till the next section, 7b)—a discussion of isotropic materials will serve as an introduction to the orthotropic case (see section 7b below). One familiar parameter that can vary in different directions is the Young's modulus, E. Another parameter that can vary is the Poisson's ratio, ν (the Greek letter 'nu'). Thus, in an artery wall with isotropic properties, E and ν are the same in any direction (see Figure 7).

It may be useful to derive what the Poisson's ratio value should be in the case of an isotropic incompressible material. In the following, strains are denoted by 'e'.

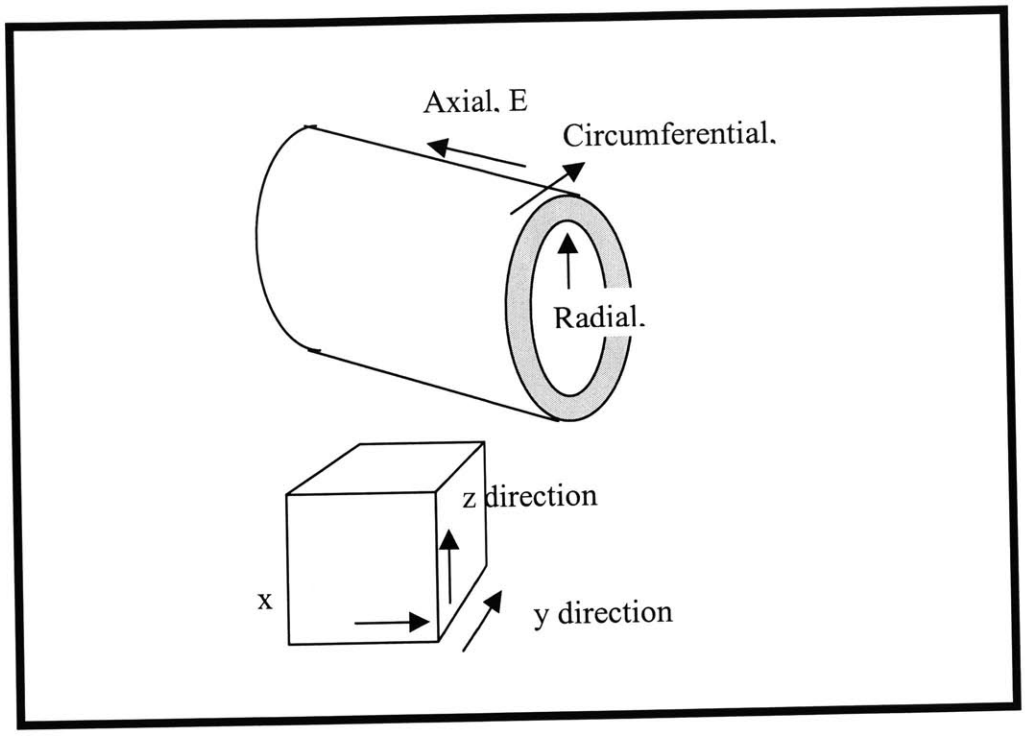

Figure 7 *Coordinate system term representation*. cylindrical coordinate system as well as the rectangular Cartesian system axes directions are shown in the top and bottom figures

Consider a cube of volume V = LWH that is deformed into a new volume

$$V_{new} = V + \Delta V = (L + \Delta L)(W + \Delta W)(H + \Delta H) \quad \text{.....(1)}$$

$$V_{new} = LWH + HL\Delta W + HW\Delta L + LW\Delta H + H\Delta L\Delta W + L\Delta H\Delta W + W\Delta L\Delta H + \Delta W\Delta L\Delta H \quad \text{.....(2)}$$

$$\Delta V = HL\Delta W + HW\Delta L + LW\Delta H + H\Delta L\Delta W + L\Delta H\Delta W + W\Delta L\Delta H + \Delta W\Delta L\Delta H \quad \text{..(3)}$$

$$\frac{\Delta V}{V} = \frac{\Delta W}{W} + \frac{\Delta L}{L} + \frac{\Delta H}{H} + \frac{\Delta L\Delta W}{LW} + \frac{\Delta H\Delta W}{HW} + \frac{\Delta L\Delta W}{LW} + \frac{\Delta W\Delta L\Delta H}{WLH} \quad \text{.....(4)}$$

For small deformations, the last four terms are nearly zero. This leads to:

$$\frac{\Delta V}{V} = \frac{\Delta W}{W} + \frac{\Delta L}{L} + \frac{\Delta H}{H} \qquad \text{.....(5)}$$

Or with,

$$\frac{\Delta W}{W} = e_x \ , \ \frac{\Delta L}{L} = e_y \ \text{ and } \frac{\Delta H}{H} = e_z, \text{ we get:} \qquad \text{.....(6)}$$

$$\frac{\Delta V}{V} = e_x + e_y + e_z \qquad \text{.....(7)}$$

For an incompressible material,

$$\Delta V = 0 \qquad \text{.....(8)}$$

Thus,

$$e_x + e_y + e_z = 0 \qquad \text{.....(9)}$$

Let us denote the stresses by σ. Now, since the material is isotropic, it will have the same Poisson's ratio, ν. The following is from [39]. For a load applied in the x direction, the following is obtained:

$$e_x = \frac{\sigma_x}{E} \qquad \text{.....(10)}$$

$$e_y = -\nu\frac{\sigma_x}{E} \qquad \text{.....(11)}$$

$$e_z = -\nu\frac{\sigma_x}{E} \qquad \text{.....(12)}$$

These are added up to get the total strain (due to a loading only in the x-direction),

$$\frac{\sigma_x}{E} - \nu\frac{\sigma_x}{E} - \nu\frac{\sigma_x}{E} = e_x + e_y + e_z \qquad \text{.....(13)}$$

But this is equal to zero. Thus, the following is obtained:

$$\frac{\sigma_x}{E} - \nu\frac{\sigma_x}{E} - \nu\frac{\sigma_x}{E} = 0 \qquad \text{.....(14)}$$

Or,

$$\nu = 0.5 \qquad \text{.....(15)}$$

For an isotropic material, this same relation can be obtained by setting the Bulk modulus to be much higher than the shear modulus [40]. This simply means that the material has a much higher resistance to changes in volume than it does to changes in shape [41]. This is what in essence is implied by incompressibility. Water has no resistance to changes in shape, but it has a high (but not infinite) resistance to change in volume. (The ratio of the bulk to the shear modulus is more important than their absolute values when we talk about incompressibility. Steel has a higher absolute resistance to changes in volume, but because its shear modulus (resistance to shape) is not zero, the ratio is not higher than water's [41]).

To obtain the same relation using the bulk-shear modulus criteria, we use the following relations:

Bulk modulus, κ, is given by,

$$\kappa = \frac{E}{3(1-2\nu)} \qquad \text{.....(16)}$$

Further, the shear modulus G, is given by,

$$G = \frac{E}{2(1+\nu)} \qquad \text{.....(17)}$$

Solving for E, from eq. 17 above follows the equation,

$$E = 2G(1+\nu) \qquad \text{.....(18)}$$

Substitute eqs.18 into 16 to obtain,

$$\kappa = \frac{2G(1+\nu)}{3(1-2\nu)} \qquad \text{.....(19)}$$

Or,

$$\frac{G}{\kappa} = \frac{3(1-2\nu)}{2(1+\nu)} \qquad \text{.....(20)}$$

For $G >> \kappa$,

$$\nu = 0.5$$

This is the classic constraint on the Poisson's ratio for as isotropic material. However, the above is valid only for small strains. Recall from equation 5 that we neglected higher order terms. For large strains, Poisson's ratio decreases, and this is explained next.

2.7.2 The relationship of Poisson's ratio to incompressibility: Isotropic case, large strain

The Poisson's ratio varies with strain with strain (Ward, [42], [43]). The following develops this in the isotropic case.

For an incompressible material Vold = Vnew;

$\lambda_x \lambda_y \lambda_z = 1$

For an isotropic material ν = constant in all directions

Vold = xyz

Vnew = xyz $(1+ex)^2(1+ez)$

(for isotropic material, ex=ey)

But Vold = Vnew

Therefore

Vold = xyz $(1+ex)^2(1+ez)$

xyz = xyz $(1+ex)^2(1+ez)$ .....(1)

1+e is the stretch ratio for small strain

In large strain analysis, $(1+2e)^{1/2}$ is the stretch ratio

It is seen that this collapses to 1+e for e small (neglecting second order terms)

$(1+2e)^{1/2} = 1+1/2*2e = 1+e$

So, if we use the large strain definition, we get

xyz = xyz $(1+2ex)(1+ez)^{0.5}$ .....(2)

Expanding 1 and 2 and setting nu = -ex/ez and ex = -nu (ez), and then collecting terms, we obtain the quadratic relations 3 and 4 respectively,

$(ez + ez^2)v^2 + (-2-2ez)v + 1 = 0$ .....(3)

$(4ez + 8ez^2)v^2 + (-4-8ez)v + 2 = 0$ .....(4)

These are then solved for different values of ez to obtain the variation of Poisson's ratio with stretch in one direction (z direction in this example).

Large strains are defined by:

$$e_x = \frac{\partial u}{\partial x} + \frac{1}{2}\left\{\left(\frac{\partial u}{\partial x}\right)^2 + \left(\frac{\partial v}{\partial x}\right)^2 + \left(\frac{\partial w}{\partial x}\right)^2\right\},$$

$$e_y = \frac{\partial v}{\partial y} + \frac{1}{2}\left\{\left(\frac{\partial u}{\partial y}\right)^2 + \left(\frac{\partial v}{\partial y}\right)^2 + \left(\frac{\partial w}{\partial y}\right)^2\right\},$$

$$e_z = \frac{\partial w}{\partial z} + \frac{1}{2}\left\{\left(\frac{\partial u}{\partial z}\right)^2 + \left(\frac{\partial v}{\partial z}\right)^2 + \left(\frac{\partial w}{\partial z}\right)^2\right\}$$

The shear strains have not been shown because by a suitable choice of coordinate axes, the strains above become the principal strains, and the shear strains vanish. In small strain analyses, all the second order terms are neglected.

Figure 8 below shows the variation of Poisson's ratio with strain. Appendix G gives the Matlab code used to extract the above plot. Next is shown how the Poisson's ratios are expressed for the orthotropic situation.

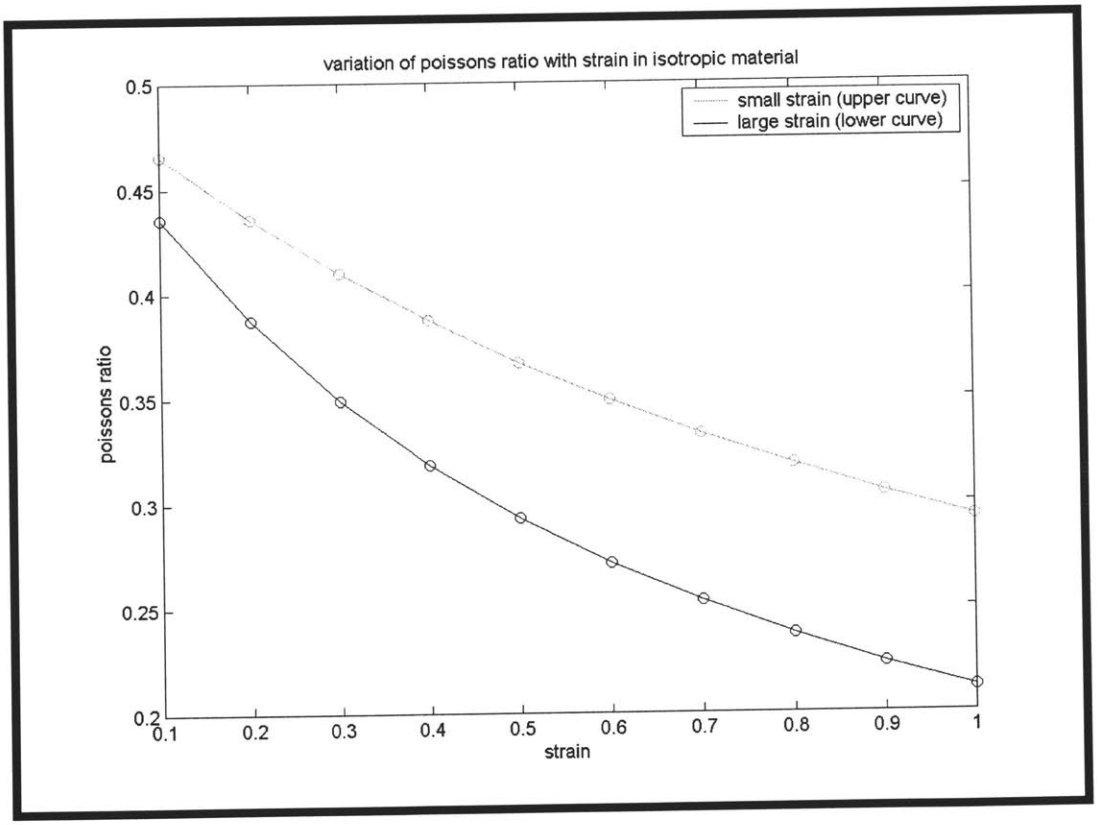

Figure 8 ***Poisson's ratio variation with strain in an incompressible material.*** **The upper curve was obtained through use of small strain equations, while the lower curve was obtained through the application of large strain analysis.**

2.7.3 Orthotropic Incompressible Poisson's ratio value constraints

An anisotropic material has different properties in all directions. It contains no plane of symmetry. Also, there is coupling between the shear modulus and normal stresses. An

anisotropic material can have as many as 21 different independent constants that need to be specified to characterize it.

$$\begin{bmatrix} \sigma_1 \\ \sigma_2 \\ \sigma_3 \\ \tau_4 \\ \tau_5 \\ \tau_6 \end{bmatrix} = \begin{bmatrix} C_{11} & C_{12} & C_{13} & C_{14} & C_{15} & C_{16} \\ & C_{22} & C_{23} & C_{24} & C_{25} & C_{26} \\ & & C_{33} & C_{34} & C_{35} & C_{36} \\ & \text{symmetric} & & C_{44} & C_{45} & C_{46} \\ & & & & C_{55} & C_{56} \\ & & & & & C_{66} \end{bmatrix} \begin{bmatrix} \varepsilon_1 \\ \varepsilon_2 \\ \varepsilon_3 \\ \gamma_4 \\ \gamma_5 \\ \gamma_6 \end{bmatrix}$$

A subset of an anisotropic material is an orthotropic material. This material has three planes of symmetry and there is no coupling between shear strains and normal stresses. This material is characterized by 9 independent constants as shown in the following matrix:

$$\begin{bmatrix} \sigma_1 \\ \sigma_2 \\ \sigma_3 \\ \tau_4 \\ \tau_5 \\ \tau_6 \end{bmatrix} = \begin{bmatrix} C_{11} & C_{12} & C_{13} & 0 & 0 & 0 \\ & C_{22} & C_{23} & 0 & 0 & 0 \\ & & C_{33} & 0 & 0 & 0 \\ & & & C_{44} & 0 & 0 \\ & \text{symmetric} & & & C_{55} & 0 \\ & & & & & C_{66} \end{bmatrix} \begin{bmatrix} \varepsilon_1 \\ \varepsilon_2 \\ \varepsilon_3 \\ \gamma_4 \\ \gamma_5 \\ \gamma_6 \end{bmatrix}$$

A further subset of this is a transversely isotropic material, in which one of the principal planes is a plane of isotropy. In this plane, the properties are the same in all directions (the axial-circumferential or θ-z (curved) plane in an artery). An artery falls in this category, with the axial-circumferential plane defining a plane of isotropy [44]. Five independent constants for a transversely isotropic case are obtained.

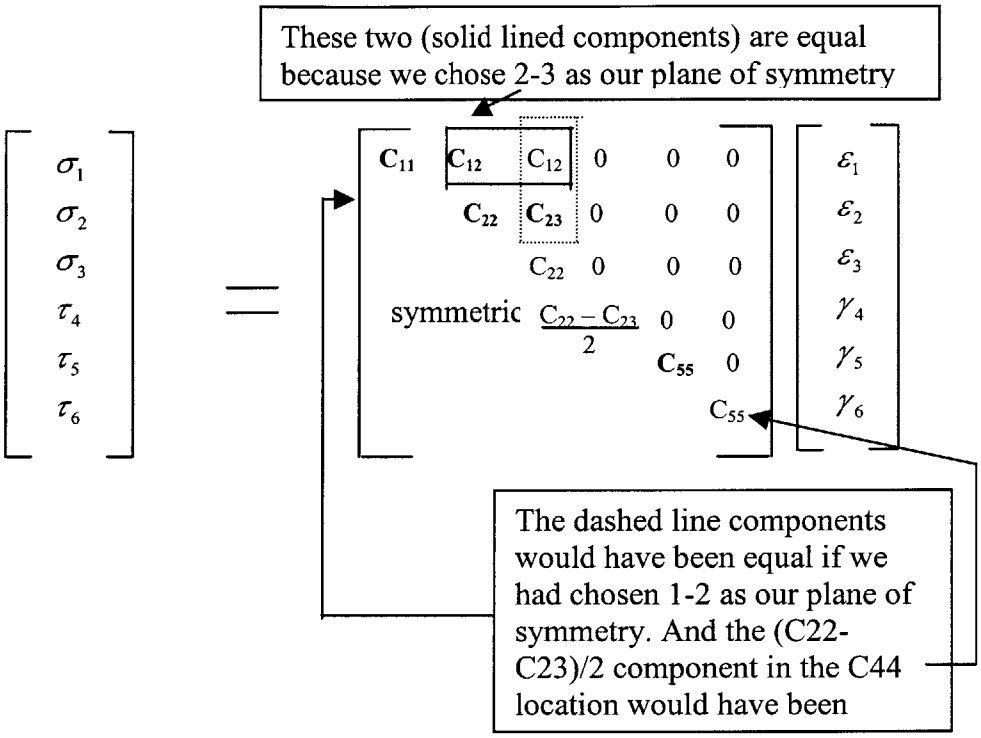

The independent constants are shown in bold. It is clear that there is no coupling between the normal stresses and shear strains.

2.7.4 ADINA—using orthotropic material properties

Although this study eventually discarded use of an orthotropic model in favor of an isotropic model, it is instructive to see how an orthotropic analysis can be carried out using finite element packages such as ADINA. It is presented here for completeness.

What have been shown above are the constants in the stiffness matrix. In short, the stiffness matrix is defined by C in the equation:

$$\sigma = C\varepsilon$$

where σ and ε are the stress and strain tensors respectively. The C matrix (or tensor) is related to the engineering constants E (Young's modulus) and ν (Poisson's ratio) in a

complicated way. However, the inverse of the C matrix, the compliance matrix, has a simple relationship to the engineering constants. The compliance matrix is given by S. It is shown here for a transversely isotropic material with the 2-3 plane defining a plane of isotropy (the plane in which all properties are the same in all directions—or the θ-z plane in the case of an artery ([44], Page 45)):

$$\begin{bmatrix} \varepsilon_1 \\ \varepsilon_2 \\ \varepsilon_3 \\ \gamma_4 \\ \gamma_5 \\ \gamma_6 \end{bmatrix} = \begin{bmatrix} S_{11} & S_{12} & S_{13} & 0 & 0 & \\ S_{12} & S_{22} & S_{23} & 0 & 0 & \\ S_{12} & S_{23} & S_{33} & 0 & 0 & \\ & & S_{44} & 0 & 0 & \\ \text{symmetric} & & & S_{55} & 0 & \\ & & & & S_{66} & \end{bmatrix} \begin{bmatrix} \sigma_1 \\ \sigma_2 \\ \sigma_3 \\ \tau_4 \\ \tau_5 \\ \tau_6 \end{bmatrix}$$

In terms of the engineering constants, the compliance matrix S is given by:

$$\begin{bmatrix} \frac{1}{E_r} & -\frac{\nu_{\theta r}}{E_\theta} & -\frac{\nu_{zr}}{E_\theta} & 0 & 0 & 0 \\ -\frac{\nu_{r\theta}}{E_r} & \frac{1}{E_\theta} & -\frac{\nu_{z\theta}}{E_z} & 0 & 0 & 0 \\ -\frac{\nu_{rz}}{E_r} & -\frac{\nu_{\theta z}}{E_\theta} & \frac{1}{E_c} & 0 & 0 & 0 \\ & & & \frac{1}{G_{\theta z}} & 0 & 0 \\ & \text{symmetric} & & & \frac{1}{G_{rz}} & 0 \\ & & & & & \frac{1}{G_{r\theta}} \end{bmatrix}$$

The 9 constants for orthotropic material properties are given below—there are equalities between these constants that give five independent constants (for the transversely isotropic artery):

$E_a = E_r$ (1^{st})

$E_b = E_\theta = E_c = E_z$ (2^{nd} and 3^{rd})

$\nu_{bc} = \nu_{\theta z}$ (4^{th})

$\nu_{ab} = \nu_{ac} = \nu_{r\theta} = \nu_{rz}$ (5^{th} and 6^{th}) .....(21)

$G_{ac} = G_{rz} = G_{ab} = G_{r\theta}$ (7^{th} and 8^{th}) and finally

$G_{bc} = G_{\theta z}$ (9^{th})

Where a, b, and c are coordinates in ADINA [45] and r, θ, and z are the familiar cylindrical coordinates with r being the radial coordinate, θ the circumferential coordinate, and z the axial coordinate. Calculation of the above parameters is given in appendix A.

2.7.5 Incompressibility—orthotropic material

The incompressibility requirement for an orthotropic material [39] is next derived:

For a force in the x direction:

$$\varepsilon_x = \frac{\sigma_x}{E_x}$$

$$\varepsilon_y = -\frac{\sigma_x \nu_{yx}}{E_y} \qquad \text{.....(22)}$$

$$\varepsilon_z = -\frac{\sigma_x \nu_{zx}}{E_z}$$

These are added up to get the total volume change as in 7 above to get:

$$\varepsilon_x + \varepsilon_y + \varepsilon_z = 0$$

Thus,

$$\frac{1}{E_x} - \frac{\nu_{yx}}{E_y} - \frac{\nu_{zx}}{E_z} = 0 \qquad \text{.....(23)}$$

Now, the same steps as in 21 above are carried out to get the strains from forces in the y and z directions to get the following two equations:

$$\frac{1}{E_y} - \frac{\nu_{xy}}{E_x} - \frac{\nu_{zy}}{E_z} = 0 \qquad \text{.....(24)}$$

$$\frac{1}{E_z} - \frac{\nu_{xz}}{E_x} - \frac{\nu_{yz}}{E_y} = 0 \qquad \text{.....(25)}$$

Add equations 22, 23 and 24, and take all the 'ν' terms to the right to get:

$$\frac{1}{E_x} + \frac{1}{E_y} + \frac{1}{E_z} = \left(\frac{\nu_{xy}}{E_x} + \frac{\nu_{xz}}{E_x}\right) + \left(\frac{\nu_{yx}}{E_y} + \frac{\nu_{yz}}{E_y}\right) + \left(\frac{\nu_{zx}}{E_z} + \frac{\nu_{zy}}{E_z}\right)$$

Setting terms with common coefficients on the LHS and RHS to get the incompressibility requirement on the Poisson's ratio in the case of an orthotropic material:

$$\begin{aligned} \nu_{xy} + \nu_{xz} &= 1 \\ \nu_{yx} + \nu_{yz} &= 1 \\ \nu_{zx} + \nu_{zy} &= 1 \end{aligned} \qquad \text{.....(26)}$$

Equations 26 give the orthotropic incompressible relations (the equivalent of the isotropic $\nu = 0.5$).

Patel [46] has obtained the Poisson's ratios for canine aorta. His reported values are (for the highest circumferential stretch ratio):

$$\begin{aligned} \nu_{r\theta} &= 0.79 \\ \nu_{\theta r} &= 0.59 \\ \nu_{\theta z} &= 0.27 \\ \nu_{z\theta} &= 0.21 \end{aligned} \qquad \text{.....(27)}$$

$\nu_{rz} = 0.72$

$\nu_{zr} = 0.41$

From [44] $\nu_{r\theta} = \nu_{rz}$. Also, from [44],

$$\frac{\nu_{r\theta}}{E_r} = \frac{\nu_{\theta r}}{E_\theta}$$

$$\frac{\nu_{rz}}{E_r} = \frac{\nu_{zr}}{E_z} \qquad \text{.....(28)}$$

$$\frac{\nu_{\theta z}}{E_\theta} = \frac{\nu_{z\theta}}{E_z}$$

Also, the condition for transverse isotropy gives:

$$\nu_{r\theta} = \nu_{rz}$$

All the above values cannot be reconciled with the condition for incompressibility given above. As a first approximation then, it may be relevant to choose values that ensure a positive definite stiffness matrix, as was done by Kamm in [47]. The stiffness matrix calculation is given in Appendix A.

However, in light of our analysis above which shows that Poisson's ratio varies with strain, it becomes unclear which Poisson's ratio value is in fact 'correct'. Kamm et al dealt with situations in which the strains were small—or certainly were small compared to our extreme strains. It is true that the arterial wall is not completely incompressible, and this may give the lower Poisson's ratio value. However, in light of our large strains, perhaps our Poisson's ratio may need to be further reduced, keeping in mind that the artery is not isotropic but is transversely isotropic.

The literature, as far as the author is aware of, has never reported any experiments that have measured the Poisson's ratio values for the large strains seen in stenting. Patel et al's classic experiments all dealt with small strain analyses.

The significance of requiring a positive definite stiffness matrix is that the strain energy for a given deformation should be positive. Thus if C is the stiffness matrix, and x is the deformation vector, then the requirement for positive definite stiffness matrix is simply that $\frac{1}{2} x^T Ax > 0$ (Page 18, Watkins [48]).

The ν's obtained from Patel's paper [46] are all incremental Poisson's ratios. The definition of an incremental quantity was first specified by Krafka [19]. An incremental modulus, for example, is the modulus created for an additional stretch produced on a specimen that has a pre-specified tension on it. In the artery, incremental quantities are typically calculated (rather than the regular quantities), because different components come into action depending upon the loading on the artery [19], [11]. The three components are the smooth muscle, elastin, and collagen (collagen comes into play at the highest loading).

The influence of the three different components causes the artery to have a non-linear strain response to increasing stresses. However, in this analysis, a linear constant relationship (which means that the Young's modulus as well as the Poisson's ratios will remain constant with the different strain levels) is assumed.

2.8 Axial stretch ratio of 1.5—explanation and discussion

Arteries in a normal male have a stretch ratio of 1.5 [49], [40]. This axial stretch exists not from the flow of blood but from the tethering that exists on the arteries [50], [41]. The fact that the artery is not in a zero state of stress with no flow imposition as also the fact that there is a constant (average) pressure loading because of the flow may perhaps also be causative factors in this value. An analysis was run to see what axial stretch is produced from the stent expansion. It was found that a uniform strain of around 8 was produced in the zz direction. This is much higher than the 0.5 strain from axial tethering. Based on this, it was decided to neglect the 0.5 axial tethering in the stented vessel.

Chapter 3 Materials, Methods

Six experiments were carried out. Experiment 1 characterized the force-displacement relationship for a self-expanding stent. Experiment 2 was used to find the recoil force of the artery on the stent. This was done to get order of magnitude comparisons on the forces set up by the stents vis-à-vis those set up on the artery from the blood shear and pressure fluctuations. Experiment 3 was used to find the stresses in different arterial beds from stenting. Experiment 4 was used to show the inapplicability of using thermal shell elements in modeling stent expansion in arteries. Experiment 5 comprised the simulations that were run on FEA models without the use of thermal shell elements, and that were also used in validating the analysis in experiment 3. Finally experiment 6 was the fatigue analysis that was carried out to see whether stents do in fact fail through fatigue.

Materials

All Simulations were run on PCs using ABAQUS (HKS, RI), ADINA 7.3 (ADINA R&D, Watertown, MA), and MATLAB (Mathworks, Natick, MA).

Experiments

3.1 Force-displacement (F/D) characteristic for a self-expanding stent

The experimental setup used is borrowed from Sawada et al [51]. A photograph of the setup is shown in Fig. 9 below.

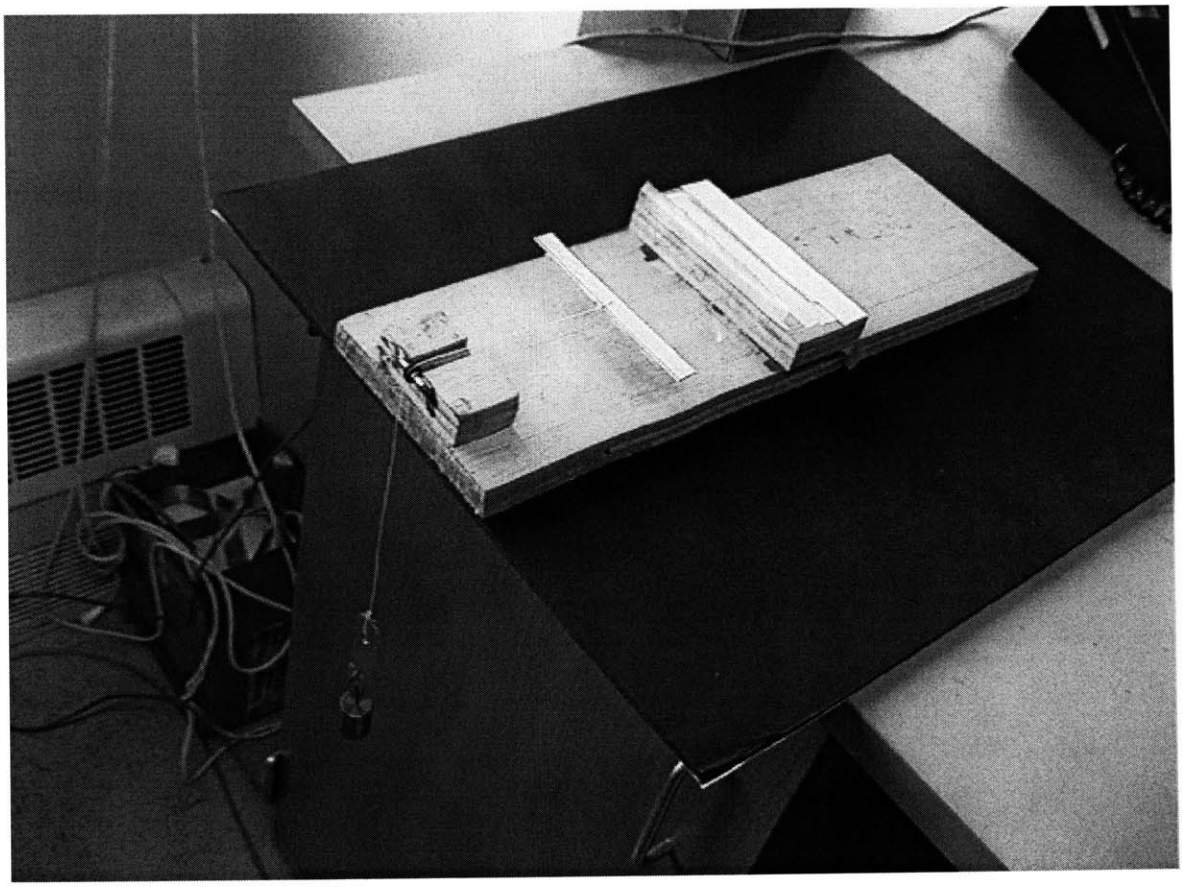

Figure 9 *Force-displacement analysis setup.* Photograph of the setup used to obtain the force-displacement characteristic for the self-expanding stent. The stent is placed within the cylindrical transparency (which in the above photograph looks white because of the lighting) at the left of the figure. As the force on the transparency is increased by adding weights on the pulley at right, the stent is pulled inwards

A plastic transparency was used to hold the stent in place. To obtain a more compliant material, the transparency was rubbed with another material with a high friction coefficient. Once an overall desired compliance was achieved, the transparency was cut up and attached as shown in the photograph in Figure 9 and the schematic in Figure 10. All measurements made were at steady state (in other words, transient effects such as might have come in from the pulley's own inertia were not relevant).

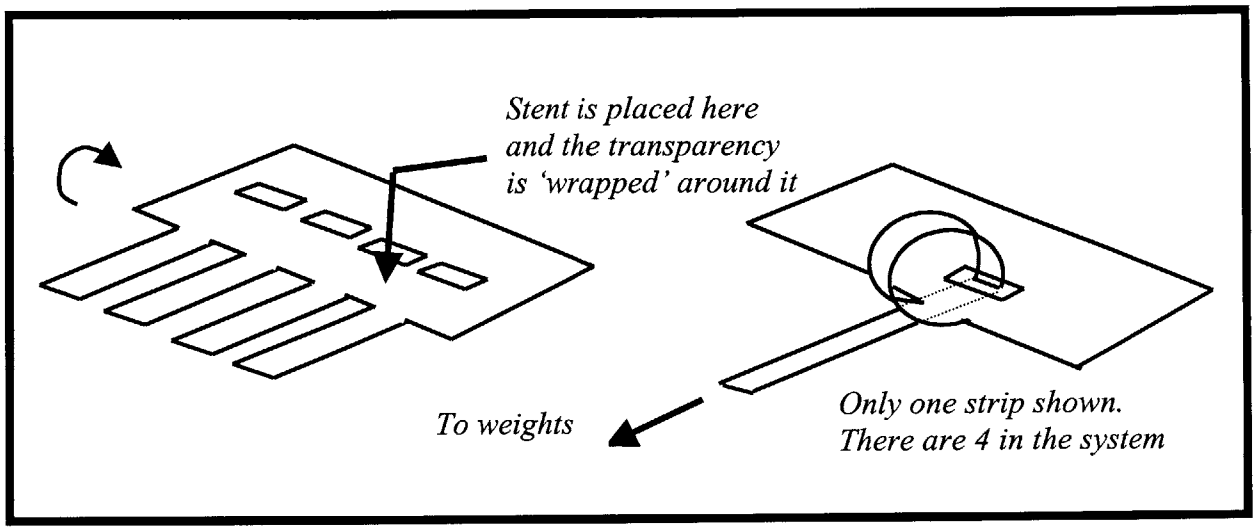

Figure 10 *Detail of the transparency set up.* The stent is placed within the curved section shown above. The flat section at the back is held while the strip (in the direction of the arrow) is pulled.

The force-displacement characteristics were measured with and without the stent in place. This was done because the transparency itself has a force displacement response. Both loading and unloading were measured to make sure there were no hysteresis effects (there weren't any). More data points were obtained with the stent as without for the simple reason that the transparency approaches a small and immeasurable circular profile far more quickly than the stent with the transparency does.

The two sets of data points were then plotted and curve fit both with an exponential equation and an equation from the literature derived by Loshakove [52]. The stent characteristics alone were obtained by subtracting the two curves obtained.

3.2 Recoil

In experiment 2, the acute recoil force of stent expansion was determined. Within a 1.3mm lumen modeling the renal artery (OD=3mm), a displacement of 1.5mm (which

brings the lumen size back to 'normal) was applied. The maximum stress was calculated. The rationale for determining this force was to see what magnitude differences exist between the forces on the artery due to the blood flow and the forces imposed by stents. The application of this displacement boundary condition in 3D analysis is not straightforward in ADINA. Direct application of displacements in 3D analysis is not allowed. This can be circumvented by use of a 3D shell element on the inner wall of the artery (explained next). Although this technique was discarded in the cross-sectional analysis comparing different arterial beds, it still gives an order of magnitude number on the acute recoil force on a stent.

To specify a displacement boundary condition, a shell element was created on the inside of the tube. This shell element had temperature dependent material properties. The shell element was given a temperature loading that expanded it (as a stent) to the opened up displacement of the artery. The bottom of the tube was fixed in all degrees of freedom to prevent rigid body motion.

The Young's modulus for the shell element (a finite element with no thickness) was set high so that there is no buckling, and the Poisson's ratio was set to zero to discard expansion in the directions not required to expand (the radial and axial).

3.3 Arterial Bed

Table 1 shows some of the assumptions that were made in the analyses, and problems attendant with those assumptions.

	Assumptions	Problems
1	*Membrane model (t<<r)*	*Fails when t is not small compared with r as in coronary arteries; does not apply to tapered vessels*
2	*Pressure constant in the curved artery which does not necessarily lead to a circular stent profile*	*In the real system, the stent forces the artery to obtain a circular profile*
3	Small strains	Most strains imposed cannot be considered small. This is not a serious problem because we are looking at differences
4	$Strain_{ave} = strain_{global}$	
5	Thermal shell element applies 'no slip' condition	This element imposes incorrect local strains
6	FEA	Curved vessel cannot be modeled using displacements.

Table 1 assumptions/ problems. This Table presents some of the assumptions that were made in the modeling along with their attendant drawbacks or limitations.

3.3.1 derivation of longitudinal and circumferential stresses in different types of arterial geometries

An artery is essentially a pressure vessel, where the internal and external pressures are different from each other. Any tube that is pressurized internally develops stresses in its walls.

In general, for a 3 dimensional system, three principal stress directions are relevant. For a symmetric pressure vessel, these are radial, longitudinal and circumferential stresses. That these three are the principal stresses can be appreciated from symmetry arguments. Consider a cylindrical section of a tube that has a constant pressure applied to its inside walls. The circumferential stress could in general be in any three directions: in the horizontal direction, in a direction with a vertical component (shown with the upward slanted arrow), or in the downward component arrow. Since the artery is symmetric, it is unlikely that the maximum will be differentially toward the top, because then it is just as likely to be toward the bottom (an observer from the top is equivalent to an observer looking from the bottom). Therefore, the most likely direction is horizontally outward.

Similar arguments lead to the axial stresses pointing straight up. The radial stress then is orthogonal to both of these stresses and points radially inward toward the cylinder axis.

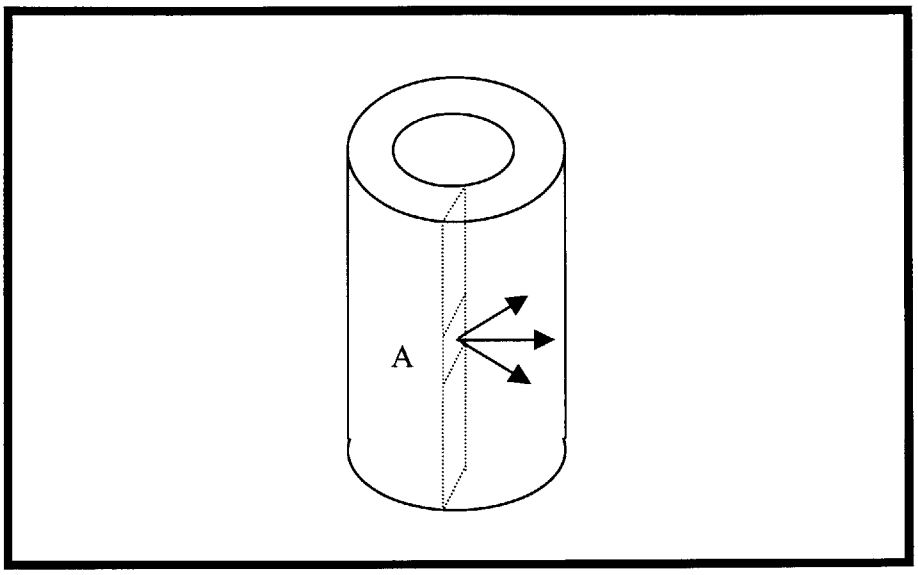

Figure 11 ***Direction of principal stresses in a cylinder.*** **In this figure the middle arrow represents the circumferential direction, and the upper and lower arrows represent directions at an angle to the circumferential direction. The principal stress is along the middle arrow. upper and bottom curves are equivalent, and therefore cannot represent the principal stress from symmetry arguments. From symmetry, both the top and bottom curves are equivalent.**

The circumferential stress is usually the largest stress component [53](Spence, pg. 20). The longitudinal stress component is zero for an open vessel. The arterial system is closed, however, and therefore shows longitudinal stresses. A free body diagram shows the longitudinal stresses in arteries.

In Fig. 12, thickness is t, and the internal radius is r_i. The pressure load is balanced by the longitudinal component of stress, σ_z.

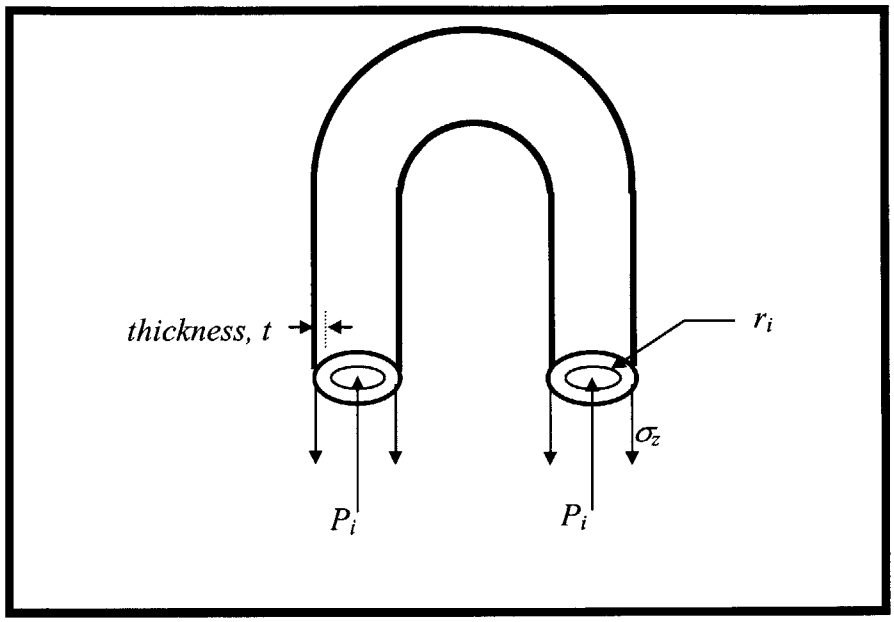

Figure 12 *derivation of longitudinal stresses.* The axial stresses (pointing down) are balanced by the pressure on the shaded area.

The pressure acts over the area, πr_i^2.

The longitudinal stress acts over the approximate area, $2\pi r_i t$ (for t small). Equating the forces set up by the stress and pressure, we get,

$P_i \pi r_i^2 = \sigma_z 2\pi r_i t$

or,

$\sigma_z = P_i r_i/(2t)$ ...(1)

or more correctly,

$\pi(r_0^2 - r_i^2)\,\sigma_z = \pi r_i^2 P_i$

$\sigma_z = P_i/(2t + t^2/r_i)$

which collapses to equation 1 when the thickness is small in relation to r_i

The above shows that even if a vessel is not "closed" in the sense of having a wall around it, but still is a closed system, such as a toroid, then there is a longitudinal component of stress equal to a system with closed walls.

The three different geometries studied were tapered, curved, and eccentric geometries. In obtaining the equations relating stresses to pressures in the tapered and curved vessels, a membrane assumption was made. In the case of the eccentric vessel, the Lamé equation for a thick-walled cylinder was used.

A constant strain boundary condition was found to be inappropriate in modeling stent expansion in different arterial beds. It is instructive to look at the effects of balloon expansion on the arterial wall, and how the applied boundary conditions translate to wall boundary conditions. In a concentric non circular vessel—what in other words we have been calling the normal vessel—the global strain corresponds to the local strain imposed at each point around the circumference. This will hold as long as the arterial wall responds equally at each circumferential point to an applied pressure. However, an eccentric vessel, by definition, imposes non-uniform circumferential resistance as does a curved vessel. Imposing a constant local strain, such as might be achieved form a temperature dependent thermal element, then incorrectly models the vascular wall's response to stenting. A temperature dependent element is an element whose length can be made to change through the use of a suitable coefficient of thermal expansion, α, and the application of a temperature. This can be seen from the following equation,

$$\varepsilon = \alpha T$$

where ε is the strain, and α is the coefficient of thermal expansion. T is the temperature.

Thus an equivalent pressure application may be more relevant than a strain application in the case of both a curved and an eccentric vessel. However, in the case of a concentric tapered vessel, the maximal strains, and therefore the maximal stresses occur at the lower end of the stented section. The median section should not show a deviation from the non-tapered vessel. These issues will be explained in more detail in subsections 2, 3, and 4 that follow and that deal with the boundary condition derivations.

Another issue that is relevant to stent expansion in arteries is the issue of shape. A balloon that expands in an artery obtains a circular cross-sectional profile, forcing the arterial inner wall to conform to this shape. It is not completely clear whether a constant pressure load—as in the case of an equivalent pressure—will model this behavior exactly. However, it is more accurate than the imposition of a constant strain. Finite element methods were used to obtain the correct shape and the correct global strains.

In the case of an eccentric vessel, application of a constant (local) strain gives us the maximum stresses at the thickest section. This is clearly not correct, as the maximum strains should occur at the thinnest sections—because this section would be expected to stretch the most with the application of a balloon assisted displacement.

Finite element techniques find their use in obtaining stresses in vessel shapes that are no longer restricted to simple tapered, eccentric, or curved independently. Also finite element methods can be used to test the hypothesis that stress contributions from each geometry found independently are superimposable in the case where the vessels assume a combination of the above geometries.

The following deals with the derivation of the equations dealing with each type of arterial bed:

3.3.2 Non tapered, concentric, straight (non-curved) vessels

Above, we derived the longitudinal stresses in a straight vessel,

$\sigma_z = P_i r_i/(2t)$

The circumferential stresses can similarly be derived to be:

$\sigma_c = P_i r_i/t$ ...(2)

The pressure P_i acts over the projected area of the inside hollow hemi-cylinder above. This area is given by $2r_i.(L)$. By equating the stress acting over the thickness to the pressure over the projected area, we obtain equation 2.

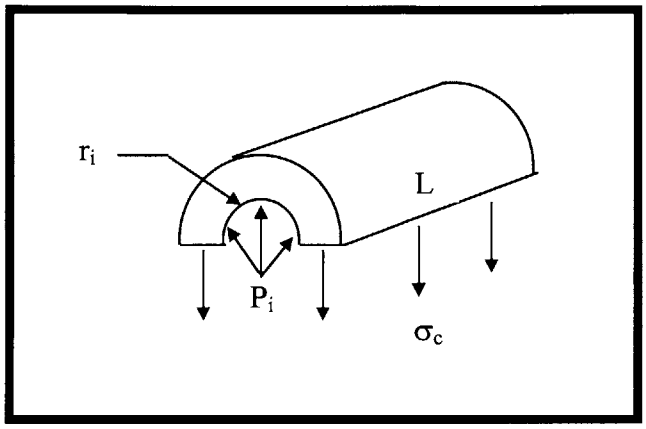

Figure 13 ***circumferential stresses in normal vessels.*** **As before, the pressure counteracts the circumferential stresses.**

The circumferential strain is related to the stress,

$$\varepsilon_c = \sigma_c/E - \nu\sigma_z/E \qquad \ldots(3)$$

Since we are dealing with the isotropic case, E and the Poisson's ratio are constant in all directions—in other words, they are axisymmetric. There is no term for the radial stress, because we are dealing with a membrane assumption, and as such radial stresses are zero.

Back solving for P_i by inputting a known strain gives the equivalent pressure that must be applied to the artery to obtain that strain. In a 'normal' vessel, strains don't vary circumferentially, and therefore the global strains and the local strain are identical. The stresses are then obtained by using the given pressure. Or alternately, a simpler way to do the analysis is to recognize that the circumferential stresses are twice the longitudinal stresses, and to set them so in equation 3, and obtain the circumferential stress for a given strain.

The pressure analysis was given above because it assumes importance in the case of a curved vessel where the local strain is no longer known as explained next:

3.3.3 Curved vessel

With the application of a constant pressure load on the inside of a curved vessel, the development of stresses around the circumference is first calculated. In this curved vessel case, it is no longer known what the local strain values are based on the global strain. This is because the stress around the circumference is now not constant (Figure 14). For a given pressure, stresses were calculated around the circumference of a transverse section of a curved vessel.

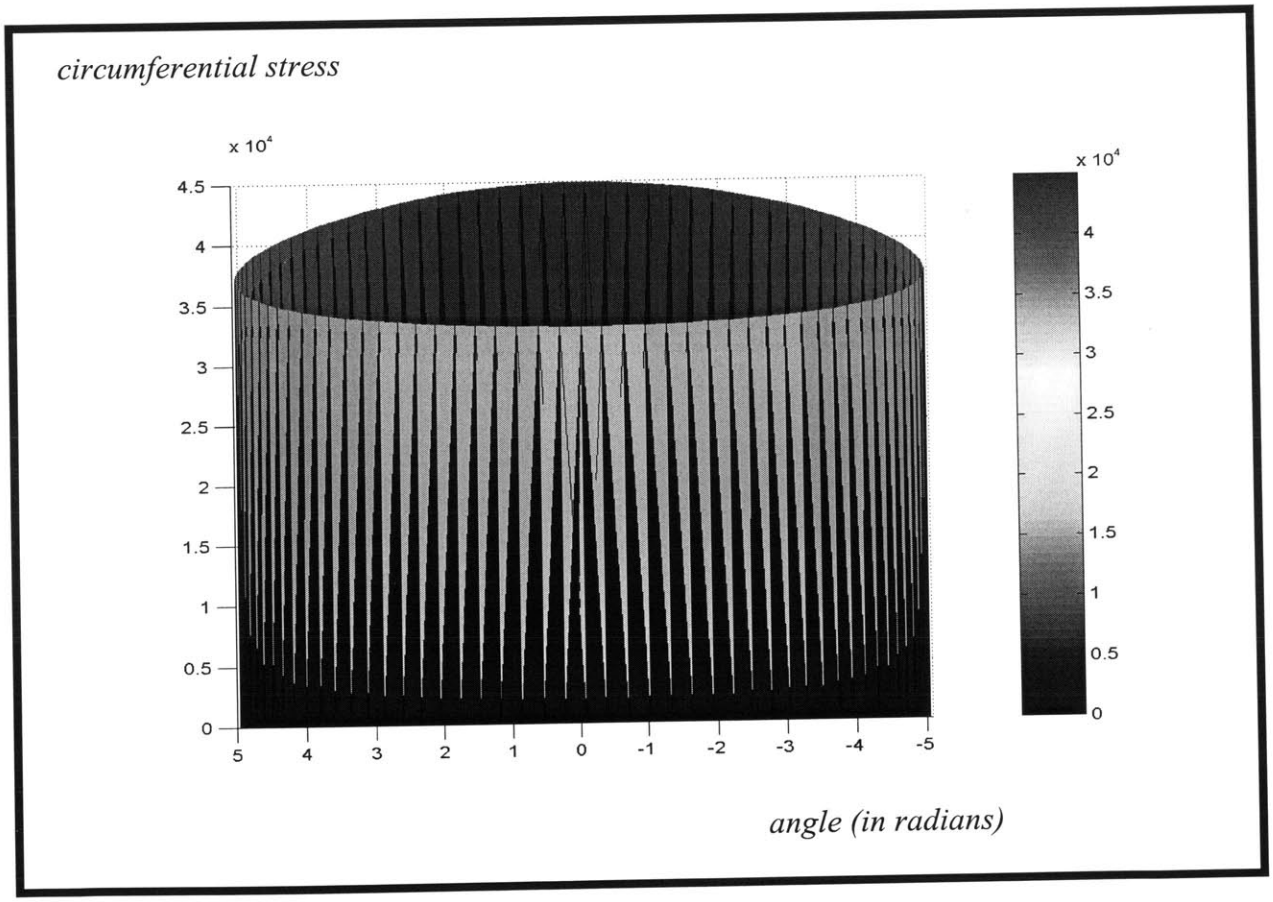

Figure 14 *Circumferential stresses in curved vessel.* As can be seen, two points (at right and left show the same stresses. The top and bottom points correspond to the max and min stresses.

The longitudinal stress, however, remains constant. Thus, the two stresses (circumferential and longitudinal) in this case do not have a two to one relationship. Therefore, it is not simply a matter of solving for the stresses directly in terms of strains.

The analysis chosen was to input a starting pressure, which was then used to solve for the local strains at 100 equally spaced points around the circumference. These strains were then averaged. If the average was lower than the required global strain, the pressure was increased. If it was higher, the pressure was decreased. The iterations were repeated until the error was below a specified value. The highest pressure occurs at the crotch point in a curved vessel (see figures 14 and 15). The strains, therefore, are expected to be the highest at such points as the curvature was varied. The Matlab file is given in appendix E.

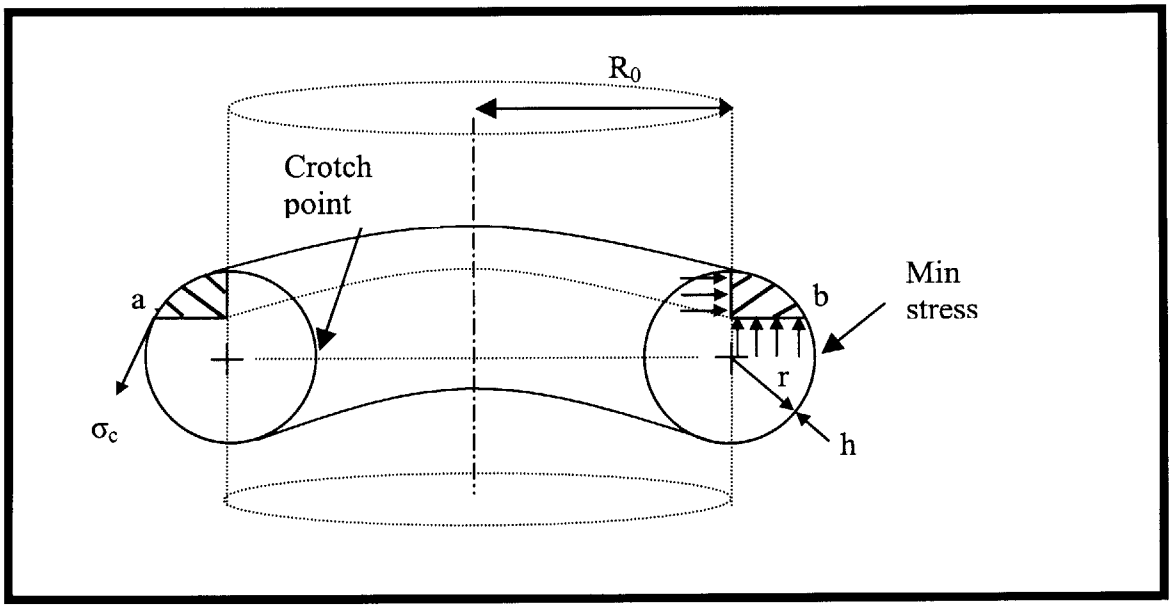

Figure 15 ***derivation of stresses in a curved vessel.*** **The free body diagram is used to obtain the circumferential stresses from a force balance (adapted from Harvey).**

In the figure above, a free body diagram was constructed by using a cylinder of radius R_0 cutting through the curved vessel. The vessel was then cut by a horizontal plane passing through the points a and b. By summing forces in the vertical direction, the circumferential stress can be calculated as given below. For a complete treatment refer to (Harvey [54]).

Another way this analysis could have been chosen is to use the equations for the two stresses in terms of strains directly in the stress strain relationship bypassing the pressure. The circumferential stress could have been solved for in terms of longitudinal stress, and this could have then been used to solve for local strains. The strains would then have been averaged as above, and the stresses varied until the strain was within a specified error. The circumferential stresses could then have been solved using the value of longitudinal stress at the crotch point. This analysis, however, would have been no less computationally intensive and perhaps less intuitive. The results would have been the same. For example, the circumferential stress is:

$\sigma_c = P_i r/(2h)*(2R_0+r\sin\theta)/(R_0+r\sin\theta)$

$\sigma_z = P_i r/(2h)$

Where h is the vessel wall thickness, r is the radius (for a membrane, it is not quite important which radius is used. However, in this analysis, the internal radius was chosen). R_0 is the radius of curvature, and θ defines the angle around the circumference as shown in the figure above.

3.3.4 Eccentric vessel

The eccentric vessel was analyzed by looking at the Lamé equations for a thick-walled cylinder (Wright, [55]). The derivation of the Lame equations follows next. Assuming transverse planes remain plane, the longitudinal stresses are forced to remain constant around the circumference. In the derivation, it is assumed that the tangential stresses on the two faces of the element are equal. This is not true for a general point in an eccentric cylinder. However, it holds at the line of symmetry, where the thickness is the biggest and smallest. Also, the center of the element in Fig. 16 is taken as the inner curve center. The derivations that follow are thus an approximation. The derivation that follows is from (Wright, [55]).

In the following, $\gamma = (r/r_i)^2$

On doing a force balance on the element shown, we obtain:

$\sigma_r\, r\, d\theta - (\sigma_r + d\sigma_r)(r + dr)d\theta + 2\sigma_t\delta_r \sin(d\theta/2) = 0$

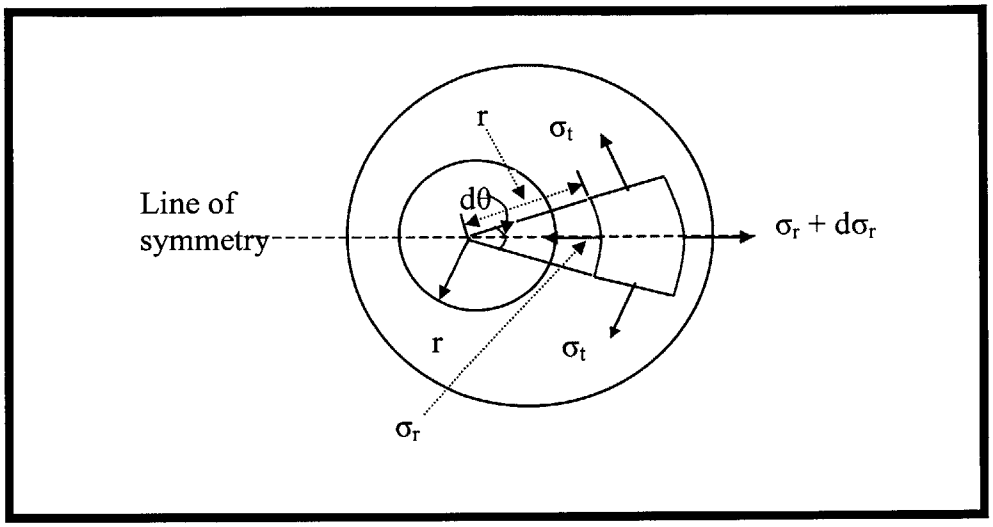

Figure 16 ***Derivation of eccentric stresses.*** **The center of the system is approximated to be at the inner circle center**

On expanding, and neglecting terms of order greater than 1, we obtain,

$(\sigma_t - \sigma_r)\, dr = r\, d\sigma_r$

...(1)

Assuming constant axial strain or e_a = constant (e = strain)

$Ee_a = \sigma_a - \nu(\sigma_t+\sigma_r)$ = constant (independent of r)

Since σ_a is also constant in the r direction, therefore,

$\sigma_t + \sigma_r = 2\sigma_m$, where σ_m is some constant

Now eliminate σ_t from (1),

$d\sigma_r / (\sigma_r - \sigma_m) = -2\, dr/r$

integrate w.r.t. γ to obtain,

$\sigma_r = \sigma_m - \sigma_v / \gamma$

where σ_v is another constant.

Using

$\sigma_r = \sigma_m - \sigma_v = -p_i$ at $r = r_i$, and

$\sigma_r = \sigma_m - \sigma_v / \gamma_0 = -p_0$ at $r = r_0$

we get,

$\sigma_m = (p_i - \gamma_0 p_0) / (\gamma_0 - 1)$ and

$\sigma_v = (p_i - p_0) \gamma_0 / (\gamma_0 - 1) = \sigma_m + p_i$

Thus, we obtain,

$\sigma_t = \sigma_m + \sigma_v / \gamma$

$\sigma_r = \sigma_m - \sigma_v / \gamma$ (either negative or zero)

$\sigma_a = \sigma_m$

It was assumed that the strains are linearly distributed from the thickest point (where they are the lowest) to the thinnest point (where they are the highest) for a given pressure. Thus, once the pressures for the same strain were found at the thickest and thinnest points, an average pressure was used in the analysis. The eccentricity was then varied and the average pressure at each value of eccentricity was then used to obtain the highest stresses in the vessel—found in the thickest sections. Appendix E contains the Matlab code that finds the maximum stresses as a function of eccentricity.

3.3.5 Tapered Vessel

A tapered vessel is different from both a curved section as well as an eccentric section in that the stresses are constant around the circumference. In other words, in a section with pure taper (and no eccentricity or curvature), the stresses are the same at any angle value for a given radius. A global strain applied at any point around the circumference then equals a local strain at any point. However, the situation is different axially. The same amount of displacement at one axial location produces a strain at one axial location that is different from the strain at another axial location. This is because the displacement is fixed. This is the case with a tapered stent that displaces equally at every axial point. In a

stent that is non-tapered, one has non-constant displacements of the arterial wall, but constant displacement in the stent. This type of stent forces the arterial wall to displace even further at the narrowest location. The ideal case arises in a set of stents that for any given taper can be sized such that the strains are constant axially. As we shall see in the following discussion, both the non-tapered and the tapered stents have the maximum strain (and therefore the maximum stress) at the thinnest or narrowest locations, with the non-tapered stent showing the higher strain. The author is not aware of any stent that displaces in such a way that the strains are constant axially.

The circumferential stress in a conical pressure vessel (thin membrane assumption) is (Harvey, [54])

$\sigma_c = pr/(h \cos \theta)$

where r is the internal radius, h is the thickness, and θ is the taper angle defined below.

The axial stress is given by,

$\sigma_z = pr/2(h \cos \theta)$

The axial stress is constant around circumference and is half the circumferential stress

3.3.5.1 Tapered stent in a tapered vessel

Now we derive the stress at the narrowest location in a tapered vessel when a tapered stent is input given the strain at the median location (it is assumed that the stent is sized such that the median location sees the input strain).

Given a strain at the median location m, and the taper angle, θ, we find the strain at the bottom location.

The circumferential strain is given by,

$\varepsilon_c|_m = R_2/R_1 - 1 = \varepsilon$ (say) ← at median location m

$\varepsilon_c|_n = R_6/R_5 - 1$ ← at bottom location n

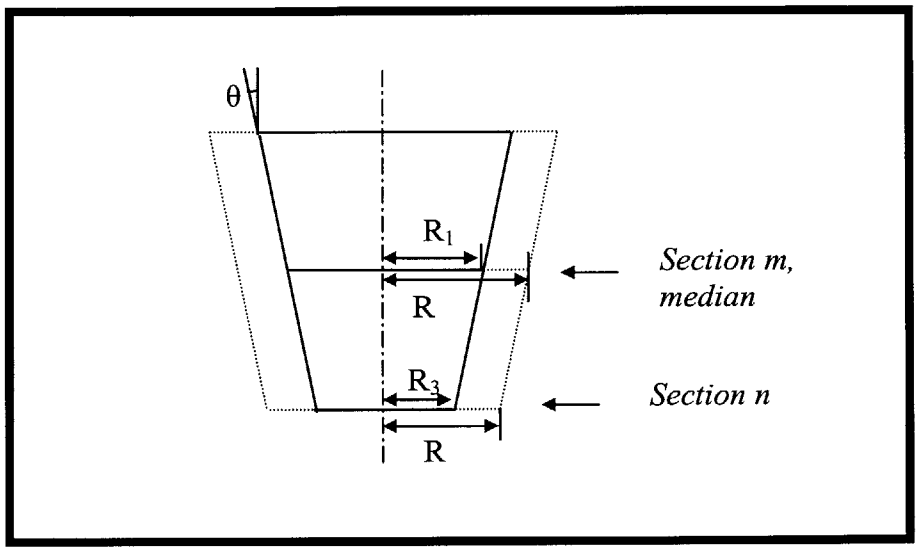

Figure 17 ***Tapered vessel, tapered stent.*** **Section being stented. Deformed shape shown by dashed lines. Wall thickness not shown. The stent is sized such that after it is expanded with the balloon, the middle section, m sees the known strains while the strain at section n will depend on the applied strain at section m along with the level of taper in the vessel wall.**

Now we need to obtain the strain at $\varepsilon_c|_n$ in terms of ε.

Now, in general,

$\varepsilon_c = \sigma_c / E - \nu\, \sigma_z / E$

But $\sigma_z = 0.5\, \sigma_c$

$\varepsilon_c = (2\, \sigma_c - \nu\, \sigma_c)/(2E)$

$\sigma_c = (2E\varepsilon_c)/(2-\nu)$ ... (1)

setting $\varepsilon_c = \varepsilon$ at median location, we get the stress at median location for a given strain ε.

$\sigma_c|_m = (2E\varepsilon)/(2-\nu)$

This is the same as the stress for the same strain in a strain vessel.

Now for a given strain at m, ε, we find the strain at the narrowest section in terms of ε. The stress at the narrowest point, n, is then simply obtain by substituting into the equation above

$\sigma_c|_n = (2E\varepsilon_c|_n)/(2-\nu)$

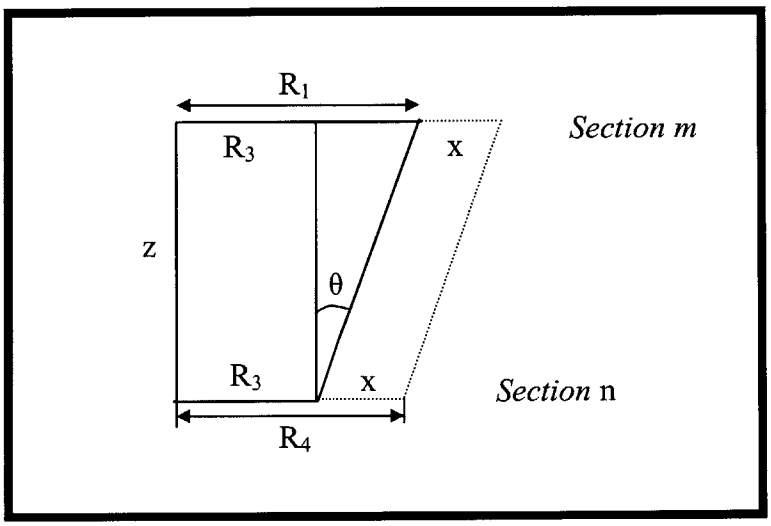

Figure 18 *tapered stent in tapered vessel (cut-away).* θ is the angle of taper. This figure shows that the inner wall (shown by the slanted dashed line) moves parallel to itself in a stent that is tapered. Thus both the middle section, m and the lower section, n see the same *displacement* and consequently a different *strain*.

$R_4 = x + R_3$

$\tan\theta = (R_1 - R_3)/z$

$R_3 = R_1 - z\tan\theta$

$\varepsilon_c|_n = R_4/R_3 - 1$

$R_4 = R_3 + x$

But $x = R_2 - R_1$

$R_4 = R_3 + R_2 - R_1$

$R_2 = R_1\varepsilon + R_1$ giving

$R_4 = R_1\varepsilon + R_1 - z\tan\theta$

$R_3 = R_1 - z \tan \theta$

$\varepsilon_c|_n = R_4 / R_3 - 1$, or

$\varepsilon_c|_n = R_1 \varepsilon / (R_1 - z \tan \theta)$

Putting the above into eq. 1, we obtain the needed stress in a tapered stent in a tapered vessel,

$\sigma_c|_n = 2E/(2\text{-}\nu) * [R_1 \varepsilon / (R_1 - z \tan \theta)]$

3.3.5.2 Non-tapered stent in a tapered vessel

Uptil equation 1 in the previous section, the derivation remains the same. The rest of the derivation is given below.

As before,

$R_3 = R_1 - z \tan \theta$

$R_4 = R_2$

$\varepsilon_c|_n = R_4 / R_3 - 1 = (\varepsilon R_1 + z \tan \theta)/(R_1 - z \tan \theta)$

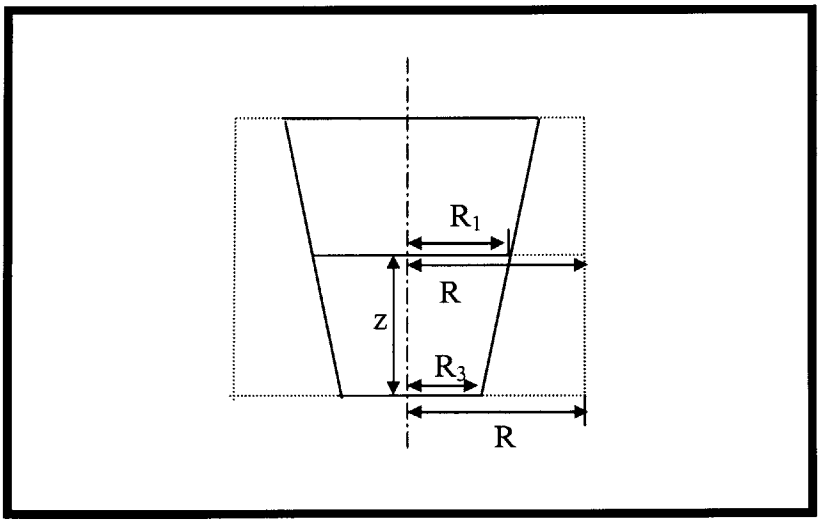

Figure 19 ***Non-tapered stent in a tapered vessel.*** **As before, only the inner wall is shown. The dotted lines are the internal artery profile post-stenting. In this case, the arterial wall does not move parallel to itself. Rather, it is forced to obtain a rectangular profile (because the stent being used is non-tapered.**

Finally we input this into eq 1 from the previous section to obtain the stress,

$\sigma_c|_n = 2E/(2\text{-}\nu)*[(\varepsilon R_1 + z \tan\theta)/(R_1 - z \tan\theta)]$

Since arteries have a varied level of taper, curvature, and eccentricity, these parameters were varied to get a range of situations. The definitions of taper, eccentricity, and curvature are given below. The curvature, C, is simply the inverse of the radius of curvature of the curved artery. The taper, T, is the change in radius over the change in length over which the radius change occurs, and E or eccentricity is the distance between the two radii over the outer radius of the artery.

The curved vessel bed was modeled as a simple curvature in the artery. The representative vessel had a cross sectional area of $\pi(R_1^2\text{-}R_2^2)$ where R_1 and R_2 are the outer and inner vessel radii, and these were chosen to be 5 and 7mm respectively. The representative tapered vessel had the same cross section at the center of the taper. The level of taper was chosen such that T was equal to 0.1 (this was then varied to 0.2 and 0.3). The eccentric representative bed had an eccentricity given by an intra-center distance of 1mm (the outer and inner radii were kept the same as in the normal vessel at 5mm and 7mm). Wall stress was determined for a range of values within the expected physiological domain.

The same cross sections were chosen for the different arterial beds to keep comparisons between sections meaningful (the area in any cross section depends only on the inner and outer radii, not their concentricity or eccentricity). The values of Poisson's ratio of 0.27 and E of 100KPa were chosen based on previous published work [47].

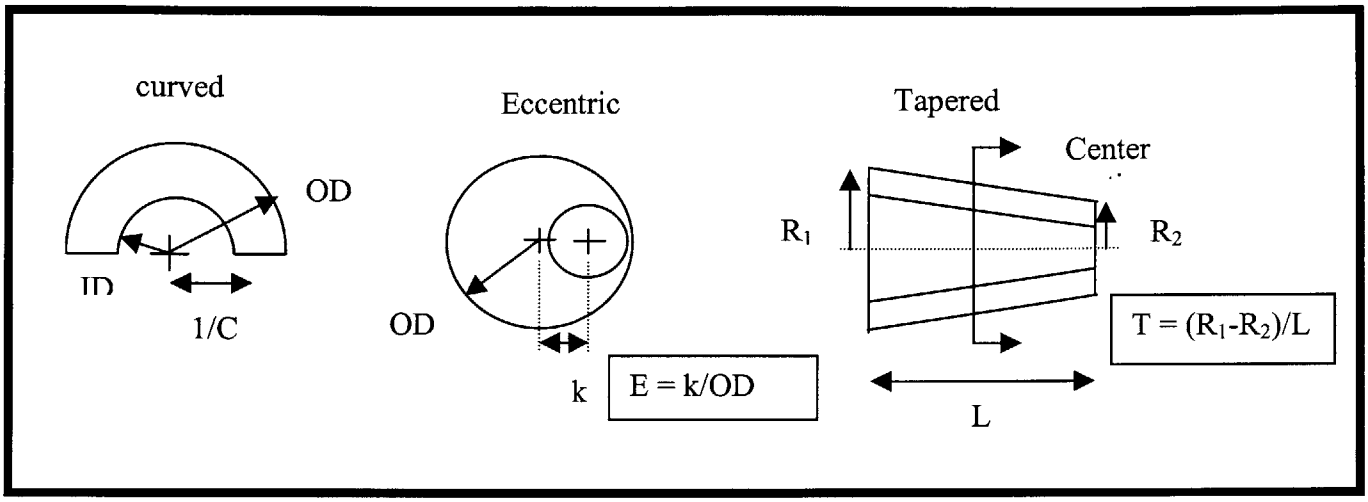

Figure 20 ***definition of C, E, and T (curvature, eccentricity, and taper).***

Arterial bed	Parameter (C, E, T)	% parameter variation
Curved	C = 0.08 0.06 0.05	50
Tapered	T = 0.1 0.2 0.3	100
Eccentric	E = 0.07 0.14 0.24	121

Table 2 variation in parameters. In this study, E, C, and T were given the above ranges.

3.4 The inapplicability of using thermal shell elements in modeling stent expansion within arteries

The stent was modeled by using a thermal stress element. At uniform temperature of unity, the strain and

coefficient of thermal expansion were 0.3 ($\varepsilon = \alpha\Delta T$)—a simple calculation shows that a strain of 0.3 correlates to a stenosis of 90% (a stenosis is a change in area of the lumen divided by the original lumen area). For all but the axial stress measurement, stresses were measured at the center arterial location to minimize errors from the axial expansion of the thermal element (the isotropic thermal element chosen creates both circumferential and axial stresses). The following figure shows the curved vessel with the thermal shell element and without the thermal shell element.

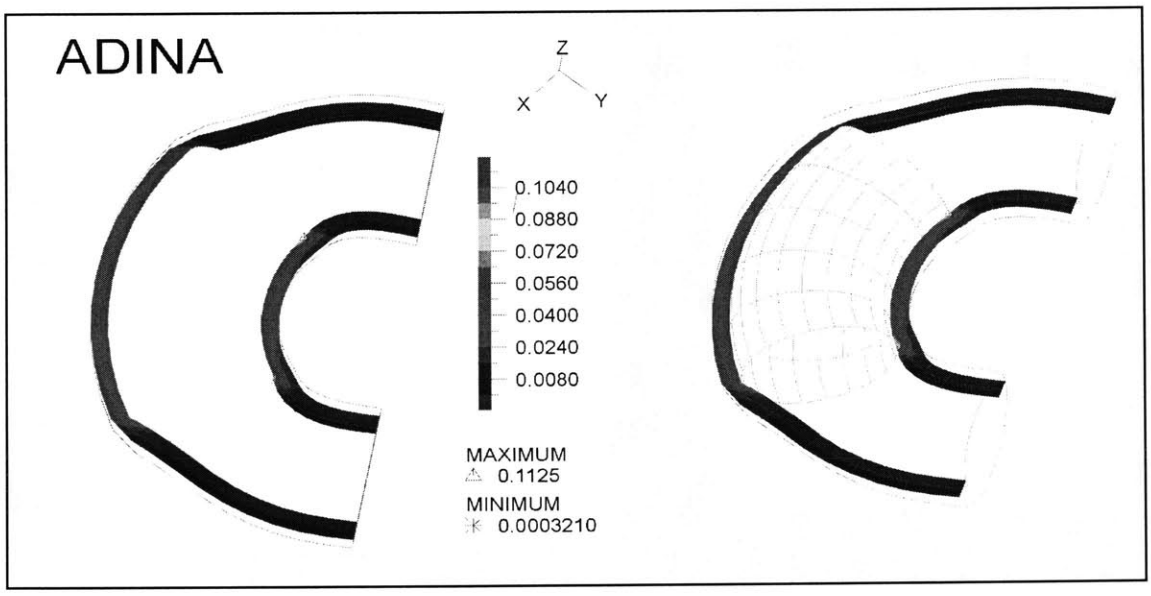

Figure 21 ***Finite element model of the curved vessel.*** **The two models show the results of stenting using a thermal shell element. The right figure shows the element explicitly.**

Curvature in the arterial bed was modeled by extruding a circular section through a 180 degree angle. The ends of the curved section were fixed in all degrees of freedom. A thermal shell element was then allowed to expand. The two sections shown are the same. The one on the right captures the stent-like thermal shell expansion, as well as the 3-D characteristics of the model—the sections shown are a cut in the xy plane. The artery was modeled with a 5mm internal radius and a 7mm external radius. The radius of curvature is 17mm. As can be seen above, the thermal shell element is fixed—in some ways glued—to the artery, and the strains that are locally input create unrealistic loading

conditions. The global displacements are known, giving known global strains. However, the local strains are certainly not known, and are to be solved for.

3.5 Verification of the eccentric vessel data using ABAQUS

As explained in chapter 6, discussion, the stresses obtained in the tapered vessels that are non-eccentric are exact. Those obtained for the curved and eccentric sections in the closed form analytic solutions, however, are not exact. There are thin membrane assumptions on the curved vessel, and the eccentric vessel suffers from the approximation that a thick vessel equation derived for an axisymmetric cylinder has been modified to fit the eccentric case. Further the stent profile is not necessarily circular with the use of a pressure boundary condition.

Stent expansion in the eccentric section was modeled using ABAQUS where the internal diameter is correctly sized and the internal profile is also circular. ABAQUS was used to construct a 2D model of an eccentric vessel. The dimensions in this model were made the same as in the closed form solution above. The intra-center distance was then varied to give 11 total data points (from zero eccentricity to an intra-distance of 1.5mm). Moreover, the stresses were the highest in the thinnest section. Thus, this technique is suitable for modeling stent expansion in a 2D model. The eccentricity was then varied and the circumferential stresses obtained. These numbers were then compared with the numbers obtained through the analytic closed form solutions.

One point on the inner circle in each iteration was fixed in the theta or angular direction (Figure 34 in discussion chapter). All other points were free to rotate. A boundary condition in the form of a 1.65 mm radial displacement was applied to the inner circle to model stent expansion in an arterial wall. The value 1.65 corresponds to a circumferential strain of 0.33 (the value chosen in all the analyses) as shown below:

$e_c = (C_{new} - C_{old})/C_{old}$

C = circumference

old and new refer to start and finish inner curve radii

This gives eventually,

$r_{new}/r_{old} = 1.33$

setting $r_{old} = 5$, we obtain $r_{new} = 6.65$

The change in inner radius then is 1.65

Although taper was also modeled using FEA, since the results from the closed form solution are exact, this analysis is not presented. The curved case, however, is quite different. To model a radial displacement in a curved vessel, one would have to create a curved axis that would be referenced by the cylindrical coordinate system under which the radial displacements are applied. There is no way that the author is aware of that a curved cylindrical axis can be defined in any FEA package. Perhaps a contact analysis may be used to bypass this limitation. However, because the closed form solution numbers for a curved vessel are so far off those from the eccentric and tapered cases, this may not be necessary.

3.6 Failure

Two types of forces load the artery: a *static* or mean pressure load and a *cyclic* load that varies about this mean. While arterial remodeling is likely influenced primarily by the mean pressure load, failure from fatigue in the stent material principally involves varying loads (dynamic loads). The following 2x2 matrix makes this clearer.

Type of loading **Time frame**	**Static**	**Dynamic**
Acute	On artery	--
Chronic	On artery (remodeling)	On stent

Table 3 loading vs time frame of loading

3.6.1 Chronic-dynamic case: 'Time to fatigue' determination with cyclic loading:

We first look qualitatively at the stresses that are built up within the stent. This is based on FEA class notes [56]:

3.6.1.1 Mechanics of stent deformation [56]

In the following, we look at a prototype stent with sinusoidal elements. The three stages described briefly are:

1) Crowning—The process of creating the bent shape of the stent (in the case of the stent with sinusoidal shaped elements) is called crowing (see below).

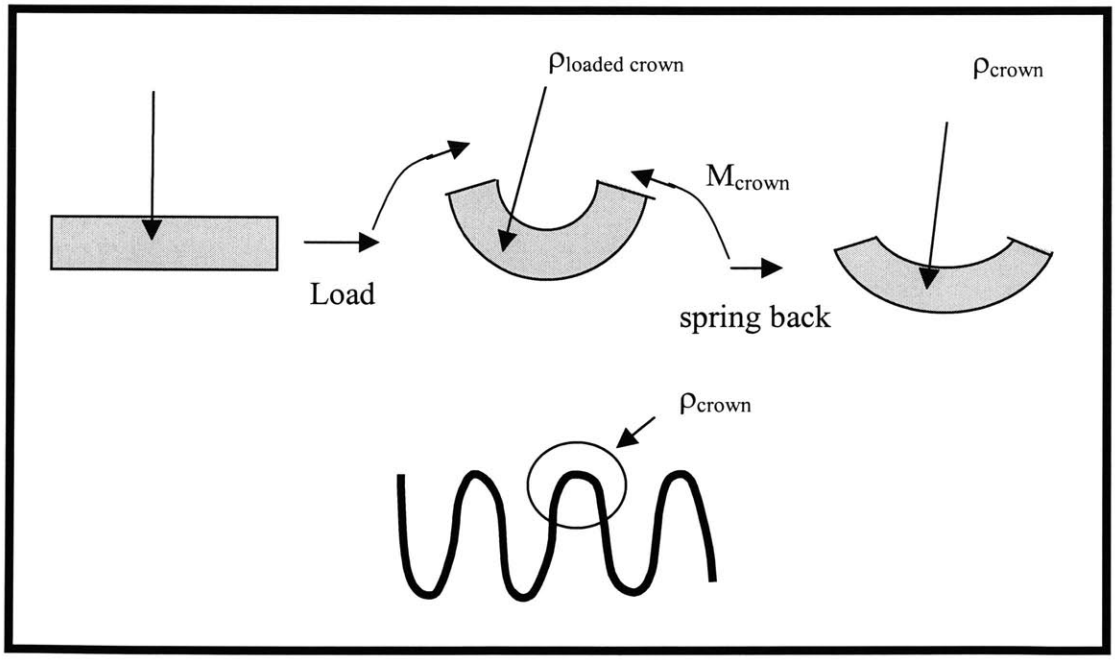

Figure 22 Crowing. The first step in the 'construction' of the stent

2) Crimping—when we further 'crimp' the stent (or bend it further) past the crown radius of curvature, ρ, we enter the crimp condition of the stent

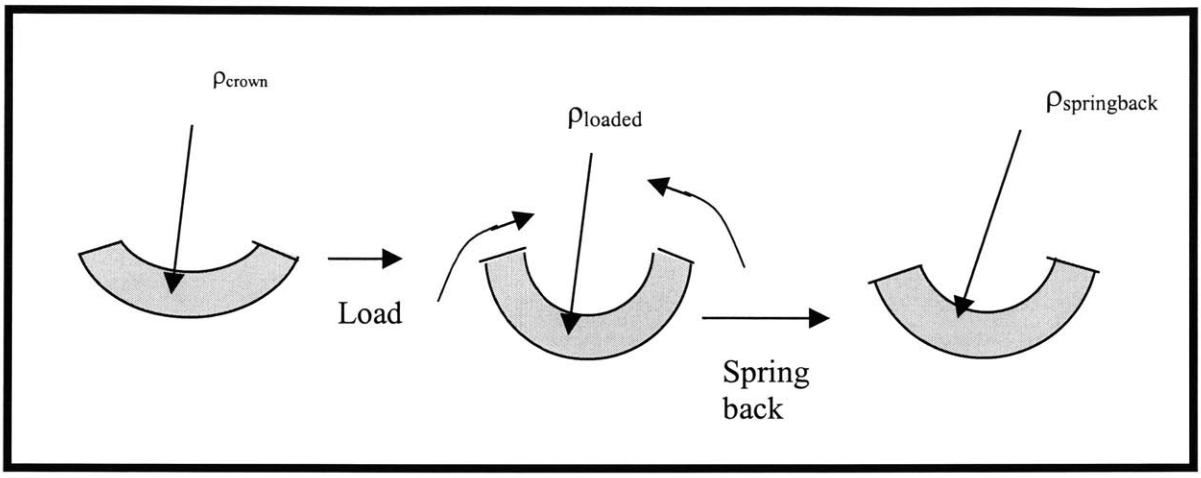

Figure 23 Crimping

3) Deployment

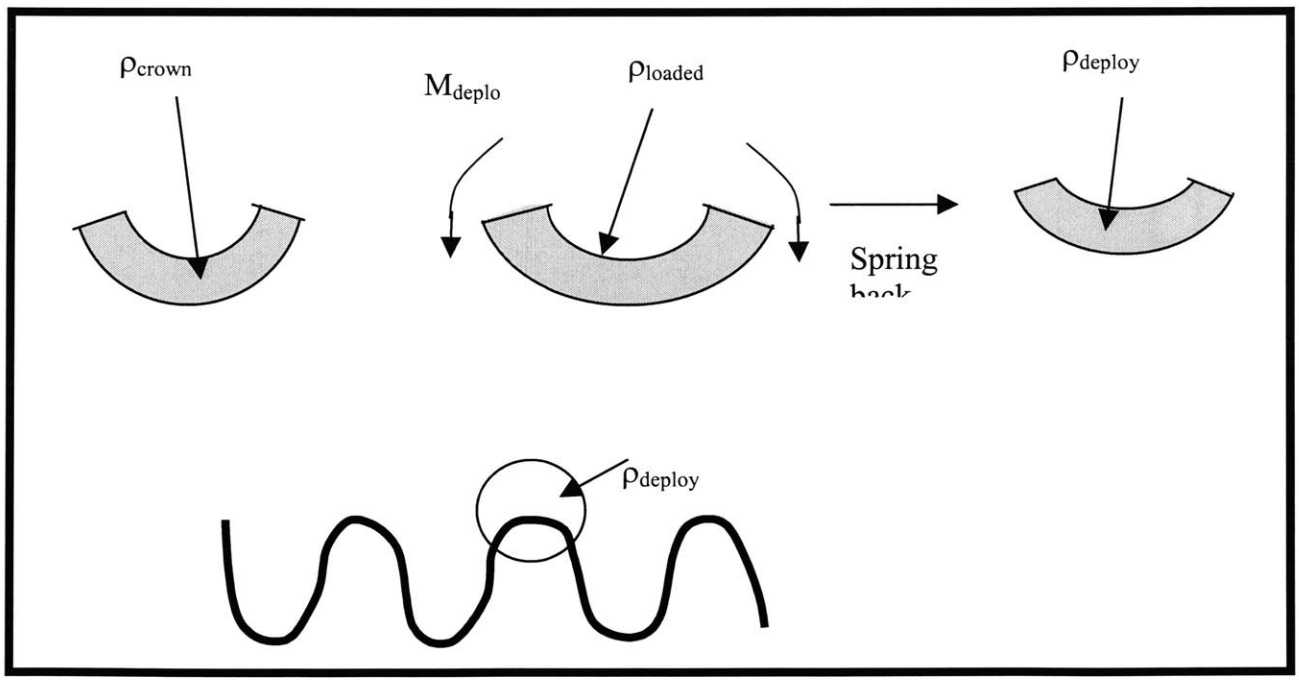

Figure 24 Deployment

Once we have the moments in the deployed configuration, we can use solid mechanics principles to find the stresses in the loaded configuration

3.6.2 Fatigue determination

Consider one of the vascular beds that we mentioned previously, for instance, the renal vascular bed. We would like to find the life to fatigue failure of the stent. Fatigue failure occurs due to a repeated loading that varies about a mean. If you take a piece of metal wire (for instance, a metal clip) and turn it back and forth, eventually the wire breaks. One turn does not break it, but a repeated or cyclic turning does.

Time to fatigue or life to fatigue is the total time it takes for a load to cause fatigue failure in a material. For instance, if each turn cycle in our example above was completed in 1 sec, and it took 4 turns to break the wire, then the fatigue life of the wire is 4 sec.

A stent within an artery, as was mentioned previously, has two types of loads applied to it by the artery: one is the mean or constant pressure load, and the other is the load that varies about this mean. The pressure load on the stent varies due to a few possible reasons. The first and main reason is perhaps obvious: the heart 'pumps' blood in repeated bursts. This 'pumping' action creates a blood pressure difference—the difference between the systolic and diastolic pressure variations. The blood in the arteries 'pulses' through. It does not flow in a constant manner. The pressure in the artery thus varies with this 'pulsing' of the blood. Any event that changes the blood pressure will cause a cyclic loading on the stent (because the load on the stent will no longer be defined by the mean pressure, but rather by a 'cyclic' variation about this mean). We have discussed the cardiac cycle as one contributory factor in blood pressure change. Other factors include exercise, posture changes, and respiratory excursion.

Each of these loads is repeated at a different rate. The heart beats at between 50-180 beats per minute (varying from person to person and varying with physical activity). We usually breathe about 17 times per minute. We see, therefore, that each event causing the change in blood pressure away from the mean can occur at a different frequency. The following Table summarizes the different pressure and frequency changes:

	Amplitude of load	Frequency of load (approximate)
The cardiac cycle	P_c	f_c = 1-2 Hz
Posture changes	P_p	f_p = low
Exercise	P_e	f_e = 0.1-10 Hz
Respiratory excursion	P_r	f_r = 0.1-0.5 Hz

'P' refers to Pressure load, and 'f' refers to frequency of this load. The subscripts stand for the various contributions to this pressure and frequency.

Table 4 The different components of the cyclic load occur at different frequencies

The following figures show possible waveforms corresponding to each loading we mentioned previously: the cardiac cycle, posture changes, exercise, and respiratory excursion.

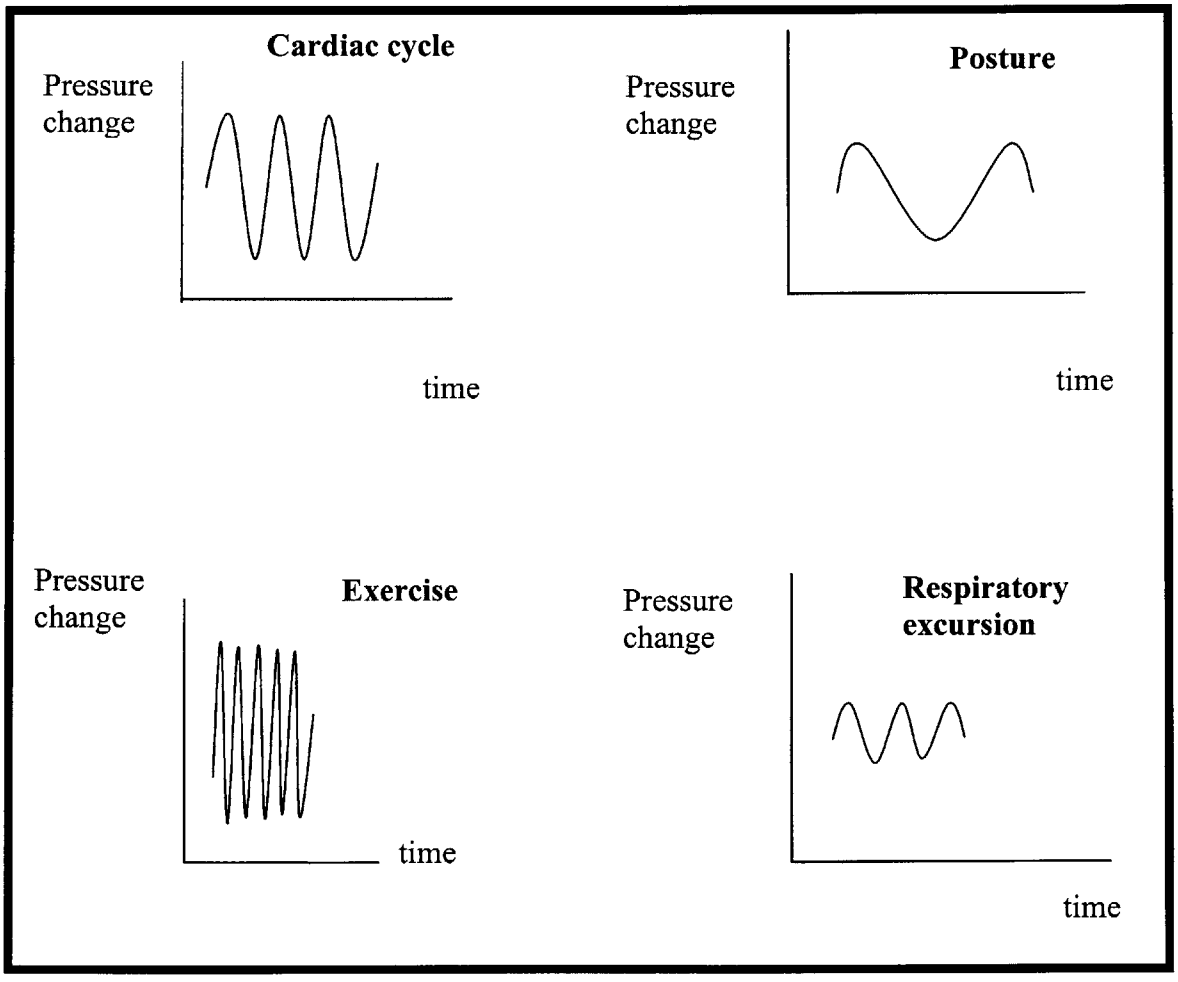

Figure 25 *components of the cyclic load shown with hypothetical profiles.* Slight postural changes and severe exercise are expected to produce the highest frequencies and amplitudes.

The load on the stent would be a superposition of all these loads, and may look something like the following figure.

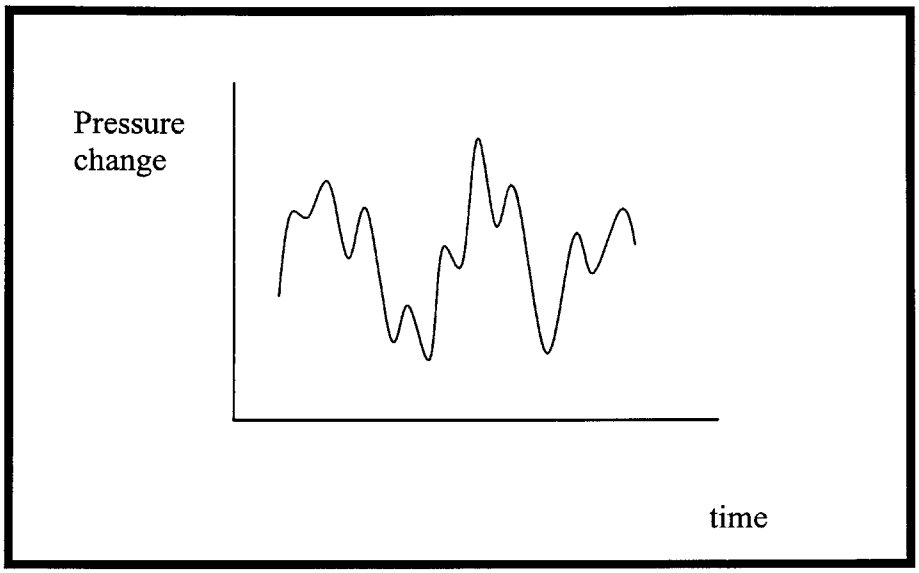

Figure 26 ***Composite hypothetical profile of the dynamic forces seen by the stent.***

In describing the composite or superimposed curve (Figure B), we need to take into account the phase differences between the different curves. However, the composite or overall loading is not needed. We only need the different components (amplitudes and frequencies). This idea is based on the Palmgren-Miner rule [57], which says that a change in the sequence of loading does not affect the fatigue life of a material.

In other words, we can replace the composite loading history curve in Figure 26 with a sequence of loadings from Figure 25. The different components in Figure A are applied one after the other (the order is not important). One possible sequence is shown in Figure 27 below:

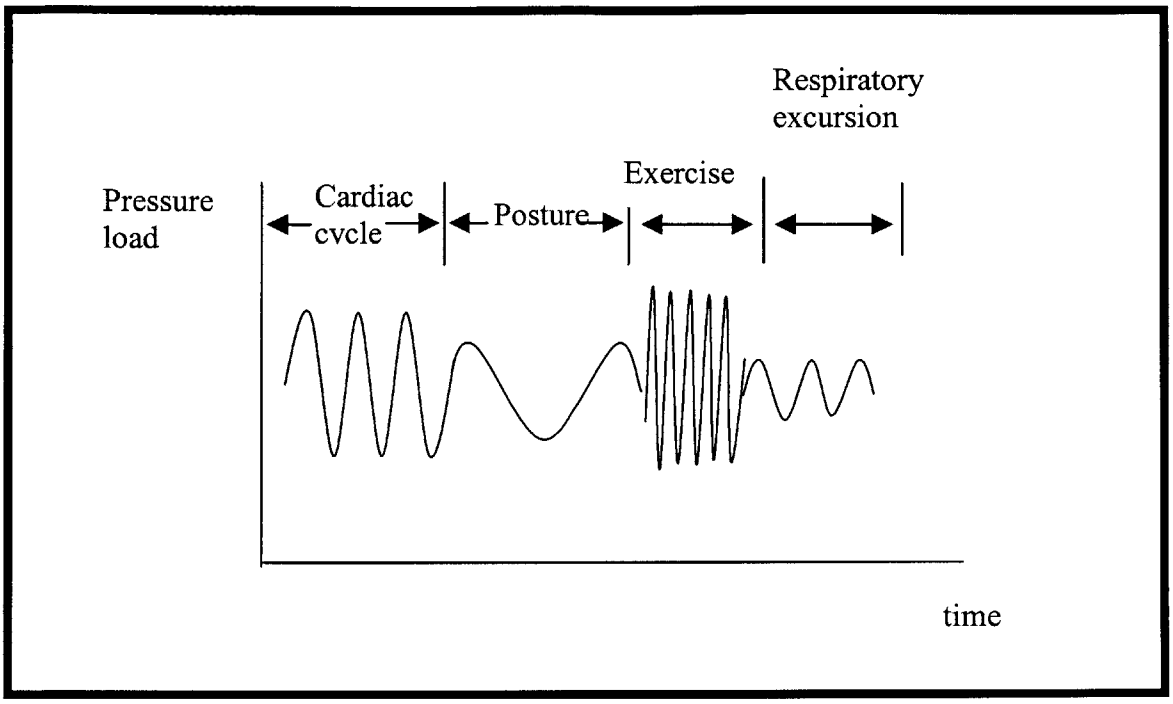

Figure 27 ***Palmgren Miner rule.*** **This rule says that the composite loading is equivalent to each load's being applied successively in turn.**

We then determine the fatigue damage from each component separately and add these up to get the total damage. Let us denote by 'N_i' the total number of cycles to fatigue if only the 'i'th load is applied. For instance, if only the cardiac cycle causes the pressure change, we look up the number of cycles to fatigue with only this load. This number is N_c. For each load then, we have an 'N' or number of cycles to fatigue when that load is applied independently on the stent. Next we introduce the variable 'n_i', or the number of cycles of the 'i'th load applied in conjunction with the other loads.

For illustrative purposes, let us assume that the cardiac cycle and exercise loads as the only two loads acting on the stent. As previously mentioned, we can find N_c (the number of cycles to fatigue with only the cardiac load), and N_e (the number of cycles to fatigue with only exercise). When the two loads are applied together, each load would end up contributing some cycles to the final fatigue. Let us call this number for the load applied

by each component acting in conjunction with the other 'n'. The ratio of 'n/N' gives us the damage from each component. Since the total damage is 1 or unity, we obtain:

$$\frac{n_1}{N_1} + \frac{n_2}{N_2} + \ldots + \frac{n_n}{N_n} = 1$$

A slightly different development may make the above derivation more concrete [58]. If 'N_i' is the number of cycles to fatigue with only the 'i'th load acting, then the damage from only one cycle is $1/N_i$. If each load contributes n_i number of cycles to final fatigue, then n_i*1/N_i gives us the contribution to fatigue from the 'i'th load. We sum up each such contribution to obtain 1 (or a 'full' damage) or the same as the equation above.

We know how to find the N's. However, we still need to find the n's. In one interval of time (any arbitrary interval), we will have a fixed number of cycles of each load. For instance, before we mentioned that the cardiac cycle load frequency is between 50-180 beats per minute. Let us use 100 beats/min in this example. Let us use 5 minutes as our arbitrary time interval. In this 5 minute time interval, we have 500 beats or cycles. Also, previously, we said that the respiratory excursion frequency is 17 cycles/min. In five minutes we would have 85 beats or cycles. Each five minute time interval in the history of use of the stent would have 500 cycles of cardiac loading and 85 cycles of respiratory excursion loading.

Let us say we have 'a' such 5 minute intervals to fatigue. Then, a*500 would be the total number of cardiac cycles to fatigue. Similarly, a*85 would be the total number of respiratory excursion cycles to fatigue. In the equation above then, the n_i's can be replaced by a constant times the number of cycles of the 'i'th load in any arbitrary time period. We thus obtain:

$$\frac{k_1.a}{N_1} + \frac{k_2.a}{N_2} + \ldots + \frac{k_n.a}{N_n} = 1$$

Where the k's are known (in a five minute interval from our example, they would be 500 and 85 beats/min for the cardiac and respiratory excursion cycles respectively). We solve for 'a' to obtain the total number of cycles to fatigue. The following figure may make this clearer:

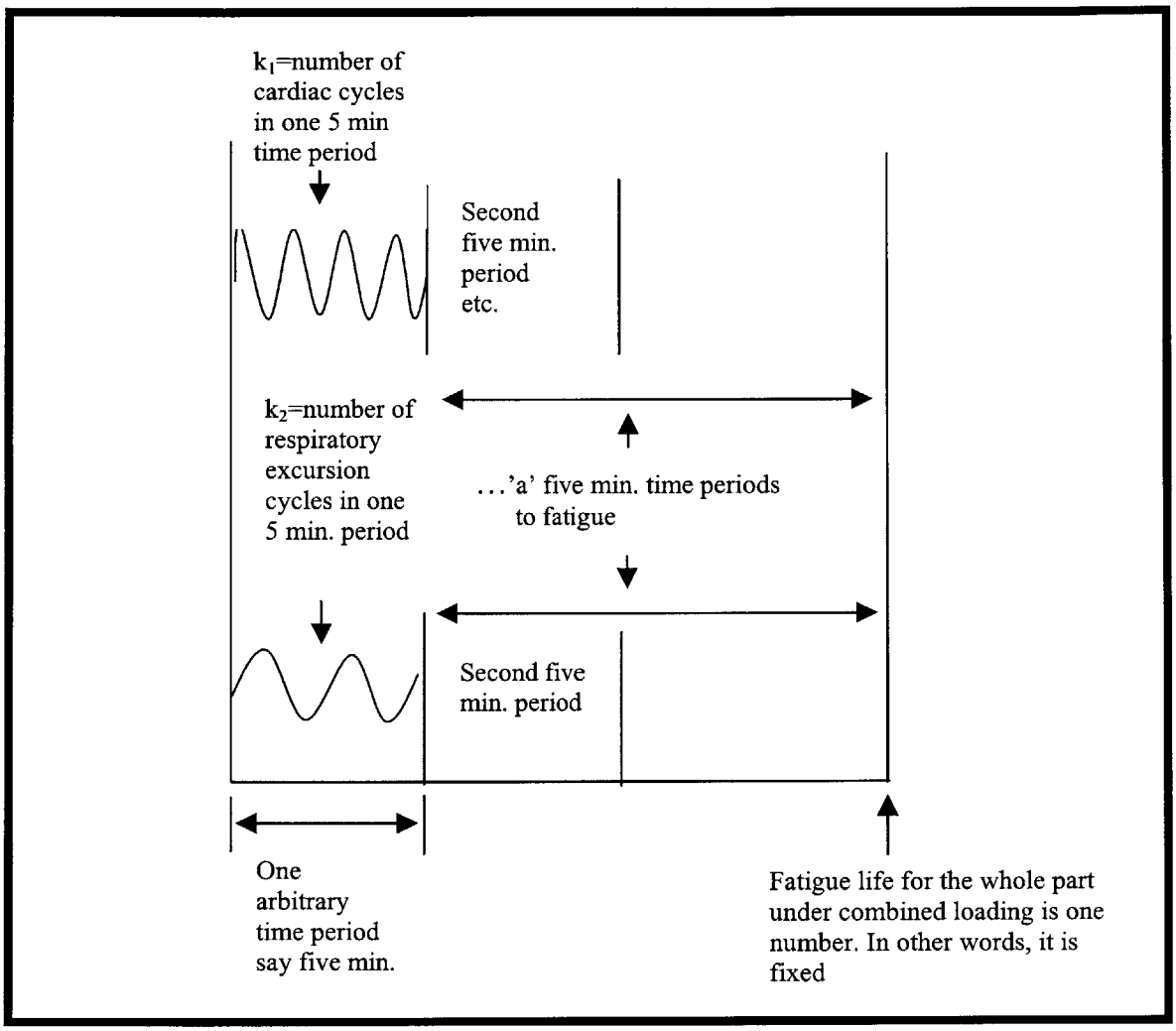

Figure 28 *determination of 'a'*. In the equation above, solving for 'a' gives us the total number of cycles to fatigue. A 5 minute interval was chosen purely for illustrative purposes. Any other number could have been used.

The possibility of failure in the stent was investigated. As explained above, the stent is subjected to a superposition of loads, of which that due to the pulsatility of the blood pressure is of the most significance. To test whether fatigue failure may occur in the

stent, a design life of 20 years was chosen (this corresponds to roughly 10^9 cycles). The stresses within the stent as it was plastically deformed to its in vivo state were evaluated. An extra force load was then applied to this load corresponding to the blood pressure load. The force load was calculated from the blood pressure using Laplace's law (explained in Appendix C). From this the stress amplitude and the mean stress were calculated. Finally, using the modified Basquin equation,

$$2N_f = (\frac{\sigma_a}{\sigma_{mean}})^{\frac{1}{b}}$$

the number of cycles to failure was found. In the above equation, N_f is the number of cycles that causes fatigue failure, σ_a is the stress amplitude calculated from,

$$\sigma_a = \frac{\sigma_{\max} - \sigma_{\min}}{2}$$

σ_{mean} is the mean stress calculated from,

$$\sigma_{mean} = \frac{\sigma_{\max} + \sigma_{\min}}{2}$$

b is –0.13 for stainless steel.

The σ_{max} and σmin were evaluated from the plastic deformation and the subsequent force loading explained above. σmax corresponded to the maximum stress in the stent after the application of the force, while σmin corresponded to the maximum stress in the stent before the force application.

Finite element analysis is employed to determine the chronic and dynamic patterns of stress distribution. Fatigue failure in the stent (not the artery) is tested by looking at the maximum stresses developed in the stent away from its baseline position during arterial expansion and contraction. The baseline position is defined by the plastically deformed shape of the stent.

Chapter 4 Results

4.1 Self-expanding force displacement relationship

The force displacement characteristics of the self expanding stent are shown in Fig 29 below. The raw data used to obtain this profile is given in Appendix B. The top curve (as explained in the methods, Chapter 3) shows the force-displacement curve for the transparency with the stent. The bottom curve shows the characteristic for the transparency alone. These curves were then curvefit using both an exponential assumption, and an assumption from an equation derived by Loshakove [52]. The exponential curvefit is remarkably close to that obtained (not shown) using an equation derived by Loshakove for a self-expanding stent [52]. The middle curve is the difference between the two to give us the stent characteristic. Only the exponential fit is shown, not the one based on Loshakove's equation. The reason the two sets of data (the top and bottom curve data) were individually first curve-fit before they were subtracted is that the stent with transparency data has a much wider range of weights over which it could be calculated.

4.2 Acute force determination

The acute force on stent was found to be 0.5 atm (or 50,000 Pa). Subsequent analyses use this value rather than the displacement value. It was found that because of the severity of loading by stents on the artery, the blood flow could be neglected in evaluating stresses on the stented artery. The shear forces were also found to be negligible in comparison to the forces imposed by the stent. The shear forces for the aorta are 0.63 N/m^2 and 0.9 N/m^2 for the renal vessels. Compared to a value of 50 kPa due to the stent, these forces are negligible.

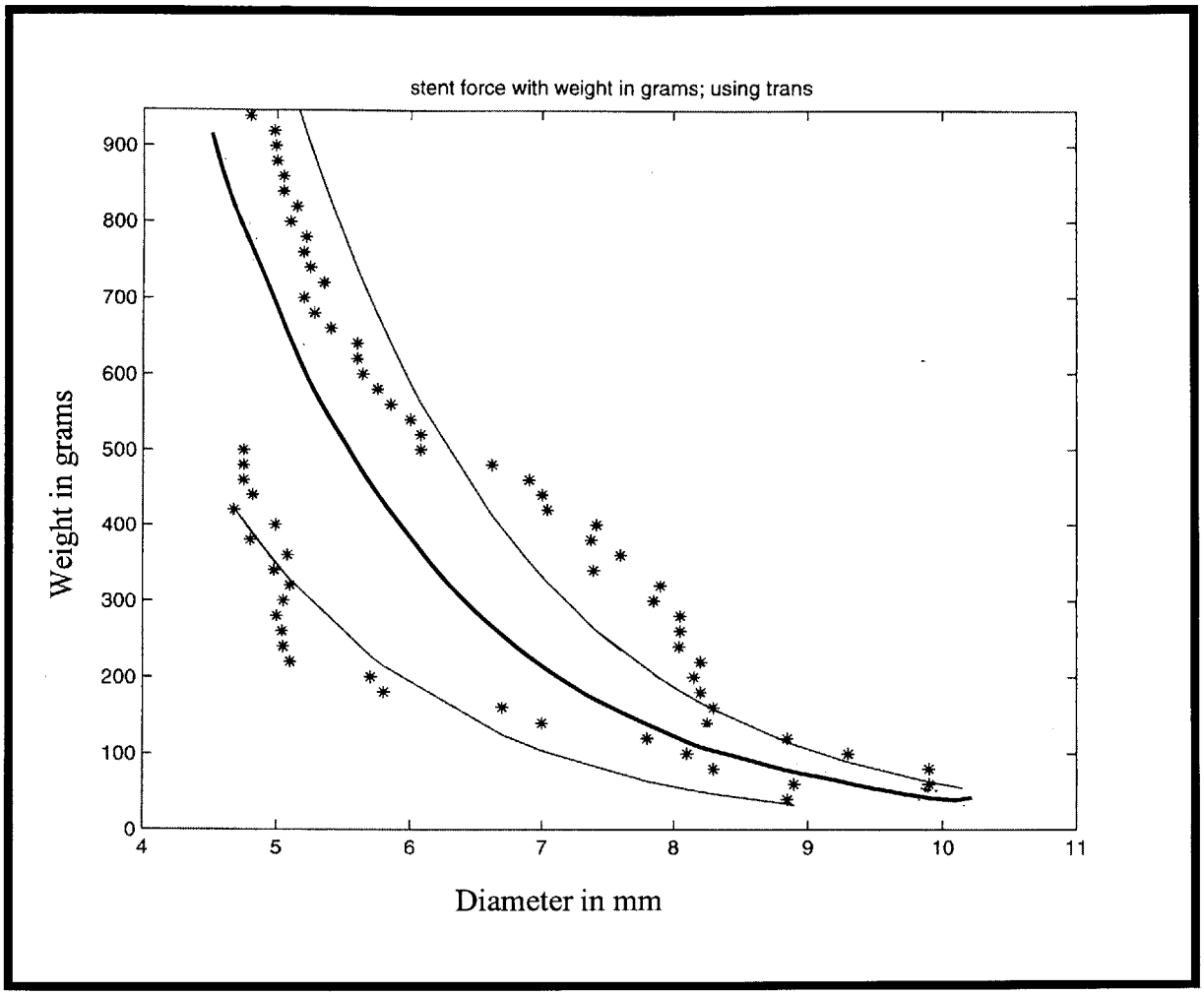

Figure 29 ***Stress-strain characteristics for a self-expanding stent.*** **The top curve corresponds to the stent with transparency, while the bottom curve is corresponds to the transparency alone. The middle curve is the stent characteristic.**

4.3 Effect of arterial bed

Figure 30 shows the variation of circumferential stress with curvature. Circumferential stress in a normal vessel (with a thin membrane assumption) is 3.815e4 Pa. Thus as the artery is made more straight (decreasing curvature), the stresses approach the value in a normal vessel. The range in variation of the stress is 0.0061% for the 50% curvature variation as given in Chapter 3, Methods.

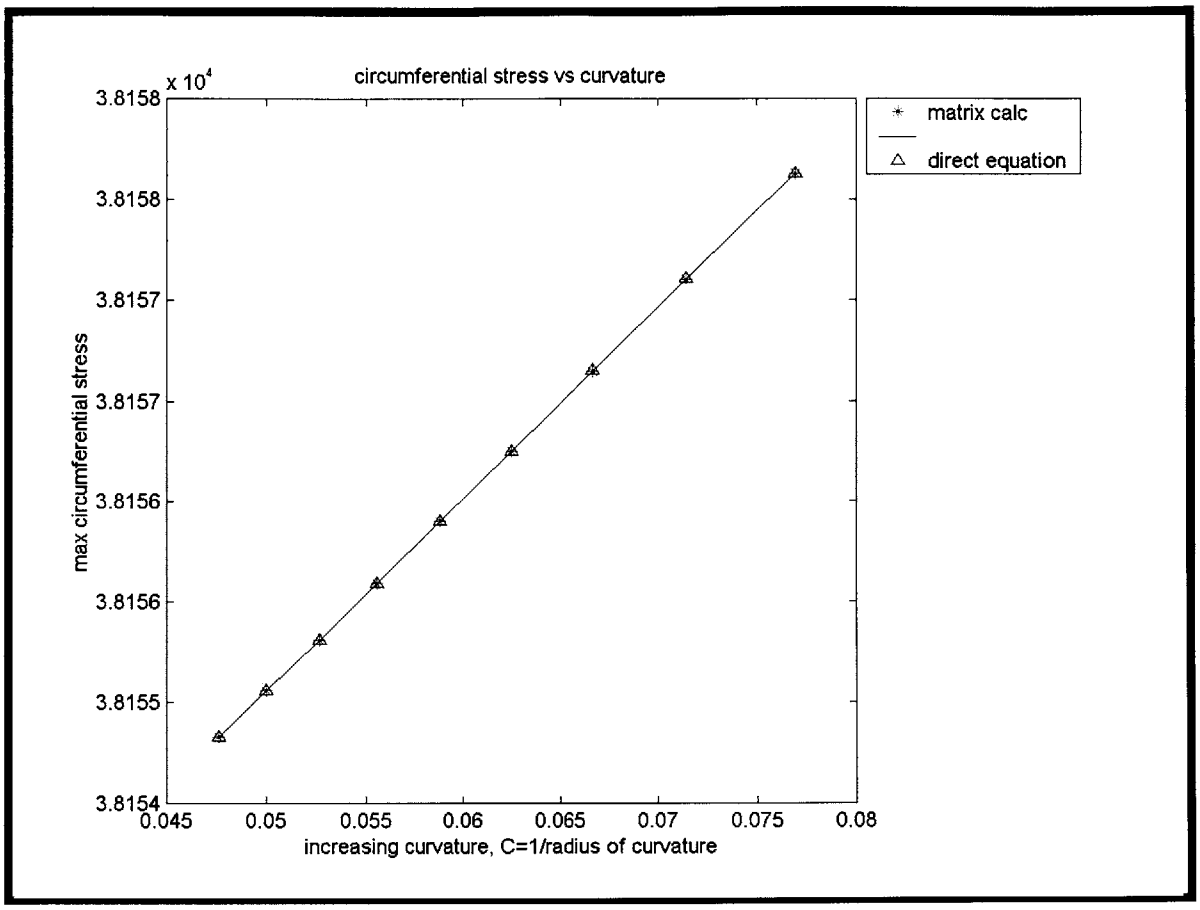

Figure 30 ***Variation of circumferential stress with curvature.*** **The variation in stresses is quite low as are the absolute numbers compared to the 'normal case (approximately 38 kPa).**

To check whether the circumference had been broken into enough points to give the maximum stress within a reasonable error, the hoop or circumferential stress was evaluated for the pressure found through iteration as explained in the theory section by using both the equation at the crotch point, and also by finding the maximum stress of the n points used (100 in this case). As can be seen the matrix maximum stresses fall within the triangles, which represent the direct equation calculation.

Figure 31 shows the effect of stenting a tapered vessel with a tapered and a non-tapered stent. As in the curved vessel case shown above, and as expected, there is an increase in the circumferential stress as the level of taper in the vessel is increased (using a tapered stent. The increase in stress, for the taper range used, however is 26%. Stenting with a

non-tapered stent, also shows, as expected, even higher stresses. This is because the non-tapered stent essentially creates a straight profile in the tapered vessel post stenting. The stress difference now is approximately 71%, a far higher number. To make comparisons with the eccentric case meaningful, all numbers were compared to a non-tapered vessel.

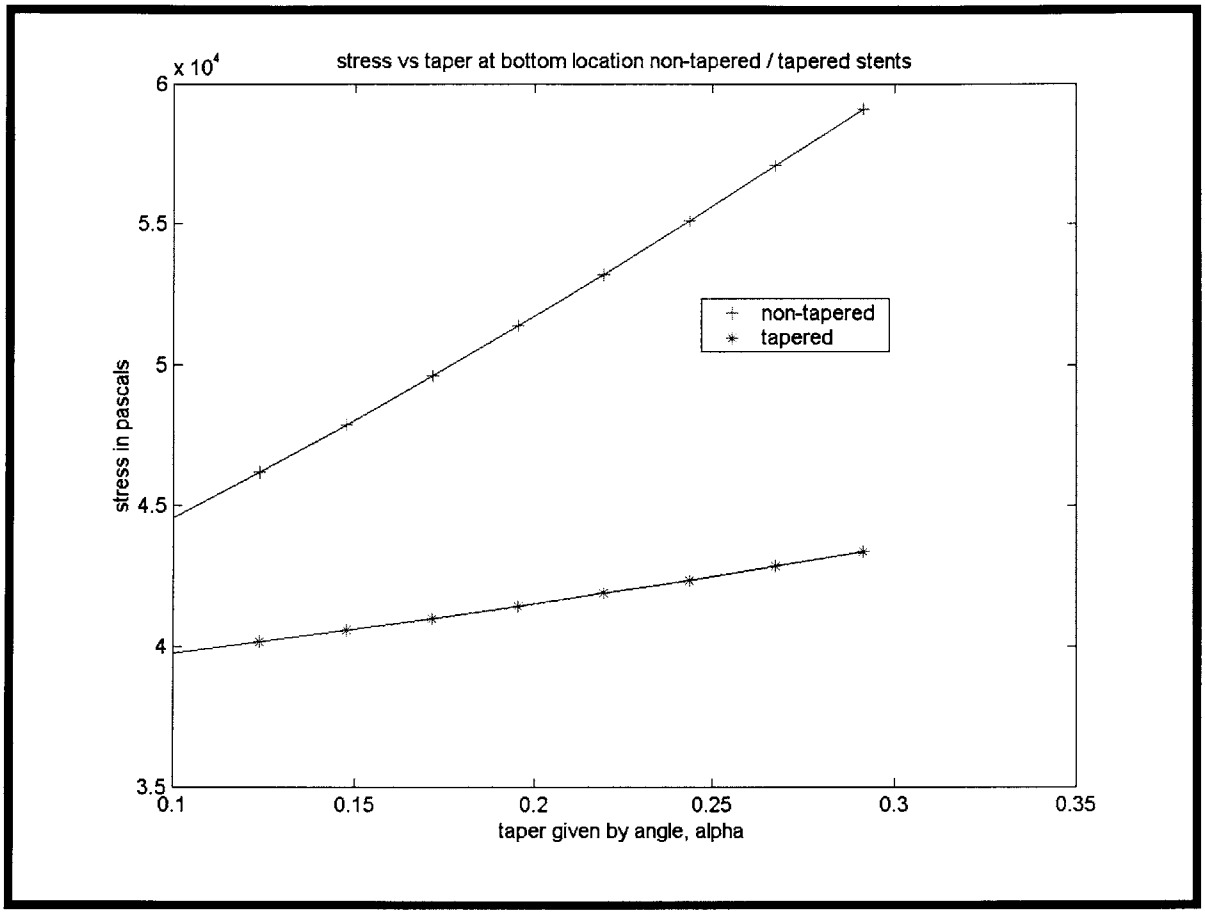

Fig 31 ***Effect of stenting a tapered vessel with tapered and non-tapered stents.*** **The non-tapered stent shows a larger variation and absolute values.**

Figure 32 shows the effect of stenting an eccentric vessel with a stent. The upper curve is the analytic closed form plot, while the lower curve was obtained through use of ABAQUS. Both curves follow essentially the same profile. However, the FEA results show a persistent downward bias. The variation in stresses in the upper curve is around 188% (using the non-eccentric section as the baseline), while the absolute value of stresses is quite high also. To test the validity of the equations used to obtain the

circumferential stresses in an eccentric vessel, a 2D eccentric model was created in ABAQUS. Again using the non-eccentric values as the baseline, the variation in stresses obtained in the FEA solution is around 155%.

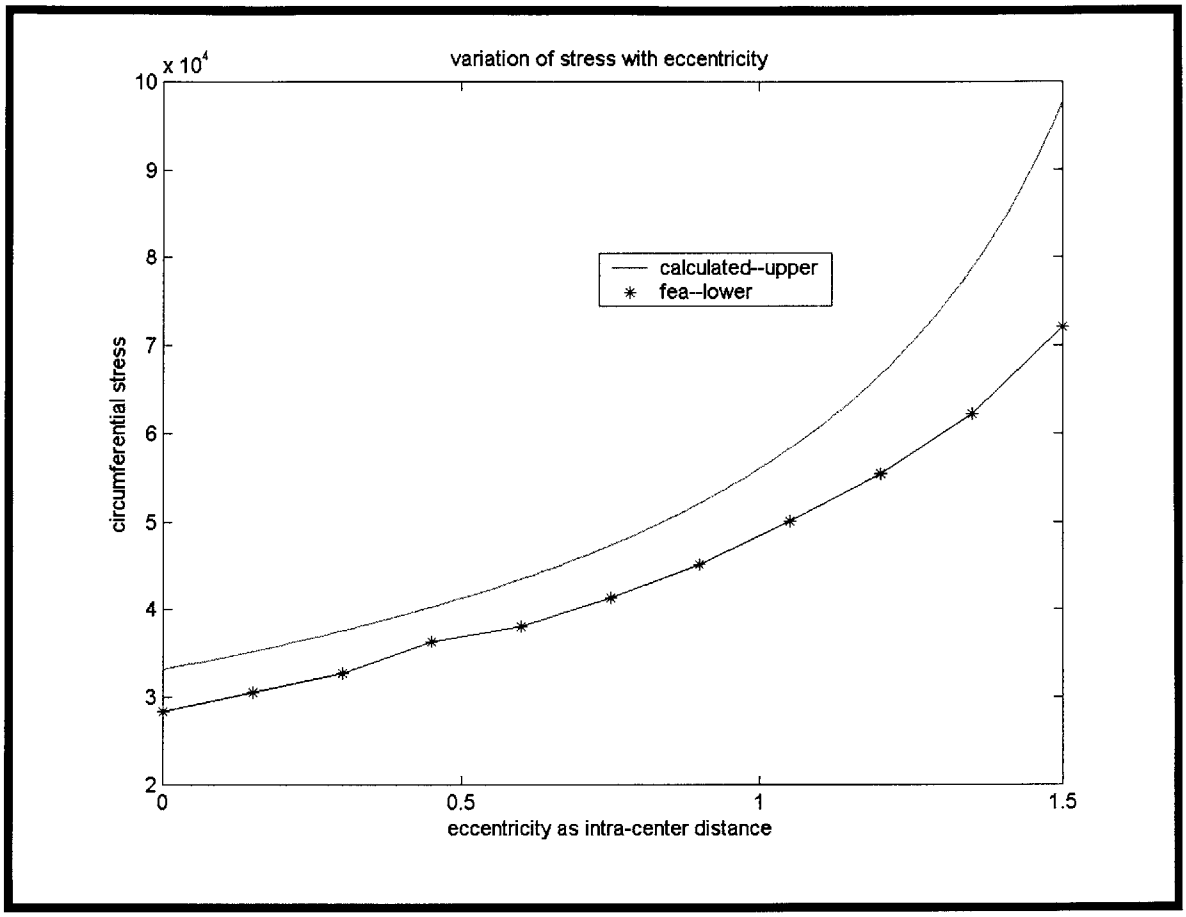

Figure 32 ***Eccentric vessel. Comparison of FEA results with the closed form analytic solution.*** **The upper curve shows calculated values, while the lower curve represents the FEA results.**

4.4 Inapplicability of using thermal shell elements

The inaccuracy inherent in using thermal shell elements is exemplified by Fig. 33. As can be seen, with increasing curvature, there is a decrease in the stress in the eccentric vessel.

However, as we saw in the curvature analysis in section 3 above, the circumferential stresses should increase with an increase in curvature. Thus, the results from the thermal shell element turn out to be exactly opposite to what we would expect. The putative mechanism by which this happens is explained in chapter 5, discussion. Although there we make use of the eccentric vessel as our main example, the explanation is directly applicable to the curved vessel. This comes mainly from the fact that in both the eccentric and curved vessels, the local strains do not coincide with the global strains. Thus, any analysis that imposes equal local strains around the circumference will produce results opposite to what is expected.

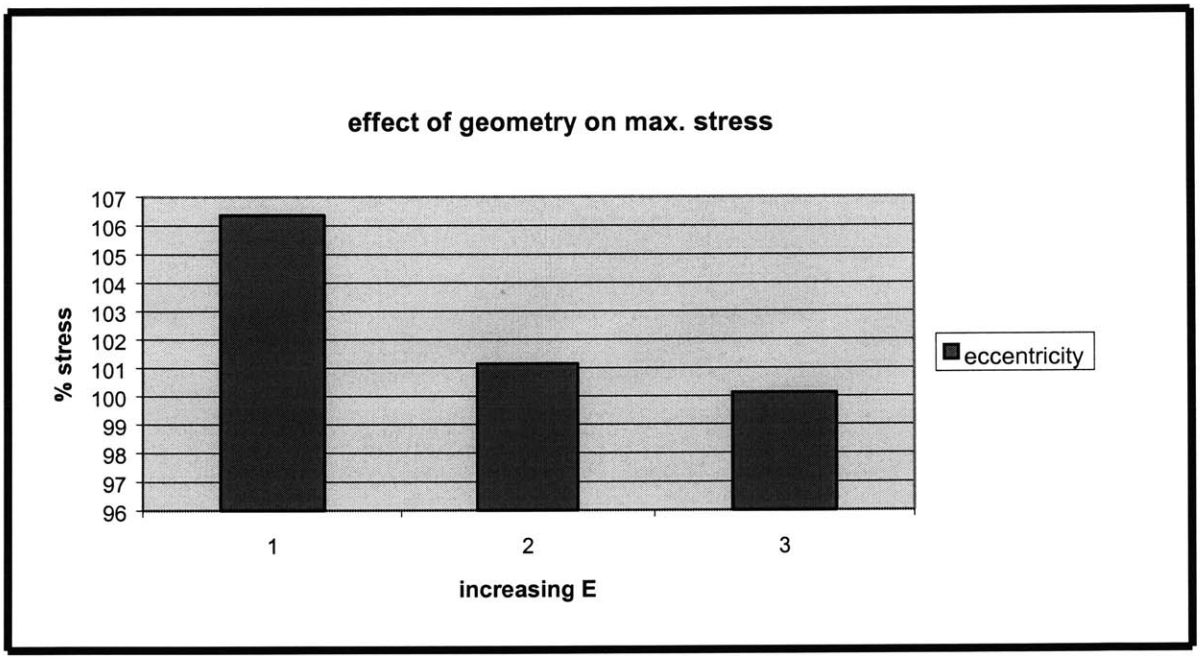

Figure 33 ***variation of maximum stress with eccentricity through use of thermal shell elements.*** **The observed trend is opposite what is expected through the analytic solution.**

4.5 Fatigue life determination

As shown by the Matlab file in Appendix D, the fatigue life of the stent is 5.1e10. A useful life of 20 years corresponds to around 10^9 cycles. The calculation shown in

appendix D gives an order of magnitude of safely in the use of the stent and therefore it is highly unlikely that failure from stent fatigue is likely to occur. It must also be kept in mind that this was a conservative set of numbers for the following reasons:

a. In Chapter 3 is mentioned the stages in the expansion of a stent within an arterial wall. At deployment of the stent, the stent is expanded the most—the stress strain response is in the plastic regime of the material that makes the stent. In our analysis, the stent was deployed or expanded but not allowed to 'relieve' stresses due to a 'fall-back' (i.e. after the displacement loading is removed, the stent—which has undergone plastic deformation, recovers from its maximum displacement slightly to relieve the stresses. This stress relief can result in stresses that are about half as large as were used.

A fall back analysis was not possible, because ADINA does not allow a restart analysis where the results from one analysis can be input in another analysis. In our case the boundary conditions that make up the first part of the analysis, which are the forces that load the stent strut would have had to be removed before the spring back could be found.

b. The stresses in the section were computed using Laplace's law. However, the section because it is 'snaked' sees stresses much lower than that predicted by Laplace's law. What this means is that in a real system, the snaked nature of the geometry allows radial expansion that produces far smaller stresses than if we simply use a radial loop to find the stresses through an application of Laplace's law. Consequently, the force applied to the stent should be lower than the one used. Thus, it is unlikely that the stent fails due to fatigue.

Chapter 5 Discussion

This chapter summarizes some of the conclusions obtained from this thesis. An eccentric vessel was found to impose stresses much higher than those obtained through a tapered vessel, while the stresses obtained in the curved vessel could be neglected. Although a membrane assumption was made in the curved vessel model, it was not used in modeling the eccentric vessel. The membrane assumption, however, especially does not apply to a tapered vessel. Let us see why this is so.

We have learned from all of the analyses that a uniform set of boundary conditions is not adequate in looking at similar events in different arterial beds. For example, in our analytic closed form solution, it was found that the tapered vessel equations and the assumptions behind those equations are quite distinct for the curved case which itself is quite distinct from the eccentric vessel case. In the eccentric and the curved vessel, because of the non-uniformity of the local strain values around the circumference, an intermediate pressure boundary condition was used to mimic the final achievement of a known global strain. This intermediate pressure strain relationship introduced approximations into our analysis. If we had a-priori known the local strains at each and every point, no pressure relationship analysis would have been called for, and this is precisely the case for a tapered vessel.

The solutions for the tapered vessel are exact. There are no thin-membrane approximations. One might argue that FEA may still find use because the strain is not related to stress in a simple way. The answer to that is simply that the relationship of stress to strain is controlled by the anisotropy-isotropy formulation, and this is input into any FEA program. In an isotropic case, the relationship between stress and strain is:

Stress = function(strain xx, strain yy, strain zz)

There are no shear cross-coupling terms, and even if there were, the use of FEA would also require the inputting of the relevant anisotropic values. FEA finds use more in cases

where the local strain values are not obvious from the global boundary conditions, which in our case are fixed displacements imposed by the stents on the arterial wall.

In experiment 3, the difference between arterial beds was evaluated using i) A tapered, vessel, ii) An eccentric vessel, iii) A 'normal' non-tapered, non-eccentric vessel, and iv) A curved section

The equations given in Chapter 3, Materials, Methods were used to obtain the maximum stresses for each of the geometry types given above. An understanding of the boundary conditions and how they cause the resulting stresses within the vessel wall is essential in formulating the equation that is used to solve for the maximum stresses. For instance, the equations show that there is a variation in stresses around the circumference in a curved vessel with an applied pressure. This then implies that the local strain is no longer the same as the global strain around the circumference. The first analysis that was carried out to study the effects of geometry on maximum stresses did not take this into account. As explained in 5.2 below, this is why a temperature dependent shell element was found inadequate to model stent expansion within an artery. More detail is given in the next section on this.

The equations for both the curved vessel were obtained using a membrane assumption, while the equations for the eccentric case by definition had to use the thick vessel assumption. Although normalizing the data to account for the membrane assumption in the curved vessel (the tapered case does not use the membrane assumption) would be useful in making comparisons, the very small absolute values and the small range in the curved vessel case made such an analysis extraneous.

The solutions to the different arterial bed loading were obtained analytically and solved for using Matlab. The value of finite element analysis in this work is still quite high, however. Even though the equations can predict maximum stresses in simple geometries, they are inadequate in predicting geometries that are a combination of the types listed above. It may just be, as hypothesized in Chapter 6, Future work, that simple geometries

superimpose in their effects, and in that case the result may simply be a superposition of the results obtained for each geometry type. However, there is another caveat. The analysis above makes use of a membrane assumption in the derivations and results. This is clearly not the case, at least where the thickness to diameter ratio of the vessel is high. Thus the membrane model is more appropriate as one moves to larger diameter vessels (where the concomitant rise in thickness with diameter is small), such as the renal arteries, and the aorta. It may fail in the case of the coronaries.

The other caveat is that the stent assumes a circular shape, at least right after expansion. Although this shape is almost very likely to be contorted into a less circular profile after the balloon is removed, it is certainly true that a uniform pressure will not lead to a completely circular profile. Thus finite element methods, insofar as they are amenable to modeling the boundary conditions of stent expansion (to a circular profile) are a more accurate representation of the stenting of a vessel. ABAQUS was used in obtaining stresses, as it was in obtaining a circular profile, in an eccentric vessel.

Finally, the equations obtained are valid for a small strain analysis. The strains imposed on the arterial wall are high however. But this is not a particularly restrictive condition, because the focus of this work was not to model correct arterial stresses. Rather it was to look at differences in stresses between the different types of sections studied.

5.1 Effect of arterial bed

This study did not seek to reproduce faithfully the arterial wall. Its intent was to look at differences between the different beds. The equations used are appropriate for small strains, whereas stenting imposes large strains. Values obtained from this study don't have relevance to particular arterial beds. Their value lies in determining relative importance of the different parameters studied.

The results show that curvature does produce a change in maximal stress compared with a normal vessel. However, this change is quite small (0.0061%), while taper creates a 27% change in the case of the non-tapered stent and around 9% for the tapered stent. It must be kept in mind that these values can be appropriately scaled. However, it is hard to see how the curvature can be such that there is a 27% increase in stress with the curve profile shown in the results section.

A linear, isotropic, homogeneous assumption was made on the arterial modeling. No pre-stress was assumed to act on the artery in its closed state (in other words, prior to a loading with a stent, the stress in the artery was set to zero). Further, the axial stretch that exists on the arterial wall [49] was also neglected for two reasons. One, the stresses produced on the arterial wall because of a stent load are far higher than those due to the stretch. Second and more important, the axial stretch exists everywhere in the body's arterial bed and therefore is not important in the relative study of arterial bed. Blood flow effects were similarly neglected.

Figures 31 and 32 from chapter 4, results, show that the eccentric section shows the highest stresses followed by the tapered vessel, while those in the curved vessel are the lowest. Although the curved vessel numbers were not normalized to take into account thickness effects, it is hard to see how these numbers can be made to be as large as the eccentric or the tapered vessels. The effects of stent expansion (on the artery) usually manifest themselves as a biologic response in the arterial wall (in addition to the mechanic response). The maximum stress, tells us less about the arterial mechanical response than it does about the effect of stent expansion on the biological response in the artery. This biologic response can take the form of neointimal hyperplasia. If the biologic response is sensitive to stress changes of 12%, then one would expect a slightly eccentric section to show more neointimal hyperplasia than other sections, while the effects of taper are more patent at the highest taper levels.

The FEA model for an eccentric vessel constructed using ABAQUS shows values that although follow the same profile as the closed form values, show consistent downward

bias. The advantage of the FEA model is that it does not rely on an approximation. Also, the final geometry obtained is circular. There is however a discrepancy in the values even at the zero eccentricity point, and this could simply be due to the way the FEA values were read off. Because of the symmetry of the situation, the output coordinate system was not chosen to be a cylindrical system. Rather, as shown in Figure 34, because of the location of the thinnest point (where the highest stresses occur), the yy stress was used in lieu of the circumferential stress. This is correct, as long as the exact location of the stress corresponds to the thinnest location. If it is even slightly off, as it can be because of mesh errors, then the value that is read off can be off.

The difference if it is due to random mesh errors then should not be systemic as it is in Figure 32 in chapter 4, Results. Perhaps there are other errors that may be inherent in the FEA (the closed form Lame equation is probably more accurate in a non-eccentric cylinder).

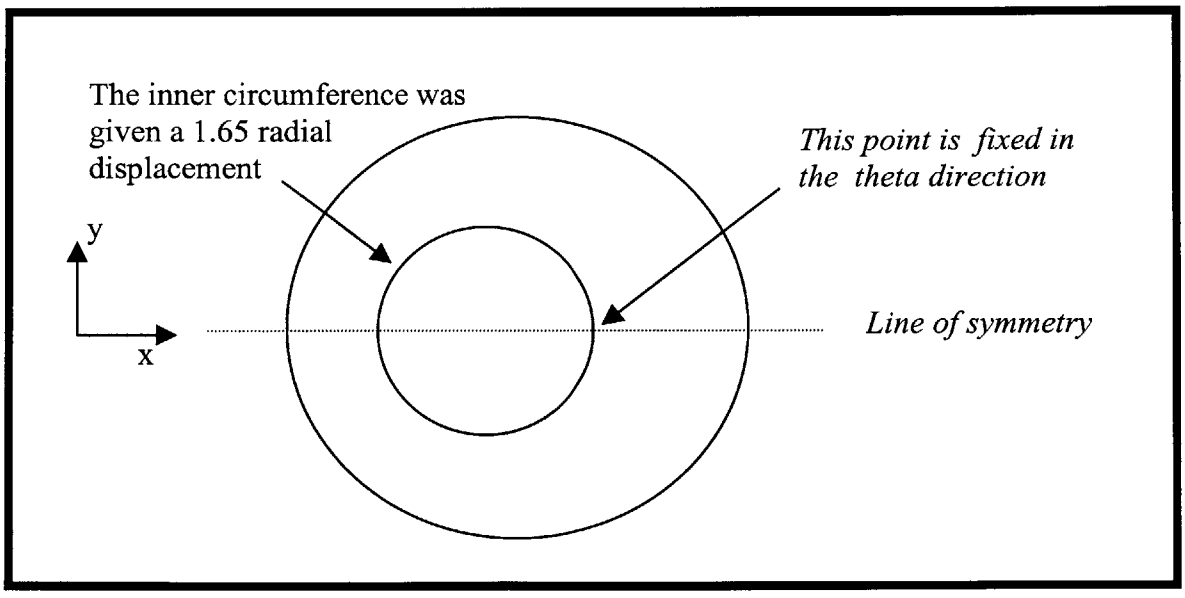

Figure 34 ***Model of the eccentric vessel in ABAQUS***

Oniki et al [23] report that "a lesion localized in a smaller area tends to result in luminal narrowing with less arterial enlargement." Clarijs et al [59], however, report that they

found no correlation between eccentricity and compensatory enlargement. Perhaps compensatory enlargement mechanisms rely on a global versus a local change in vessel diameter.

It is also important to realize that the experiments pertain to boundary conditions, which due to the placement of stents, are severely different from those arising from in-vivo non-stent 'normal' boundary conditions. For example, in this analysis effects of blood flow on the stresses produced within the artery were largely ignored. This is reasonable because the deformations produced through stenting create strains (and therefore stresses) that far outweigh those resulting from blood flow in the region. Others have looked at non-stent boundary conditions, and their effects on the rupture potential of a region of the artery. For instance Aoki et al looked at the reduction in transmural pressure leading to collapse of a stenosed vessel [60].

The results of this analysis show that taper and eccentricity may be more pressing problems than curvature in stent expansion. There are stent designs that currently address this issue by providing taper in the stent. The issue of eccentricity may be harder to solve—partially because the extent of eccentricity or its direction is not known with complete certainty. Further, the stent placement currently cannot be controlled such that one side faces the thicker and one side the narrower region of eccentricity. It may also be argued that no stent design may significantly manage the issue of eccentricity. Eccentricity plays its role mainly in the resistance of the vessel to applied load. The thinner section tends to take on most of the stretch (and therefore the stress—assuming constant material properties around the section). The eccentric section is not as simple as was modeled in this analysis. It is often seen in conjunction with varying material properties (in particular lipid pools).

5.2 Inappropriateness of using thermal elements

The thermal shell element is not suitable in modeling stent expansion in arteries. Local strains within curved and the eccentric sections are different from the globally applied

strain. The shell element that is temperature dependent applies the global strain at all points equally. The application of the same strain at each point works the problem backwards incorrectly (Fig. 35). The end result of an expansion is that one wants to obtain the stresses, but the stresses are dependent on the strains. Applying a known strain works if the global strains equal the local strains, but if they don't, as they do not in the two cases discussed above, the results come out opposite what would be expected. The highest stresses are obtained at the thickest section.

The expansion of the thermal element with an applied temperature equally in all directions. Thermal elements create unreal axial stresses. Although a real artery is subject to an axial stress, this stress is the result of the tendency of the arterial wall to maintain an overall constant volume (this comes from the incompressibility assumption talked of before) with a change in the circumference with stenting. If additional axial displacements are created, as they are with thermal shell elements, the overall stresses will be higher. It may seem that this can simply again be circumvented by holding only one end of the arterial wall fixed, while allowing for free translation, or at least axial translation of the other end.

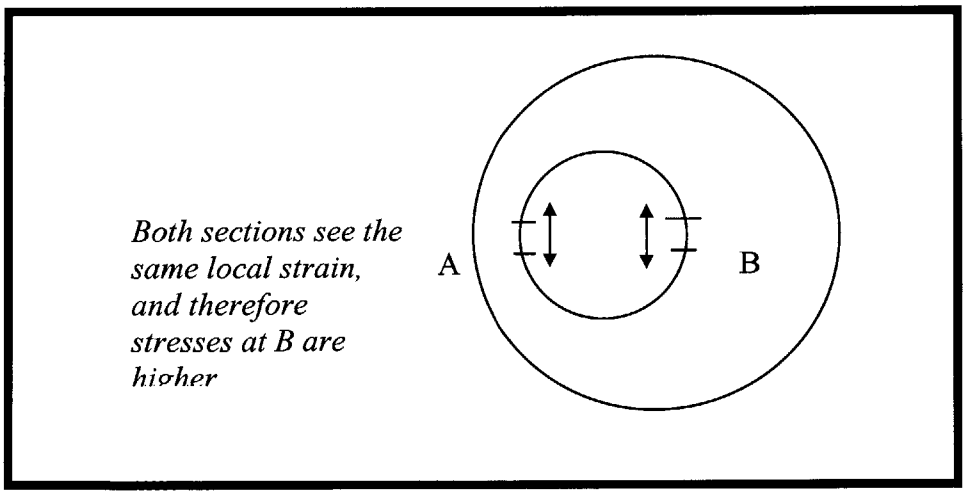

Figure 35 ***Application of the same strain at two different points leads to stresses opposite to what is expected***

This perhaps may reduce the stresses, but will still be incorrect, principally because of the no-slip boundary condition between the thermal element and the arterial wall. The no-slip exists because the surface of the shell element is one to one with the inner surface of the arterial wall. Any axial translation of the shell element will cause an axial translation and stretch in each element block as shown in Fig. 36.

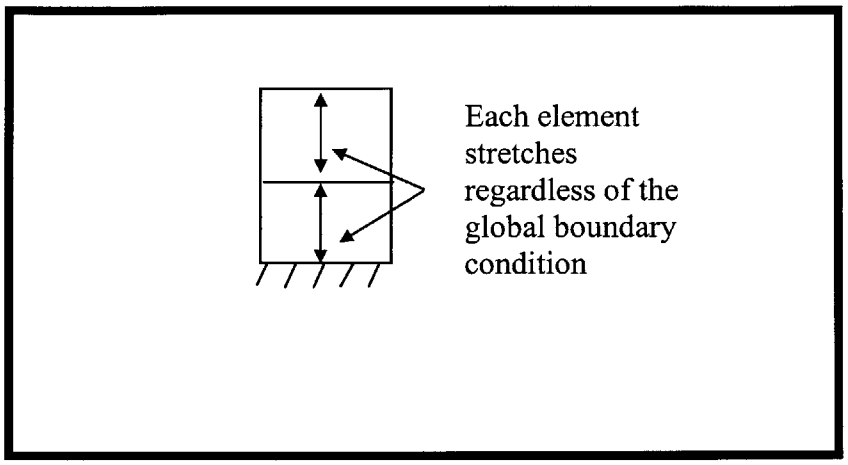

Figure 36 ***Each thermal shell element shows strain regardless of global constraints.*** **This occurs because of the element being 'fixed' to the arterial wall.**

Chapter 6 Future work

Having looked at the effect of arterial bed in predicting the type of stenting that should be performed in those beds, we now discuss possible future work that builds on this thesis. We discuss 'viscoelastic' effects defined broadly as the artery's tendency to stretch slowly with an applied stress. Next we discuss the possibility of using superposition in predicting stresses in complicated geometries, and finally we talk about how comparisons between self-expanding and balloon-expanded stents can be made more meaningful.

It was mentioned in the discussion that viscoelastic effects may be responsible for the time lag seen between the forces imposed by the self-expanding stent and their 'resolution' by the artery by an expansion. This was compared to compensatory enlargement (and in the strictest definition of compensatory enlargement, it is so). However, whether the cause is purely mechanical remains to be verified. It is true that a self-expanding stent continues to impose an outward force on the artery. Does the artery stretch automatically in response to this force imposition through viscoelastic effects, or is there a biologic mechanism that plays a middle role? Remodeling in general and compensatory enlargement in particular are not very well understood. Future work that looks at the viscoelasticity of the artery (taking into account its non-linear stretch characteristics) in terms of its stretch may resolve the question of a mechanical versus a biological reason behind the enlargement seen.

It is more likely that a combination of biologic and mechanical events are responsible for the enlargement seen. However, researchers have noted the viscoelastic character of the arterial wall, so this may also be a valid mechanism.

One question that may be relevant deals with the possibility of superimposing the stresses found in simple geometries in predicting stresses in mixed or complicated geometries. For instance, the stresses predicted for simple geometries could be added for geometries that are a composite of the different geometries that were studied in this thesis. These numbers could then be verified using Finite element models of the composite geometries.

In Chapter 2, Theory, we discussed the possibility of compensatory enlargement with stents. In a study by Carter [22], self-expanded stents were compared to balloon inflated stents. The self-expanding stent diameter was higher than the balloon expanded stent diameter. The question is: why were the arteries that were balloon expanded not expanded further? Perhaps further expansion would have led to a tear in the arterial wall. To get meaningful comparisons between the two stent types, perhaps a route for future work may be that the balloon expanded stent is expanded to a diameter that a self-expanding stent finally obtains, and that the self-expanding stent is also concomitantly also balloon expanded. This way, the neointimal hyperplasia comparisons will be valid and the relevance of injury to the difference in outcomes between the two types of stenting clearly established.

Appendix A

Matlab file to calculate the stiffness matrix entries (from [44]):

```
clear
E1=10000;          %% E1=E radial
E2=100000;         %% E2=E circumferential
E3=100000;         %% E3=E axial
v12=0.01;          %% v12=v13
v23=0.27;

%% the following calculates the compliance matrix
s(1,1)=1;          %% s is the compliance matrix or C^-1
s(1,2)=-v12*E2/E1;
s(1,3)=-v12*E3/E1;
s(2,1)=-v12;
s(2,2)=1;
s(2,3)=-v23;
s(3,1)=-v12;
s(3,2)=-v23;
s(3,3)=1;
s
delta=(1/E1*1/E2*1/E3)*det(s)

%% The following calculates entries in the stiffnes matrix
C11=(1-(v23)^2)/(E2*E3*delta)
C22=(1-(v12)^2*E3/E1)/(E1*E3*delta)
C33=(1-(v12)^2*E2/E1)/(E1*E2*delta)
C12=(v12+v12*v23*E3/E2)/(E1*E3*delta)
C23=(v23+v12*E2/E1*v12)/(E1*E2*delta)
C13=(v12+v12*v23)/(E1*E2*delta)
C44=(1-v23-2*(v12)^2*E3/E1)/(2*E1*E3*delta) %%G23=C44
C55=50000          % C55=G12=G13 (due to transverse isotropy)
C66=50000          % C66=G12=G13 (same as above)
C44=(C22-C23)/2    % (due to transverse isotropy) check on C44 above
```

The output from the above file is:

```
s =     1.0000   -0.1000   -0.1000
        -0.0100    1.0000   -0.2700
        -0.0100   -0.2700    1.0000

delta = 9.2456e-015

C11 = 1.0027e+004
C22 = 1.0805e+005
C33 = 1.0805e+005
```

C12 = 1.3736e+003
C23 = 2.9311e+004
C13 = 1.3736e+003
C44 = 3.9370e+004
C55 = 50000
C66 = 50000
C44 = 3.9370e+004

The delta matrix given above is shown more clearly below:

$$\Delta = \frac{1}{E_1 E_2 E_3} \begin{bmatrix} 1 & -\nu_{21} & -\nu_{31} \\ -\nu_{12} & 1 & -\nu_{32} \\ -\nu_{13} & -\nu_{23} & 1 \end{bmatrix}$$

The above Δ is then used to calculate the entries in the stiffness matrix, C. For example, C_{11} is given by:

$$C_{11} = \frac{1 - \nu_{23}\nu_{32}}{E_2 E_3 \Delta}$$

Appendix B Data used to obtain the force-displacement characteristics of a self-expanding stent

Transparency alone

mass (gm)	diameter (mm)	length (cm)
40	8.85	16
60	8.9	14.7
80	8.3	13.6
100	8.1	11.15
120	7.8	10.8
140	7	10.1
160	6.7	9.65
180	5.8	8.76
200	5.7	8.5
220	5.1	8.14
240	5.05	8.1
260	5.04	7.95
280	5	7.94
300	5.05	7.75
320	5.1	7.75
340	4.98	7.82
360	5.08	7.82
380	4.8	7.82
400	4.99	7.85
420	4.68	7.8
440	4.82	7.9
460	4.75	7.74
480	4.75	7.78
500	4.75	7.85

Transparency with self-expanding stent

mass (gm)	diameter (mm)	length (cm)
40	10.15	14.3
60	9.9	13.75
80	9.9	13.05
100	9.3	11.9
120	8.85	11.15
140	8.25	10.4
160	8.3	10.15
180	8.2	10.25
200	8.15	9.9
220	8.2	9.2
240	8.04	9.1
260	8.05	9.35
280	8.05	9.2
300	7.85	9.1
320	7.9	8.94
340	7.4	8.75
360	7.6	8.8
380	7.38	8.75
400	7.42	8.3
420	7.04	8.32
440	7	8.1
460	6.9	8.05
480	6.62	8.24
500	6.08	7.98
520	6.08	7.85
540	6	7.65
560	5.85	7.5
580	5.75	7.35
600	5.64	7.38
620	5.6	7.5
640	5.6	7.3
660	5.4	7.4
680	5.28	7.42
700	5.2	7.4
720	5.35	7.32

740	5.25	7.3
760	5.2	7.4
780	5.22	7.45
800	5.1	7.15
820	5.15	7.45
840	5.05	7.12
860	5.05	7.35
880	5	7.4
900	4.99	7.2
920	4.98	7.22
940	4.8	7
960	5	7.2
980	5.02	7.2
1000	4.8	7.3
1020	5.08	7.25
1040	5.1	7.15
1060	5.1	6.9
1080	4.98	7
1100	5.02	6.92
1120	4.75	6.85
1140	4.95	6.8
1160	4.85	6.8
1180	5.05	6.78
1200	4.82	6.75
1220	4.95	6.7
1240	4.95	6.75
1260	4.72	6.85
1280	4.9	7
1300	4.78	6.9
1320	4.92	6.72
1340	4.9	6.82
1360	4.74	6.75
1380	4.92	6.95
1400	4.92	6.8
1420	4.78	

Table 5. ***Data used to obtain the self-expanding force displacement characteristic.***

Appendix C: Determination of force to be used in fatigue testing

Determination of the force to be applied to the stent at the end of in vivo placement of the stent (the in vivo stent placement was simulated by displacing the stent the length of an in vivo expanded stent, and then finding the equivalent force to effect this displacement.

Let us assume that the blood pressure variation is 100 mmHg. Also, let us assume that the surfaces of the stent that face the blood vessel are completely apposed to the vessel wall. This is important, because if the stent is not completely in apposition with the wall, blood pressure will not be able to effect any stent expansion (for expansion to occur, pressure has to be applied only to one set of surfaces—see figure below using an example of a simple ring shaped object substituting for the stent).

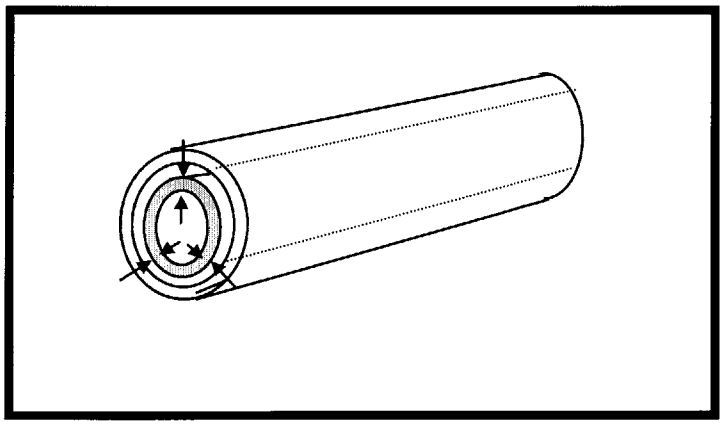

Figure 37 ***Forces on a stent modeled as a cylindrical tube.*** **The inner tube (darker shade) is not properly apposed to the artery wall (lighter shade). No resultant pressure acts on the tube→no displacement**

Pressure difference, dP = 100 mmHg = 0.013 MPa

Now use Laplace's law (the derivation is given below) to find the circumferential force on the stent due to this applied pressure.

Assume, as in the figure above that the stent is a longitudinal tube with a thickness t (see also figure below)

P0 – Pi is the blood pressure difference given above.

'l' is the length of the tube under consideration (it will eventually cancel out in the derivation)

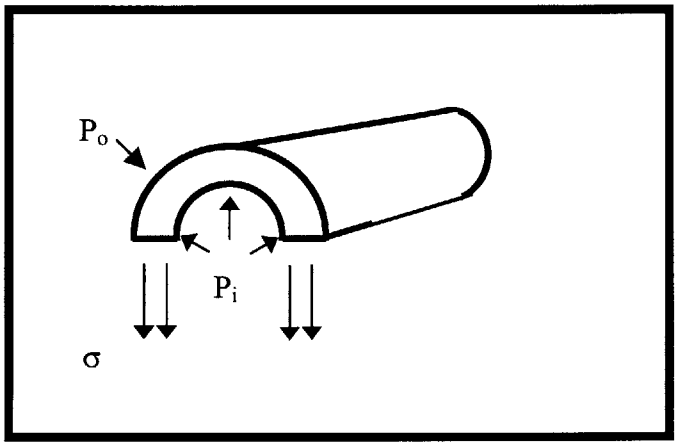

Figure 38 ***Force balance on a tube.*** **The circumferential stresses (shown facing down) are balanced by the pressures acting on the tube or arterial wall.**

$$2(\sigma)(t)l = (P_o - P_i)(2r_i)l$$

A force balance on the tube gives,

Or,

$$\sigma = \frac{(P_o - P_i)r_i}{t}$$

With r_i = internal radius of artery (or expanded stent radius) = 1.6mm

P = 0.013 MPa

$t = 0.178$ mm

$A = t^2 = 0.032$ mm^2

Stress, $\sigma = 0.0037$ = approx. 0.004 N

Appendix D Calculation of fatigue life

Matlab input file

```
sigma_max=659
sigma_min=612
sigma_a=(sigma_max-sigma_min)/2
sigma_mean=(sigma_max+sigma_min)/2
Nf=((sigma_a/sigma_mean)^(-1/0.13))/2
```

Matlab output file

```
sgma_max = 659
sigma_min = 612
sigma_a = 23.5000

sigma_mean =  635.5000

Nf =  5.1847e+010
```

Appendix E: Matlab file to find the pressure that will cause ave($strain_{local}$) = a specified global strain in a curved vessel

```
clear
%repeat analysis for 9 values of curvature varying
%from a low of 13 to a high of 21
%13 14 15 16 17 18 19 20 21
%This first for loop will calculate max stresses for values %of curvature from 13 to 21
step 1
%The output is the max. stress at 3pi/2 for max. stress vs %curvature. The values fo max.
stress for each curvature %will be saved in maxstress(diff)
%This matrix will have 9 entries with entry 1 corresponding %to curv=13

diff=1 % set diff equal to 1. Increment as each value of curv is changed
for curv=13:21 % cycle through different values of curvature
R0=curv

%calculation of the pressure for a given strain
%define intermediate variables
E=100000;
ec=0.33;
nu=0.27;
r=0.005;
h=0.002;

theta=0  %this is the best starting point for pressure
      %calc since it gives a good average pressure
a=(2*R0+r*sin(theta))/(R0+r*sin(theta));
b=nu*r/(2*h);
c=r/(2*h);
d=E*ec;
P(1)=d/(c*a-b)

%the following will calculate the strains for each pressure %value at 100 points around
the vessel circumference

%create 100 equally spaced angles between 0 and 2*pi
theta=linspace(0,2*pi);

%calculate ec at each of these angles
for number = 1:100
  aa(number)=(2*R0+r*sin(theta(number)))/(R0+r*sin(theta(number)));
  cc = r/(2*h);
  bb = nu*r/(2*h);
```

```
  ec(number)=(cc*aa(number)-bb)*P(1)/E;
end
%now we average over the strains calculated
ec_mean1=mean(ec)
aaaa=0.0000001
%compare this to the strain wanted=0.33

k=0.1;
t=0;
while(abs((ec_mean1-0.33)/0.33)>0.001)
  (ec_mean1-0.33)/0.33
  if(ec_mean1>0.33)
    P(1)=P(1)-k*P(1);
    for number = 1:100
        aa(number)=(2*R0+r*sin(theta(number)))/(R0+r*sin(theta(number)));
        cc = r/(2*h);
        bb = nu*r/(2*h);
      ec(number)=(cc*aa(number)-bb)*P(1)/E;
    end
    ec_mean1=mean(ec)
  end

  if(ec_mean1<0.33)
    P(1)=P(1)+k*P(1)
    for number = 1:100
        aa(number)=(2*R0+r*sin(theta(number)))/(R0+r*sin(theta(number)));
        cc = r/(2*h);
        bb = nu*r/(2*h);
      ec(number)=(cc*aa(number)-bb)*P(1)/E;
    end
    ec_mean1=mean(ec)
  end
  if(ec_mean1==0.33)
    P(1)
  end
  if(t>=100)
    k=0.05;
  end
  t=t+1;
end

%Now we spit out the final pressure
'the pressure is'
P(1)

% we use this pressure to find the stress sigma_c at each point around the circumference
```

```
theta=linspace(0,2*pi);
for number = 1:100

sigma_c(number)=P(1)*r/(2*h)*(2*R0+r*sin(theta(number)))/(R0+r*sin(theta(number));
end
%sigma_z is constant and is given by
'axial stress sigma_z is'
sigma_z=P(1)*r/(2*h)

maxst(diff)=max(sigma_c); %find the max value of stress at
                    %given curv
maxst2(diff)=P(1)*r/(2*h)*(2*R0+r*sin(3*pi/2))/(R0+r*sin(3*pi/2));      %find max
stress through equation
diff=diff+1;  %increment the value of diff

end         %this is the end of the first for loop

%we should now have 2 matrices.
%one matrix contains the max stress from the calculated %values around circ.
%the other calculates max stress from the formula using %P(1) calculated.

%we now plot each of these matrices separately, and then %compare the results
%the way maxst and maxst2 are ordered now is from %increasing curvature to
decreasing curvature.
%We want to reverse this
for revcount=1:9
  maxstrev(revcount)=maxst(10-revcount)
  maxstrev2(revcount)=maxst2(10-revcount)
end
count1=linspace(21,13,9)
count=1./count1
plot(count,maxstrev,'m*',count,maxstrev,'k-',count,maxstrev2,'k^')
title('circumferential stress vs curvature')
legend('matrix calc','','direct equation',-1)
xlabel('increasing curvature, C=1/radius of curvature')
ylabel('max circumferential stress')
```

Appendix F: Matlab file to find the stress vs strain curve for an eccentric vessel

```
clear
% calculation of the pressure for a given strain
% define intermediate variables
E=100000;
ec=0.33;
nu=0.27;
%for this trial intercenter distance=0.5

%for the min and max thickness, calculate the pressure. First
%define the variables for the geometry for the min and max
%radius
ri=5;  %ri=internal radius (fixed) see page 131 lab notes for dig.
%vary eccentricity. r0 is the radius at the thickest point, r1 at the thinnest point
r0=linspace(7,8.5,100);
r1=linspace(7,5.5,100);
g0=(r0./ri).^2; %g stands for gamma
g1=(r1./ri).^2;

%now calculate the pressure at thick point (corresponding to var. 0)
Pi0=E*ec./[(1+g0)./(g0-1)-nu.*(2-g0)./(g0-1)];
%now pressure for the thin point or point 1
Pi1=E*ec./[(1+g1)./(g1-1)-nu.*(2-g1)./(g1-1)];

%average these two pressures
Pave=(Pi0+Pi1)/2

%now find circ stress at the thin points (point 1) using the about Pave values
sigmacthin=Pave.*(1+g1)./(g1-1);
%now plot sigmac versus eccentricity. Define eccentricity as simply distance between
%centers
ecc=linspace(0,1.5,100);
plot(ecc,sigmacthin,'r-')
xlabel('eccentricity as simply intracenter distance')
ylabel('circumferential stress')
title('circumferential stress versus eccentricity')

hold

%The following circumferential stresses were found at the thinnest
%sections in eccentric vessels using a 2D model in ABAQUS
stress=[2.827 3.045 3.266 3.625 3.805 4.130 4.509 5.004 5.545 6.223 7.205]*10^4;
eccen=linspace(0,1.5,11);
```

```
plot(eccen, stress, 'k*', eccen, stress, 'k-')
xlabel('eccentricity as intra-center distance')
ylabel('circumferential stress')
title('variation of stress with eccentricity')

legend('calculated--upper', 'fea--lower')
```

Appendix G: Matlab file to find the stress vs strain curve for a tapered and non-tapered stent in a tapered vessel

```
clear
%%%% NON TAPERED STENT
E=100000
nu=0.27
% calculate strains and stresses at bottom
alpha=linspace(atan(1/10),atan(3/10),9)
for k=1:9
  strain(k)=[0.33*5+2*tan(alpha(k))]/[5-2*tan(alpha(k))]
  stress_c(k)=(2*E)/(2-nu)*strain(k)  % find stresses at bottom
end

% find stress at median location
'stress at median location'
stress_m=2*E*.33/(2-nu)

plot(alpha, stress_c,'m*', alpha, stress_c,'k-')
title('stress vs taper at bottom location for non-tapered stent')
xlabel('taper given by angle, alpha')
ylabel('stress in pascals')

%%%% TAPERED STENT
% strains and stresses at bottom
for k=1:9
  strain1(k)=0.33*5/(5-2*tan(alpha(k)))
  stress_c1(k)=(2*E)/(2-nu)*strain1(k)  % find stresses at bottom
end

% stresses at median plane for tapered stent are the same as before.
% No variation

% plot stresses
figure
plot(alpha, stress_c1,'m*', alpha, stress_c1,'k-')
title('stress vs taper at bottom location for Tapered stent')
xlabel('taper given by angle, alpha')
ylabel('stress in pascals')
```

Appendix H: Matlab code to find variation of poisson's ratio with strain

```
% the following code uses the quadratic formula to obtain the
% poisson's ratio variation with strain. The strain is allowed
% to vary from 0.1 to 1 in 10 increments. Both the small strain
% equation and the large strain equation are used in obtaining
% the poisson's ratios. It is seen from the plot that the error
% (or difference in calculated poisson's ratios) grows larger
% as the strains are increased

clear
ez=linspace(0.1,1,10)
a=ez+ez.^2;          % a, b, c are coefficients from the general
b=-(2+2*ez);  % quadratic formula: root=(-b+/-(b^2-4ac)^0.5)/2a
c=1;
nu1=(-b+(b.^2-4.*a).^0.5)./(2*a);
nu2=(-b-(b.^2-4.*a).^0.5)./(2*a)

a1=4*ez+8*ez.^2;
b1=-(4+8*ez);
c1=2;
nu1a=(-b1+(b1.^2-4.*a1*c1).^0.5)./(2*a1);
nu2a=(-b1-(b1.^2-4.*a1*c1).^0.5)./(2*a1)

plot(ez,nu2,'g-',ez,nu2a,'k-',ez, nu2,'go',ez,nu2a,'ko')
title('variation of poissons ratio with strain in isotropic material')
xlabel('strain')
ylabel('poissons ratio')
legend('small strain (upper curve)','large strain (lower curve)')
```

References

1. Baboolal, K., C. Evans, and R.H. Moore, *Incidence of end-stage renal disease in medically treated patients with severe bilateral atherosclerotic renovascular disease.* Am J Kidney Dis, 1998. **31**(6): p. 971-7.
2. Strandness, D.E., Jr., *Natural history of renal artery stenosis.* Am J Kidney Dis, 1994. **24**(4): p. 630-5.
3. Blum, U., *et al.*, *Treatment of ostial renal-artery stenoses with vascular endoprostheses after unsuccessful balloon angioplasty [see comments].* N Engl J Med, 1997. **336**(7): p. 459-65.
4. van de Ven, P.J., *et al.*, *Transluminal vascular stent for ostial atherosclerotic renal artery stenosis [see comments].* Lancet, 1995. **346**(8976): p. 672-4.
5. Tuttle, K.R. and R.D. Raabe, *Endovascular stents for renal artery revascularization.* Curr Opin Nephrol Hypertens, 1998. **7**(6): p. 695-701.
6. Ho, D.S., W.H. Chen, and C. Woo, *Stenting of a renal artery bifurcation stenosis.* Cathet Cardiovasc Diagn, 1998. **45**(4): p. 445-9.
7. Henry, M., *et al.*, *Stents in the treatment of renal artery stenosis: long-term follow-up.* J Endovasc Surg, 1999. **6**(1): p. 42-51.
8. van Lankeren, W., *et al.*, *Stent remodeling contributes to femoropopliteal artery restenosis: an intravascular ultrasound study.* J Vasc Surg, 1997. **25**(4): p. 753-6.
9. Faxon, D.P., W. Coats, and J. Currier, *Remodeling of the coronary artery after vascular injury.* Prog Cardiovasc Dis, 1997. **40**(2): p. 129-40.
10. Ohki, T., *et al.*, *Ex vivo human carotid artery bifurcation stenting: correlation of lesion characteristics with embolic potential.* J Vasc Surg, 1998. **27**(3): p. 463-71.
11. tickner, g., *Theoretical and experimental study of the elastic behavior of the human brachial and other human and canine arteries.* vidya report, 1964. **162**.
12. Greenwald, S.E., *et al.*, *Experimental investigation of the distribution of residual strains in the artery wall.* J Biomech Eng, 1997. **119**(4): p. 438-44.
13. Silver, F.H., *Biological materials : structure, mechanical properties, and modeling of soft tissues.* New York University biomedical engineering series. 1987, New York: New York University Press. xx, 228.
14. Mintz, G.S., *et al.*, *Arterial remodeling after coronary angioplasty: a serial intravascular ultrasound study.* Circulation, 1996. **94**(1): p. 35-43.
15. Hoffmann, R., *et al.*, *Patterns and mechanisms of in-stent restenosis. A serial intravascular ultrasound study [see comments].* Circulation, 1996. **94**(6): p. 1247-54.
16. Young, T., *The Croonian Lecture. On the functions of the Heart and Arteries.* Philosophical transactions, 1808: p. 1-31.
17. Bank, A.J., *Physiologic aspects of drug therapy and large artery elastic properties.* Vasc Med, 1997. **2**(1): p. 44-50.
18. Roach, M.R., Burton, A.C., *The reason for the shape of the distensibility curves of arteries.* Can. J. Biochem. Physiol., 1957. **35**: p. 681-90.
19. krafka, j., *Comparative study of the histo-physics of the aorta.* American journal of physiology, 1939. **125**: p. 1-14.
20. kutryk MJB, S.P., *Coronary stenting current perspectives. A companion to the handbook of coronary stents*. 1999: Martin Dunitz Ltd.

21. Oesterle, S.N., *et al.*, *The stent decade: 1987 to 1997. Stanford Stent Summit faculty.* Am Heart J, 1998. **136**(4 Pt 1): p. 578-99.
22. Carter, A.J., *et al.*, *Progressive vascular remodeling and reduced neointimal formation after placement of a thermoelastic self-expanding nitinol stent in an experimental model.* Cathet Cardiovasc Diagn, 1998. **44**(2): p. 193-201.
23. Oniki, T. and M. Iwakami, *Is arterial remodeling truly a compensatory biological reaction? A mechanical deformation hypothesis.* Atherosclerosis, 1997. **132**(1): p. 115-8.
24. Kakuta, T., *et al.*, *Differences in compensatory vessel enlargement, not intimal formation, account for restenosis after angioplasty in the hypercholesterolemic rabbit model.* Circulation, 1994. **89**(6): p. 2809-15.
25. Vavuranakis, M., *et al.*, *Impaired compensatory coronary artery enlargement in atherosclerosis contributes to the development of coronary artery stenosis in diabetic patients. An in vivo intravascular ultrasound study.* Eur Heart J, 1997. **18**(7): p. 1090-4.
26. Post, M.J., C. Borst, and R.E. Kuntz, *The relative importance of arterial remodeling compared with intimal hyperplasia in lumen renarrowing after balloon angioplasty. A study in the normal rabbit and the hypercholesterolemic Yucatan micropig [see comments].* Circulation, 1994. **89**(6): p. 2816-21.
27. Edelman, E.R. and C. Rogers, *Hoop dreams. Stents without restenosis [editorial; comment].* Circulation, 1996. **94**(6): p. 1199-202.
28. Mangell, P., *et al.*, *Are self-expanding stents superior to balloon-expanded in dilating aortas? An experimental study in pigs [see comments].* Eur J Vasc Endovasc Surg, 1996. **12**(3): p. 287-94.
29. Glagov, S., *et al.*, *Compensatory enlargement of human atherosclerotic coronary arteries.* N Engl J Med, 1987. **316**(22): p. 1371-5.
30. Polak, J.F., *et al.*, *Compensatory increase in common carotid artery diameter. Relation to blood pressure and artery intima-media thickness in older adults. Cardiovascular Health Study.* Stroke, 1996. **27**(11): p. 2012-5.
31. Eisenhauer, A., *personal communication*, . 2000.
32. Niskanen, L., *et al.*, *Carotid artery intima-media thickness in elderly patients with NIDDM and in nondiabetic subjects.* Stroke, 1996. **27**(11): p. 1986-92.
33. Gronholdt, M.L., S. Dalager-Pedersen, and E. Falk, *Coronary atherosclerosis: determinants of plaque rupture.* Eur Heart J, 1998. **19 Suppl C**: p. C24-9.
34. Lendon, C.L., *et al.*, *Atherosclerotic plaque caps are locally weakened when macrophages density is increased.* Atherosclerosis, 1991. **87**(1): p. 87-90.
35. Loree, H.M., *et al.*, *Mechanical properties of model atherosclerotic lesion lipid pools.* Arterioscler Thromb, 1994. **14**(2): p. 230-4.
36. Cheng, G.C., *et al.*, *Distribution of circumferential stress in ruptured and stable atherosclerotic lesions. A structural analysis with histopathological correlation.* Circulation, 1993. **87**(4): p. 1179-87.
37. Fung, Y.C., *Biomechanics : mechanical properties of living tissues*. 2nd ed. 1993, New York: Springer-Verlag. xviii, 568.
38. Carew, T.E., R.N. Vaishnav, and D.J. Patel, *Compressibility of the arterial wall.* Circ Res, 1968. **23**(1): p. 61-8.
39. Berrenberg, B., *Composites Newsletter*, . 2000.

40. bathe, m., *A fluid-structure interaction finite element analysis of pulsatile blood flow through a compliant stenotic artery*, in *mechanical engineering*. 1998, MIT: Cambridge.
41. Patel, D.J., Vaishnav, R.N., *The rheology of large blood vessels*, in *Cardiovascular fluid dynamics vol. 2*, D.H. Bergel, Editor. 1972, Academic Press: London, New York,. p. v.
42. Ward, I.M. and D.W. Hadley, *An introduction to the mechanical properties of solid polymers*. 1993, Chichester [England] ; New York: J. Wiley & Sons. xi, 334.
43. Ward, I.M., *Mechanical properties of solid polymers*. 2nd ed. 1983, Chichester, Sussex ; New York: Wiley. xv, 475.
44. Daniel, I.M. and O. Ishai, *Engineering mechanics of composite materials*. 1994, Oxford, [England] ; New York: Oxford University Press. xiii, 395.
45. ADINA R&D, W.M., *ADINA theory and modeling guide*. 1997.
46. Patel, D.J., J.S. Janicki, and T.E. Carew, *Static anisotropic elastic properties of the aorta in living dogs.* Circ Res, 1969. **25**(6): p. 765-79.
47. Loree, H.M., *et al.*, *Effects of fibrous cap thickness on peak circumferential stress in model atherosclerotic vessels.* Circ Res, 1992. **71**(4): p. 850-8.
48. Watkins, D.S., *Fundamentals of matrix computations*. 1991, New York: Wiley. xiii, 449.
49. Demiray, H., *Pulse velocities in initially stressed arteries.* J Biomech, 1988. **21**(1): p. 55-8.
50. Demiray, H., *personal communication by email*, . 1999.
51. Sawada, S., *et al.*, *Study of the physical properties of expandable metallic stents.* Radiat Med, 1991. **9**(6): p. 213-6.
52. Loshakove, A. and H. Azhari, *Mathematical formulation for computing the performance of self expanding helical stents.* Int J Med Inf, 1997. **44**(2): p. 127-33.
53. Spence, J. and A.S. Tooth, *Pressure vessel design : concepts and principles*. 1st ed. 1994, London ; New York: E & FN Spon. xvi, 491.
54. Harvey, J.F., *Theory and design of pressure vessels*. 1985, New York: Van Nostrand Reinhold. xiv, 623.
55. Wright, D., *notes on design of machine elements*, . 2000.
56. MIT, *FEA analysis in Computer-Aided Mechanical Design*, . 1999.
57. Juvinall, R.C. and K.M. Marshek, *Fundamentals of machine component design*. 2nd ed. 1991, New York: J. Wiley. xxvi, 804.
58. Zahavi, E. and V. Torbilo, *Fatigue design : life expectancy of machine parts*. 1996, Boca Raton: CRC Press. x, 321.
59. Clarijs, J.A., *et al.*, *Compensatory enlargement in coronary and femoral arteries is related to neither the extent of plaque-free vessel wall nor lesion eccentricity. A postmortem study.* Arterioscler Thromb Vasc Biol, 1997. **17**(11): p. 2617-21.
60. Aoki, T. and D.N. Ku, *Collapse of diseased arteries with eccentric cross section.* J Biomech, 1993. **26**(2): p. 133-42.